

**BREAST CANCER METASTATIC DORMANCY AND EMERGENCE IN THE
HEPATIC NICHE**

by

Donald Paul Taylor

B.S. Information and Decision Systems, Carnegie Mellon University, 1998

M.B.A., University of Pittsburgh, 2006

M.S. Bioengineering, University of Pittsburgh, 2006

Submitted to the Graduate Faculty of
Swanson School of Engineering in partial fulfillment
of the requirements for the degree of
Doctor of Philosophy

University of Pittsburgh

2013

UNIVERSITY OF PITTSBURGH
SWANSON SCHOOL OF ENGINEERING

This dissertation was presented

by

Donald Paul Taylor

It was defended on

November 8, 2013

and approved by

Linda Griffith, Ph.D., Professor, Departments of Biological and Mechanical Engineering,

Massachusetts Institute of Technology

Partha Roy, Ph.D., Professor, Department of Bioengineering

David Vorp, Ph.D., Professor, Department of Bioengineering

Dissertation Director: Alan Wells, MD, DMSc, Professor, Departments of Pathology and

Bioengineering

Copyright © by Donald Paul Taylor

2013

BREAST CANCER METASTATIC DORMANCY AND EMERGENCE IN THE HEPATIC NICHE

Donald Paul Taylor, Ph.D.

University of Pittsburgh, 2013

Breast cancer metastatic dormancy allows tumors to avoid clinical detection and evade treatment leading to recurrence after years or even decades, with devastating mortality rates. How the aggressive carcinoma cells that initially underwent a cancer-associated Epithelial to Mesenchymal Transition (EMT) from the primary tumor to disseminate and maintain a long-term, clinically undetectable state in an ectopic site is unknown. Clinical evidence suggests that many of the extravasated breast cancer cells partially revert their mesenchymal phenotype to an epithelial phenotype (MErT). This transition coincides with resistance to chemotherapy and may be a precursor to metastatic dormancy.

We first investigated the boundary probabilities under which proliferating micrometastases would engage dormancy. We developed a two-state Markov chain Monte Carlo simulation that modeled balanced proliferation. This modeling determined that balanced proliferation invoked dormancy only between a 49.7-50.8% survival probability range. This narrow window strongly suggests that cellular quiescence most likely explains dormancy. The implications for treatment and chemoresistance of metastases are discussed.

We also investigated early events that allow for metastatic dormancy. We postulated that the metastatic niche must be prepared by stresses that destabilize the parenchyma. Primary rat and human hepatocytes were challenged with epidermal growth factor (EGF) prior to MDA-MB-231 or MCF-7 inoculation in 2D and 3D bioreactor cultures. MDA-MB-231 cells with

exogenously modulated E-cadherin were intrasplenically injected into NOD/scid gamma mice in order to investigate E-cadherin's role in establishing liver metastases. To explore emergence from metastatic dormancy we investigated whether hepatic non-parenchymal cells (NPCs) contributed to metastatic breast cancer cell outgrowth and a mesenchymal phenotypic shift indicative of emergence. We found that the pre-stressed liver microenvironment confers a metastatic seeding advantage to the breast cancer cells at least in part by promoting a more pronounced epithelial reversion marked by E-cadherin up-regulation. *In vivo* studies confirmed that E-cadherin inversely correlates to metastatic proliferation. We also concluded that NPCs impart a partial mesenchymal shift to the MCF-7 cells thus conferring a grow-out advantage.

Taken together these investigations suggest that the metastatic microenvironment plays a role in metastatic competency through EMT/MErT plasticity and should be considered a potential target for ablating disseminated tumor cells.

TABLE OF CONTENTS

PREFACE.....	XVIII
1.0 INTRODUCTION.....	1
1.1 BREAST CANCER.....	2
1.1.1 Etiology and prevalence	2
1.1.2 Major breast cancer sub-types	3
1.1.3 Breast cancer intravasation	4
1.1.3.1 Epithelial-to-mesenchymal transition	5
1.2 LIVER AS METASTATIC SITE.....	7
1.2.1 Liver physiology and function	7
1.2.2 Parenchymal hepatocytes.....	8
1.2.3 Non-parenchymal hepatic cells.....	8
1.2.4 Hepatic injury and stress response	10
1.2.5 Metastatic extravasation to the liver.....	14
1.2.5.1 Mesenchymal-to-epithelial-reverting transition.....	16
1.3 BREAST CANCER METASTATIC DORMANCY AND EMERGENCE .	17
1.3.1 Dormancy mechanisms	18
1.3.2 Emergence mechanisms	19
2.0 THE DORMANCY DILEMMA: QUIESCENCE VERSUS BALANCED PROLIFERATION	20
2.1 ABSTRACT.....	20
2.2 INTRODUCTION TO METASTATIC DORMANCY	21
2.3 PROGNOSTIC ASSAYS FOR METASTATIC DORMANCY.....	23
2.4 COMPUTER SIMULATION REVEALING QUIESCENCE AS INTEGRAL TO METASTATIC DORMANCY	24
2.5 IN VIVO INVESTIGATIONS INTO METASTATIC DORMANCY	28

2.6	MICROPHYSIOLOGIC THREE-DIMENSIONAL BIOREACTORS TO STUDY METASTATIC DORMANCY	33
2.7	CONCLUSIONS	34
3.0	MODELING BOUNDARY CONDITIONS FOR BALANCED PROLIFERATION IN METASTATIC LATENCY.....	36
3.1	ABSTRACT.....	36
3.2	TRANSLATIONAL RELEVANCE	37
3.3	INTRODUCTION	38
3.4	MATERIALS AND METHODS	42
3.4.1	MCMC model overview	42
3.4.2	Assumptions	44
3.5	RESULTS	44
3.5.1	Survival after metastatic extravasation is rate limiting	44
3.5.2	Dormant metastases arise only for survival probabilities proximal to 50 percent.....	49
3.5.3	Dormant metastases exhibited a large range in cell numbers.....	51
3.5.4	Metastatic outgrowth was highly sensitive to small changes to survival probability	53
3.6	DISCUSSION.....	55
4.0	HEPATIC NON-PARENCHYMAL CELLS DRIVE BREAST CANCER PROLIFERATION AND PARTIAL EPITHELIAL-TO-MESENCHYMAL TRANSITION.....	61
4.1	ABSTRACT.....	61
4.2	INTRODUCTION	62
4.3	RESULTS	64
4.3.1	Endothelial cell lines confer a grow-out and survival advantage to breast cancer cells.....	64
4.3.2	Primary human non-parenchymal cells confer a grow-out advantage to breast cancer cells	68
4.3.3	Brest cancer cell outgrowth is increased in primary rat NPC co-culture versus hepatocyte co-culture.....	70

4.3.4	NPC cells confer a partial mesenchymal phenotypic shift to E-cadherin positive breast cancer cells	72
4.3.5	NPC cells initiate p38 nuclear translocation in MCF-7 cells	77
4.3.6	NPC-induced MCF-7 outgrowth is at least partially mediated by soluble factor secretion through epidermal growth factor receptor activation	80
4.4	DISCUSSION.....	83
4.5	MATERIALS AND METHODS	84
4.5.1	Cells and cell culture	84
4.5.2	Co-culture.....	85
4.5.3	Imaging	85
4.5.4	Immunoblotting	86
4.5.5	Flow cytometry.....	86
4.5.6	EGFR inhibition	87
4.5.7	Statistical Analysis.....	87
5.0	THE PRE-STRESSED HEPATIC NICHE PROMOTES BREAST CANCER METASTATIC COMPETENCY	88
5.1	ABSTRACT.....	88
5.2	INTRODUCTION	90
5.3	RESULTS	91
5.3.1	Pre-stressing hepatocytes does not significantly damage the cells while causing homotypic E-cadherin membrane delocalization	91
5.3.2	Pre-stressed hepatocytes induce an epithelial-like clustering morphology in breast cancer cells and prompt E-cadherin up-regulation.	94
5.3.3	Pre-stressed hepatocytes impart a grow-out advantage to breast cancer cells.	96
5.3.4	MErT is enhanced in the pre-stressed hepatocyte cultures.....	97
5.3.5	MDA-MB-231 cells undergo mesenchymal to epithelial reversion in spontaneous metastases derived from ectopic primary tumors in mouse models.....	99
5.3.6	E-cadherin expression in the metastatic niche correlates with proliferation and outgrowth	108

5.4	DISCUSSION.....	109
5.5	MATERIALS AND METHODS	112
5.5.1	Cells and cell culture	112
5.5.2	Animal procurement and care.....	112
5.5.3	Imaging.....	113
5.5.4	Flow cytometry.....	113
5.5.5	Quantitative real-time PCR.....	114
5.5.6	Immunohistochemistry	114
5.5.7	Statistical Analysis.....	115
6.0	3D ORGANOTYPIC BIOREACTOR SYSTEMS HOLD PROMISE TO UNCOVER METASTATIC DORMANCY AND EMERGENCE MECHANISMS	116
6.1	BIOREACTOR OVERVIEW	116
6.2	REACTOR EQUATIONS FOR OXYGEN MASS TRANSPORT.....	118
6.3	FUNCTIONAL TISSUE CONSTRUCTS.....	119
6.4	BREAST CANCER CELL INNOCULATION	124
7.0	DISCUSSION.....	127
7.1	CONCLUSION	131
8.0	SPECULATIONS AND NEXT STEPS.....	132
	BIBLIOGRAPHY	136

LIST OF TABLES

- Table 1. Five-year relative survival rates (2003 - 2009) for all women of all races (Adapted from SEER, 2013). The notable implication is that therapies directed to treat and resolve the primary tumor are largely ineffective once breast cancer metastasizes..... 2
- Table 2. Signaling cascade following partial hepatectomy (Phx). A rich diversity of secreted factors from the hepatic niche is dispersed in a predictable, highly-controlled manner. Many of these secreted factors are not found within the primary tumor microenvironment, and so may contribute to disseminated breast cancer cell dormancy, emergence, or apoptosis..... 13

LIST OF FIGURES

- Figure 1. Carcinoma associated epithelial-to-mesenchymal transition (EMT). This figure was adapted from a Wells laboratory cartoon and depicts the transforming carcinoma cells from the primary breast tumor losing their membrane-bound E-cadherin, thus enabling single-cell transit into the circulatory conduits. Autocrine EGF signaling continues to sequester E-cadherin from the membrane while also providing pro-survival signals to the breast cancer cells. Shown here is also the extravasation step where a single carcinoma cell is able to penetrate the liver sinusoidal endothelial cells and intercalate among the hepatocytes..... 6
- Figure 2. NPC cell signaling within a remodeling liver (adapted from Michalopoulos, 2007). Paracrine signaling among hepatocytes and non-parenchymal cells is triggered through tight temporal control. Hepatic stress response signaling is also maintained between non-parenchymal cells such as TGF- β 1 from stellate cells to liver sinusoidal endothelial cells. This physiologic signaling cascade may contribute to ectopic breast cancer cell dormancy and emergence given carcinoma response from cytokines such as TGF- β 1 may differ in the metastatic niche versus the primary tumor microenvironment..... 11
- Figure 3. Metastatic seeding and involvement of hepatic non-parenchymal cells (adapted from Van den Eynden et al., 2013). Panel A depicts the body's natural and uninhibited response to ablating disseminated cancer cells in the hepatic vascular conduits. For example, Kupffer cells perform phagocytosis while liver sinusoidal cells secrete apoptotic signals. Panel B depicts the extravasation process whereby certain carcinoma cells evade the body's natural response and enable metastatic seeding within the liver microenvironment. This extravasation can trigger the physiologic stress response pathways from the hepatic niche (as depicted in Figure 1) that consequently may trigger dormancy or emergence carcinoma phenotypes..... 15
- Figure 4. Probability of dormancy from *in silico* simulation. Dormancy is defined by a metastasis achieving 1,218 cycles while having a cell number greater than 0 and below 1 million. The simulated balanced proliferation yields a dormant phenotype for patients harboring 1,000 cryptic micrometastases only between 49.7% and 50.8% survival probability

regardless of starting cell number in the micrometastasis. A, the absolute number of dormant metastases at the end of the 1,218 cycles for a starting number of 2 cells per micrometastasis. B, the metastatic fate for each of the survival probabilities showing that same dormancy window (in red). The green area shows that the majority of metastases die out even at survival probabilities approaching 60%. Metastases that become clinically evident (exceed 1 million cells) are shown in purple..... 26

Figure 5. Schematic of an approach to study metastatic dormancy. The development of microphysiologic systems such as organotypic bioreactors allows for the examination of cellular events in metastatic seeding and entry into dormancy or continuous outgrowth for a multiweek period (Griffith & Swartz, 2006). Shown is a cartoon depicting the fate of the micrometastasis following from the host tissue being in a more physiologic state (upper pathway) versus a stressed, inflamed, or fibrotic organ (lower pathway). The stressed pathway prohibits micrometastases from entering dormancy while supporting emergence into frank metastases. 32

Figure 6. Metastatic cell fates are determined via a Markov chain Monte Carlo method developed in the Matlab programming environment. A, the simulation's progression starting with 1,000 metastases initialized for each of the 100 patients. Within each simulation, there exists a starting cell number denoted by n (1, 2, 4, or 8) across survival probabilities ranging from 30% to 70%. Starting with the first cell cycle (denoted by k) a random number is generated and compared with the survival probability. If n is equal to 0, the metastasis dies out, and the next metastasis simulation (up to 1,000) begins. If n reaches 1 million, the metastasis is assumed to grow out to be clinically evident. If k reaches 1,218 while n is greater than 0, the metastasis goes dormant. B, traces the fate of 100 individual metastases across 4 survival probabilities, showing the variability in metastatic progression. Once metastases reach approximately 1,000 cells, the growth rate equals the expected growth rate as depicted by the dotted lines..... 41

Figure 7. Metastatic fate for 2-cell (top) and 8-cell (bottom) starting metastases followed identical trends with the majority of metastases dying out. The metastatic fate is coded with black designating the metastases that remained dormant, gray the ones that died out, and patterned those that grew out. X-axis represents survival probability from 30% to 70% with vertical bars representing incremental probability rate changes. Shown are stochastic models; the fixed survival percentages exhibited similar fates (data not shown). 46

Figure 8. Micrometastases that die do so quickly when survival probability is low or high. As P increases mets are, on average, surviving longer, even though most still die. The symmetric, decreasing curves capture results from the increased likelihood of cell survival, meaning that those that do die out must converge to that fate quickly. Vertical bars indicate cell survival maxima and minima for non-surviving metastases. Only near

the dormancy survival ranges do micrometastases have marked increases in cell cycles to die out, but still well below 1,218 cycles..... 48

Figure 9. Dormancy only manifests between 49.7% and 50.8% survival probability. Mean number of dormant metastases per 1,000 initial nodules (ordinate) increases as starting cell number increases, although they remain bounded by the same restraints in terms of survival probabilities (abscissa). B, an enlarged view of the narrow probability window indicated in A..... 50

Figure 10. Dormant metastases exhibit a wide range of cell numbers per metastasis. The number of cells in each dormant nodule (ordinate) spanned from hundreds to nearly one million cells, with similar results between 1-cell to 8-cell starting metastases across the survival percentages. This range is highly sensitive to small changes in survival probability..... 52

Figure 11. Cycles to outgrowth between 1- and 8-cell metastases. The cumulative fraction (ordinate) of micrometastases that grow out as a function of survival probability leads to fewer cycles (abscissa) with even a one percentage point increase in cell survival reducing outgrowth time by nearly two thirds..... 54

Figure 12. Non-parenchymal cell lines co-cultured with MCF-7-RFP cells confer carcinoma outgrowth. A) Phase contrast imaging with a fluorescence overlay (Red: MCF-7 cells) are representative images on Day 1 and Day 4 across 3 conditions: HMEC-1 co-culture in HMM, MCF-7-RFP in HMM, and MCF-7-RFP in RPMI. MCF-7 cells in HMM fail to outgrow, while outgrowing exponentially in the RPMI controls as expected. The MCF-7 cells experience outgrowth in the presence of HMEC-1 cells. B) Same conditions as in Panel A but with TMNK-1 cells. Day 1 is 24 hours after MCF-7-RFP cell seeding. Greater than 95% of the MCF-7-RFP cells expressed RFP on Day 4. Scale bar 250 micrometers..... 66

Figure 13. Flow cytometry for Annexin V negative, RFP positive cells (MCF-7-RFP) used to quantify cell counts in a separate biological replicate than in Figures 12A and 12B. HMEC-1 co-culture MCF-7 cells grew out at rates similar to the MCF-7 growth medium controls. Technical replicates performed in triplicate; p value < .001..... 67

Figure 14. Human primary non-parenchymal liver cells (NPCs) confer carcinoma outgrowth. A) Representative images of MCF-7-RFP and B) MDA-MB-231-RFP cells in co-culture with primary NPCs compared to their HMM controls demonstrating carcinoma outgrowth in the presence of NPCs. Flow cytometry quantification for Annexin V negative, RFP positive breast cancer cells. One well of a single biologic sample. Scale bar 250 micrometers. 69

- Figure 15. Hepatocytes confer MDA-MB-231 outgrowth but less than non-parenchymal liver cells. Flow cytometry quantifying MDA-MB-231-RFP cell count for Annexin V negative, RFP positive cells in co-culture conditions versus positive and negative controls. Technical replicates performed in triplicate..... 71
- Figure 16. Representative phase contrast images with fluorescence overlay of MDA-MB-231 cells across four culture conditions: hepatocyte growth medium alone, hepatocyte co-cultures, non-parenchymal hepatic cell co-cultures, and RPMI MDA-231 growth medium alone. Scale bar 250 micrometers. 72
- Figure 17. HMEC-1 co-culture confers a mesenchymal phenotype to MCF-7 cells. Representative fluorescent images on Day 4 of MCF-7 cells (in red) co-cultured with HMEC-1 cells. Fluorescent imaging depicts MCF-7-RFP cells in growth medium (left column) versus in HMEC-1 co-culture in HMM (right column). Scale bar 50 micrometers..... 74
- Figure 18. HMEC-1 cells induce a partial mesenchymal shift to MCF-7-RFP cells. Confocal imaging for E-cadherin (green) shows membrane-bound staining in RPMI controls while co-cultured MCF-7 cells (red) internalize E-cadherin within the cytoplasm. Scale bar 50 micrometers. Nuclei indicated in blue. 76
- Figure 19. Immunoblot for E-cadherin in MCF-7 cells co-cultured with HMEC-1 cells (not expressing E-cadherin)..... 77
- Figure 20. HMEC-1 cells induce a stress response in MCF-7 cells. Confocal imaging for phosphorylated p38 (Green) shows a nuclear translocation in HMEC-1 co-cultures versus the RPMI control. Scale bar 50 micrometers..... 79
- Figure 21. HMEC-1 conditioned medium supports MCF-7 outgrowth. Phase contrast images of MCF-7-RFP cells with fluorescent overlay (Panel A) across three culture conditions: 1) HMEC-1 conditioned medium, 2) HMM, and 3) RPMI growth medium. MCF-7 cells in conditioned medium exhibited a grow-out advantage over MCF-7 cells cultured in the HMM controls (Panel B). Technical replicates performed in triplicate. 81
- Figure 22. EGFR inhibition blunts MCF-7 outgrowth in HMEC-1 cultures. Co-cultures were administered as described in Figure 13. 500 nM of EGFR inhibitor was introduced into

the three treatment groups while MCF-7 positive growth controls in RPMI were free from inhibitor. Technical replicates were performed in triplicate; $p < .001$ 82

Figure 23. BUN and AST levels in 2D cultures are similar between pre-stressed and non-stressed hepatic cultures with either MDA-MB-231 or MCF-7 cells. EGF was incubated for 6 hours prior to aspiration and PBS washes. 231 No and MCF7 No categories reflect cultures not incubated with EGF..... 92

Figure 24. Human hepatocytes fail to maintain membrane-bound E-cadherin in pre-stressed cultures during the 6 hour EGF incubation period. E-cadherin (shown in green) delocalizes from the hepatocyte membranes at the 6-hour timepoint (versus the No EGF controls). After 24 hours of EGF incubation the hepatocytes begin to restore membrane-bound E-cadherin suggesting that the pre-stress EGF condition provides an opportunity for breast cancer cells to intercalate for seeding, and then become incorporated into the restored heterotypic E-cadherin connections. Scale bars 50 micrometers..... 93

Figure 25. MDA-MB-231 cells form greater numbers of epithelial-like clusters in pre-stressed versus non-stressed co-cultures (Panel A) for 20nM EGF cultures (incubated for 6 hours prior to breast cancer cell inoculation). There was no significant difference in cluster area across the pre-stress conditions (Panel B). Clusters were defined as 4 or more contiguous MDA-MB-231 cells across 9 fields per well in duplicate. Scale bar 200 micrometers..... 95

Figure 26. Pre-stressing promotes cancer cell proliferation. By day 5 of co-cultures, there were 35% more MDA-MB-231 cells in the pre-stressed hepatic cultures versus the non-stressed controls as quantified by flow cytometry for Annexin V negative, RFP-positive MDA-MB-231 cells. Error bars represent the standard deviation from the mean of three technical replicate samples. P value $< .01$ 96

Figure 27. E-cadherin is more strongly expressed among breast cancer cells co-cultured in pre-stressed hepatocytes. MDA-MB-231 breast cancer cells (red) weakly re-express E-cadherin (green) in no press hepatic cultures (left panel). Pre-stressed cultures (20nM EGF) elicit a stronger E-cadherin re-expression (right panel). Scale bar 50 micrometers. 98

Figure 28. Spleens and livers were harvested from the three MDA-MB-231 variants across 18 NOD/scid gamma mice. Metastases were macroscopically apparent in all injections from their cognate ectopic primary tumors in the spleens..... 100

Figure 29. MDA-MB-231 cells injected into mouse spleens formed irregular and disorganized ectopic primary tumors while the paired liver metastases exhibited a more organized and clustered phenotype. This demonstrates that the metastases histologically appear more differentiated than their primary tumor cognates. Scale bars – 10x 200 micrometers, 40x 50 micrometers..... 101

Figure 30. The MDA-MB-231 E-cadherin knock-down cell injections maintain a de-differentiated and irregular morphology in both the ectopic primary tumors and paired liver metastases. Scale bars – 10x 200 micrometers, 40x 50 micrometers..... 103

Figure 31. MDA-MB-231 injections into NOD/scid Gamma mice. Spleens are E-cadherin negative while their cognate liver metastases stain positive for E-cadherin. Scale bars – 10x 200 micrometers, 40x 50 micrometers..... 104

Figure 32. MDA-231Ecad cells injected into NOD/scid gamma mice. Scale bars – 10x 200 micrometers, 40x 50 micrometers..... 105

Figure 33. MDA-231shEcad injections into NOD/scid gamma mice. Scale bars – 10x 200 micrometers, 40x 50 micrometers..... 106

Figure 34. E-cadherin increases in MDA-MB-231-WT spontaneous metastases to the liver (MErT). In the main graph the y-axis represents E-cadherin normalized to GAPDH with the delta CT transformation ($1/2^x$) where x = mean E-cadherin CT normalized to GAPDH CT within 3 samples of each tissue. Inset – represents the same E-cadherin quantification as in the main graph, but depicts the MDA-MB-231-WT (blue) and shEcad (red) on a linear scale. Human E-cadherin and GAPDH primers..... 107

Figure 35. Spleens strongly stain for Vimentin and Ki-67 versus their paired liver metastases. 108

Figure 36. LiverChip bioreactor plate positioned within the pneumatic pump docking station.116

Figure 37. Cross sectional schematic of the LiverChips' reactor and reservoir system (Linda Griffith lab diagram). 117

Figure 38. LiverChip scaffold..... 118

Figure 39. Evaluating LiverChip hepatic injury and function through extended culture periods.
..... 120

Figure 40. Cytochrome P450 activity in 13-day LiverChip cultures with and without non-
parenchymal cells..... 122

Figure 41. Day 15 of cryopreserved hepatic cultures (A) and freshly-harvested hepatic cultures
(B). F-actin in green, kupffer cells in red (for CD68). Nuclei are stained blue (DAPI).
Red is stained with CF45 which is a pan-leukocyte marker while green represents the
liver sinusoidal endothelial cells (stained for Lyve-1). The nuclei are stained in blue
(DAPI)..... 124

Figure 42. MCF-7 cells intercalating in the hepatic niche. A representative scaffold on Day 15 of
the metastatic culture system. Actin is labeled in green, nuclei in blue (DAPI), and the
MCF-7 cells are exogenously expressing dsRED (in red). B) is an orthogonal plan
composite from A). 125

Figure 43. Spontaneous growth attenuation among sub-populations of human immortalized
breast cancer cells. MCF-7 cells (Red) on Day 15 of co-culture in the LiverChip system.
MCF-7 cells seeded Day 3 (1,000 cells per scaffold). B) MDA-MB-231 cells Day 15.126

PREFACE

It's uncertain who first proclaimed, "Your dreams must be bigger than your fears and your actions be louder than your words." If that statement holds true, I must have dreamt big – very big – to pursue my PhD because it nearly scared me to death every step of the way. I am here at the end of my journey with so many people to thank, for without them, I'd just be all talk.

I will be ever grateful to my PhD advisor Alan Wells for taking a risk hiring me into his lab and mentoring me when I had never previously picked up a pipette. Alan provided just the right intellectual freedom for me to self-discover the highs and lows of experimental research. I sincerely thank my thesis committee: Linda Griffith, Partha Roy, and David Vorp for being vigilant in holding me to high standards of experimental design and research integrity.

I thank all members of the Wells lab past and present who invested their time in training someone so green. I thank my business mentor, Jim Jordan, who provided me with an opportunity to support my family and to maintain my passion for commercialization while knee deep in hepatocytes, mouse spleens, or coding behind a computer screen. I thank my mom and dad who taught me to be kind to other people and to persevere under hardship.

With the highs came lows, and I'm grateful to my wife Jenny who lifted my confidence when I had episodes of thinking all hope was lost for me as a research scientist. To my boys Lans and Donnie, I will always remember our weekend lab excursions where we did experiments

together. Throughout the years of long, solitary hours in the lab while you both were being best of friends or driving mom crazy I hope that you know I thought about you as much as I did my research. May you both dream big and fear not.

1.0 INTRODUCTION

Clinical emergence from dormant breast cancer metastases affects nearly 20 percent of breast cancer patients – most of these cases are refractory to treatment and result in death. Early detection and diagnosis of primary breast cancer is largely curable by surgery or radiation therapy, though nearly one third of those patients will already have disseminated disease. Half of those patients will develop clinically evident metastases within a few years of primary tumor diagnosis and successful treatment. Consequently additional clinical interventions such as surgery or adjuvant therapy will be administered to eliminate the metastases, though many patients will succumb to the disease. But for the other 50 percent, years to decades will transpire before the metastases become clinically evident – offering an extended timeframe to treat those patients with therapies directed to keeping metastases indolent, or to kill the cryptic breast cancer cells before their escape from metastatic dormancy. Unfortunately no such therapies exist. This dissertation investigates the metastatic niche as a critical axis of both dormancy and the subsequent emergence from metastatic dormancy.

1.1 BREAST CANCER

1.1.1 Etiology and prevalence

The Surveillance Epidemiology and End Results (SEER) of the National Cancer Institute (NCI) projects that 232,340 women will be diagnosed with breast cancer in 2013 with 39,620 women dying from this disease in the same year (SEER.cancer.gov, 2013).

Table 1. Five-year relative survival rates (2003 - 2009) for all women of all races (Adapted from SEER, 2013). The notable implication is that therapies directed to treat and resolve the primary tumor are largely ineffective once breast cancer metastasizes.

Stage at Diagnosis	Five-year relative survival (%)
Localized	98.6
Regional	84.4
Distant	24.3
Unknown (unstaged)	50

The five-year relative survival following breast cancer diagnosis is encouraging when cancer is either localized to the primary site or regional (adjacent lymph node involvement). Critically, however, five-year survival rates drop precipitously (approximately 60 percentage points) when breast cancer spreads to distant organs (Table 1). These data suggest at a high level that early detection for surgical, radiological, and/or chemotherapeutic interventions can save the majority of lives. Unfortunately these data also suggest that those same interventions that are successful in the primary tumor are vastly wanting at curing metastatic breast cancer.

1.1.2 Major breast cancer sub-types

Breast cancer is predominately categorized as stemming from either ductal or lobular origins, with the majority of cases derived from ductal transformations (Rakha et al., 2006). High- versus low-grade breast carcinomas are prognostic for their likelihood to invade the local stroma and metastasize to distant organs. Estrogen receptor (ER) and progesterone receptor (PR) positive samples with low p53 mutation are generally considered to be low grade. High-grade breast cancer is typically ER-negative, PR-negative, p53 mutated and 16q chromosomal deficient (Rakha et al., 2006).

Invasive ductal carcinoma (IDC) exhibits the most extensive histomorphological differences among tumor samples that have since been characterized into four major subtypes (Bombonati and Sgroi, 2011). These subtypes include estrogen receptor (ER) positive luminal A, ER-positive luminal B, ER-negative ERBB2 and ER-negative basal. Invasive ductal carcinomas tend to be E-cadherin positive, limiting their invasive propensity.

Invasive lobular carcinoma (ILC) accounts for approximately 14% of breast cancer diagnoses. ILC is characterized by 16q chromosomal loss and reduced or absent E-cadherin expression (Simpson et al., 2008).

This high molecular diversity among breast cancers poses great challenges in identifying mechanisms responsible for metastatic dormancy, notwithstanding selecting for the most effective primary tumor treatment.

1.1.3 Breast cancer intravasation

Breast cancer intravasation is the process by which the carcinoma cells enter the body's systemic conduits such as the lymph nodes or blood vessels. By this very definition, intravasation is the first step in tumor metastasis, as this represents the ability for carcinoma cells to move beyond the primary tumor. The cellular transformation preceding intravasation (discussed in detail in Chapter 1.1.3.1) consists of the epithelial cells losing their cell-cell contacts and becoming motile as single-cell deposits. The extracellular matrix (ECM) within the breast must then be degraded in order for the carcinoma cells to transit into local lymph or blood vessels.

Prompting the cells to engage these EMT and intravasation programs is thought to be largely dictated by aberrant gene expression – as well as epigenetic modifications. Oncogenes have been functionally evaluated for their ability to serve as modulators for motility and subsequent intravasation. The most notable breast oncogenes include epidermal growth factor receptors (EGFR), MNNG HOS Transforming gene (c-MET), phosphatase and tensin homologue (PTEN), and small GTPases such as Ras (Sahai, 2005).

The vast majority of carcinoma cells in the primary tumor do not possess this motility phenotype (Wang et al., 2002). Furthermore, those few motile cells tend to be clustered within a specific region in the tumor that's most proximal to the extracellular matrix (Wyckoff et al., 2000). Consequently, the primary tumor microenvironment is thought to be a potent regulator of this motility transformation in carcinoma cells.

Particular emphasis has been placed on stromal-associated cells and the degree to which those cells can influence the motility of the carcinoma cells. These stromal cells include fibroblasts, myofibroblasts, and macrophages that have been shown to secrete matrix

metalloproteinases (MMPs), epidermal growth factor (EGF), and hepatocyte growth factor (HGF) in a paracrine signaling process (De Wever et al., 2004).

The cancer cells' phenotype will also help determine to what extent those cells are capable of intravasation. Motility phenotypes are typically divided among mesenchymal motility amoeboid motility or collective motility. Nearly half of carcinomas exhibit the mesenchymal motility phenotype (Thiery, 2002) and so this phenotype is a primary focus of our research investigation.

1.1.3.1 Epithelial-to-mesenchymal transition

Epithelial-to-mesenchymal transition (EMT) is a physiologic, highly conserved process during embryogenesis whereby the mesoderm is formed from a mesenchymal transition from the embryonic epithelium (Mani et al., 2008). Subsequently those mesodermal cells differentiate into epithelial cells of tissues such as the kidneys and ovaries – which is the reverse process called mesenchymal-to-epithelial transition (MET). EMT has been implicated in pathologies such as cancer where the EMT program is through to be hijacked by transforming carcinomas allowing them to gain advantages such as invasion, single-cell survival, and proliferation (Thiery, 2003; Radisky, 2005). Thus, the cancer-associated EMT better describes a transformed carcinoma cell, though a pathophysiologic EMT is still considered.

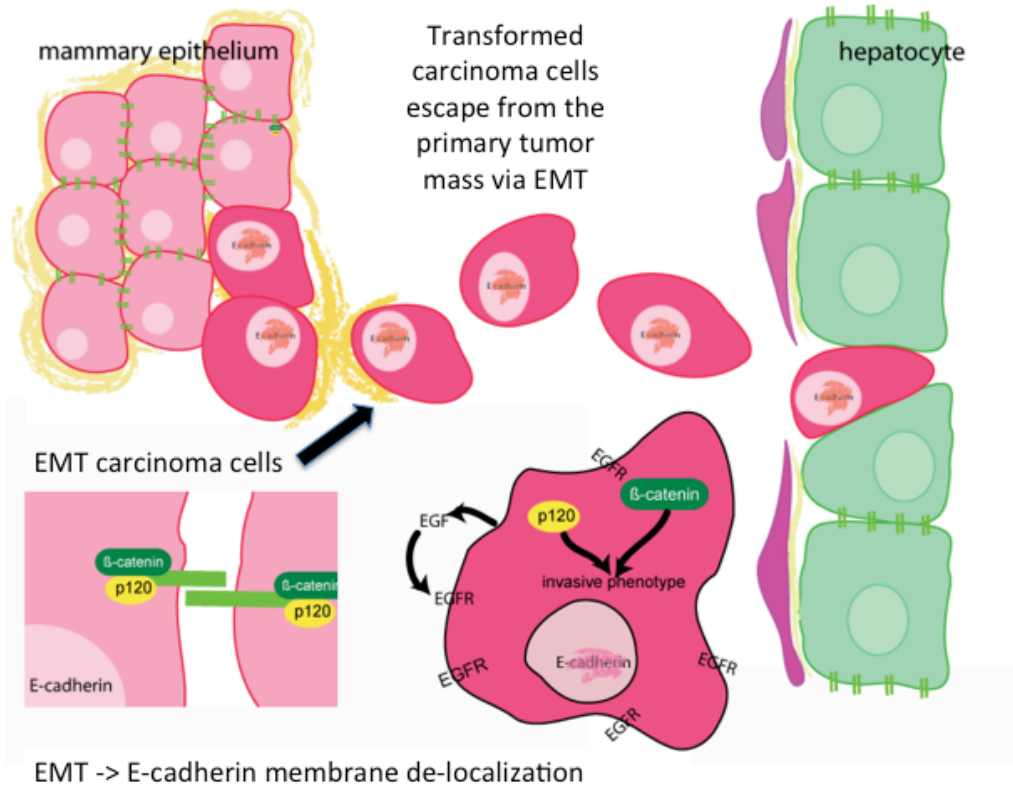


Figure 1. Carcinoma associated epithelial-to-mesenchymal transition (EMT). This figure was adapted from a Wells laboratory cartoon and depicts the transforming carcinoma cells from the primary breast tumor losing their membrane-bound E-cadherin, thus enabling single-cell transit into the circulatory conduits. Autocrine EGF signaling continues to sequester E-cadherin from the membrane while also providing pro-survival signals to the breast cancer cells. Shown here is also the extravasation step where a single carcinoma cell is able to penetrate the liver sinusoidal endothelial cells and intercalate among the hepatocytes.

EMT disrupts the apical-basal polarity orienting epithelial cells. Prior to an EMT, those epithelial cells are normally forming tight junctions among each other, as well as maintaining a strong integrin linkage to the surrounding extracellular matrix. As a consequence, those epithelial cells are sequestered from soluble factors and paracrine signaling that otherwise might disrupt their normal function.

EMT can be induced through many different ways, all of which depend on the tissue of origin as well as the surrounding extracellular milieu. Nuclear localization of SMAD proteins along with transforming growth factor beta (TGF β) activation of cell surface receptors can trigger EMT (Shi and Massague, 2003). Transcriptional repressors such as TWIST and Snail can initiate EMT by transcriptionally silencing E-cadherin (Ansieau et al.; Fendrich et al., 2009).

1.2 LIVER AS METASTATIC SITE

1.2.1 Liver physiology and function

By weight the liver is the largest organ in the human body and is divided into eight lobe segments inclusive of the caudate lobe (Dawson and Tan, 1992). The primary functional units of the liver are organized into lobules that primarily consist of hepatic plates and portal triads (portal vein, hepatic artery and bile ducts). The liver directly brokers vascular blood supply between the gastrointestinal system and the body's other organ systems, thus, the liver is exposed to a vast array of endobiotics, xenobiotics, and toxic precursors. A major liver function is therefore to metabolize these toxins into substances that can be safely purged from the body.

1.2.2 Parenchymal hepatocytes

The parenchymal hepatocytes form 1-cell thick plates within the liver lobules. Each plate consists of approximately 25 hepatocytes that form a pericentral-to-periportal orientation. Because of the steep oxygen gradient from periportal to pericentral (Jungermann and Kietzmann, 2000), the hepatocytes along this continuum have different and specialized functions (Fausto and Campbell, 2002). For example, hepatocytes neighboring the portal veins are mostly involved with glycogenolysis and gluconeogenesis while the hepatocytes proximal to the central vein express glutamine synthetase (GS).

In addition to the hepatocytes' location within the lobule, a spatial dimension (that of the plasma membrane orientation) further imposes functional heterogeneity. With respect to the hepatocyte's plasma membrane surface area, 50% contacts other hepatocytes, 37% contacts the sinusoidal space, and 13% contacts the bile canicular domain (Weibel et al., 1969). As such, the parenchymal hepatocytes are exposed to diverse cues from the extracellular microenvironment and must respond accordingly to maintain homeostasis. In order to perform their various functions, the hepatocytes are equipped with a large number of organelles: 1000 mitochondria, 300 lysosomes, 300 peroxisomes and 50 Golgi apparatus (Reddy and Rau, 1987). As a consequence of this diversity, hepatocytes have unique cellular properties that may be implicated in participating in breast cancer metastatic dormancy and emergence.

1.2.3 Non-parenchymal hepatic cells

The non-parenchymal hepatic cells (NPCs) consist of all the resident liver cells except for the hepatocytes. The major NPC types include: liver sinusoidal endothelial cells (LSEC) lining the

sinusoids), macrophage-like kupffer cells (KC) and fibroblast-like stellate cells (SC). Although NPCs contribute less than 10% of the liver volume, they represent approximately 40% of the total liver cells by number (Kmiec, 2001).

The liver sinusoidal endothelial cells form a fenestrated barrier between the parenchymal hepatocytes and the sinusoids and are therefore largely implicated in filtration functions. However LSECs are involved in regulating the hepatic microenvironment as they are highly endocytic for components such as collagen, fibronectin, and hyaluronate that can change their activated state and function (Kmiec, 2001). LSECs can also secrete factors into the extracellular matrix.

Kupffer cells are located intrasinusoidally and predominantly function as macrophage-like cells. KCs are involved in helping to mitigate the inflammation response in large part by secreting factors such as TNF- α and reactive oxygen species. KCs can overshoot their inflammation management functions and participate in liver injury especially by exposure to bacterial endotoxins such as lipopolysaccharide (Kmiec, 2001).

Hepatic stellate cells are located perisinusoidally. In their normal state, SCs align with the LSECs and assist with sinusoidal contraction. Hepatocyte damage can prompt SCs to transform into myofibroblast-like cells that can mediate fibrosis.

It is evident that the hepatic non-parenchymal cells are capable of secreting factors into the metastatic niche that could be capable of inducing metastatic dormancy or emergence from dormancy, and so they are also a focus of this thesis.

1.2.4 Hepatic injury and stress response

By the biologic nature of hepatic function, the liver is under continuous challenge from circulating toxins, metabolic stressors, and infections from bacterial or viral origins. The liver has thus adapted a complex and tightly orchestrated system to either maintain a homeostatic environment or to quickly repair itself when challenges become more severe. Hepatic stress response pathways are consequential to understanding metastasis because of the inherent nature of disseminated carcinoma cells eliciting such a response by at least their physical presence. For example, it's been well documented that a hepatic inflammation response can trigger the up-regulation of cell adhesion molecules among liver sinusoidal endothelial cells conferring enhanced ability to bind to carcinoma cells (Brodt et al., 1997; Bresalier et al., 1998). So it becomes paradoxical that both the normal state of the liver as well as the hepatic stress response pathways can both inhibit and assist metastatic development. Resolving this paradox may greatly contribute to early metastatic detection and lead to new treatments and is a key focus of my investigations.

To better understand this liver reparation pathway, partial hepatectomies have been performed on rat livers in order to disrupt the hepatic parenchyma and to study what mechanisms and in what sequence those mechanisms are initiated for liver regeneration and repair. A mini-review by Dr. George Michalopoulos in 2007 describes this pathway in rodent models in great detail (Figure 2). First, the periportal hepatocytes proliferate triggering a proliferation cascade toward the pericentral region of each liver lobule. Next the non-parenchymal cells replicate starting with the liver sinusoidal endothelial cells, but not until the hepatocytes have largely completed their proliferation. Stellate cell proliferation follows the endothelial cells that provide for the reestablishment of the extracellular matrix.

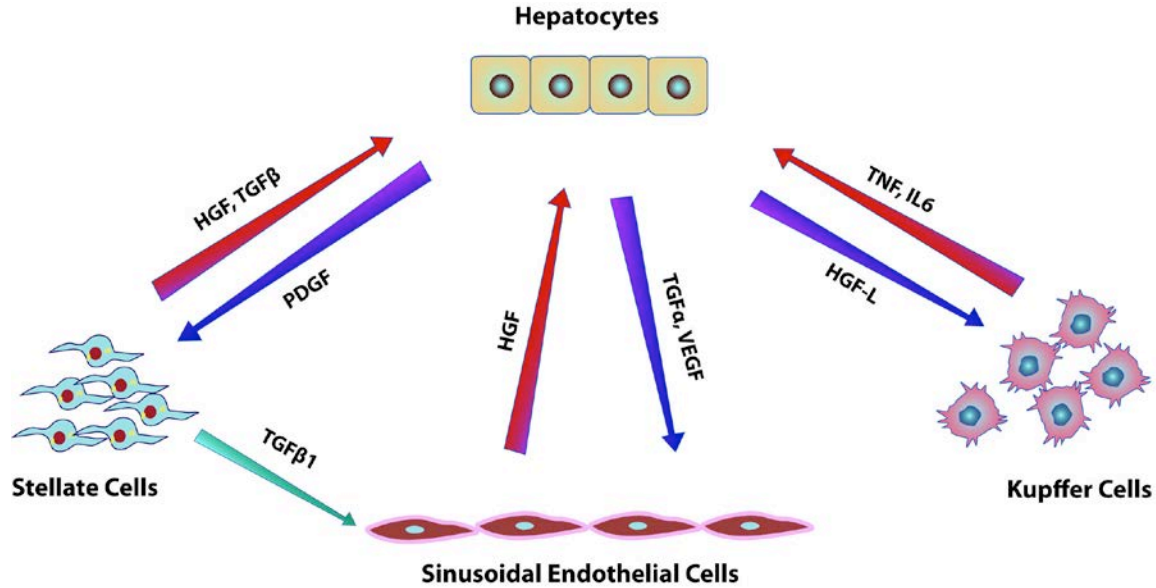


Figure 2. NPC cell signaling within a remodeling liver (adapted from Michalopoulos, 2007). Paracrine signaling among hepatocytes and non-parenchymal cells is triggered through tight temporal control. Hepatic stress response signaling is also maintained between non-parenchymal cells such as TGF-β1 from stellate cells to liver sinusoidal endothelial cells. This physiologic signaling cascade may contribute to ectopic breast cancer cell dormancy and emergence given carcinoma response from cytokines such as TGF-β1 may differ in the metastatic niche versus the primary tumor microenvironment.

Regaining the normal liver weight takes approximately 7 days in rat and 14 days in humans. Interestingly the regenerated liver lobules are larger with 2-cell hepatic plates versus the standard 1-cell hepatic plates. Thus, a regenerated hepatic plate would be capable of fully surrounding a disseminated breast cancer cell without exposing that cell to the extracellular matrix, neighboring non-parenchymal cells, or soluble factors in the hepatic sinusoids.

Partial hepatectomy induces a cascade of secreted factors that are responsible for signaling the start and end of proliferation (Michalopoulos, 2007). Table 2 below has been adapted from the 2007 Michalopoulos publication detailing many of these secreted factors.

Table 2. Signaling cascade following partial hepatectomy (Phx). A rich diversity of secreted factors from the hepatic niche is dispersed in a predictable, highly-controlled manner. Many of these secreted factors are not found within the primary tumor microenvironment, and so may contribute to disseminated breast cancer cell dormancy, emergence, or apoptosis.

Hours after Phx	Factor
< 1	Beta catenin and Notch in hepatocyte nuclei
< 1	Urokinase activity increases
<1	HGF released from the extracellular matrix
< 1	HGF and EGF receptor activation on the hepatocytes
< 1	MMP9 activation
1 – 24 hours	HGF, IL6, TNF, TGF β 1, and hyalouronic acid increases in plasma circulation
5	Increased STAT3 and NF κ B
1-24	Hepatocytes secrete increased TGF α , FGF1, VEGF, SCF, TGF β 1, and HB-EGF

1.2.5 Metastatic extravasation to the liver

Disseminated carcinoma cells reaching the liver must laboriously navigate through the hepatic sinusoids, offering a chance to become physically lodged or to form heterotypic connections with the endothelial cell lining. Though the liver is a preferential site of breast cancer metastasis, it's been experimentally determined that less than 0.02% of portally-injected carcinoma cells successfully establish metastases in mouse models (Luzzi et al., 1998). The rate-limiting factor in establishing clinically evident metastases has therefore been deduced to be the extended survival or capability of pre-angiogenic carcinoma cells to initiate outgrowth where otherwise the majority of cells perish (Figure 3). Therefore the stage of metastatic extravasation becomes a critical research focus on combatting metastatic disease.

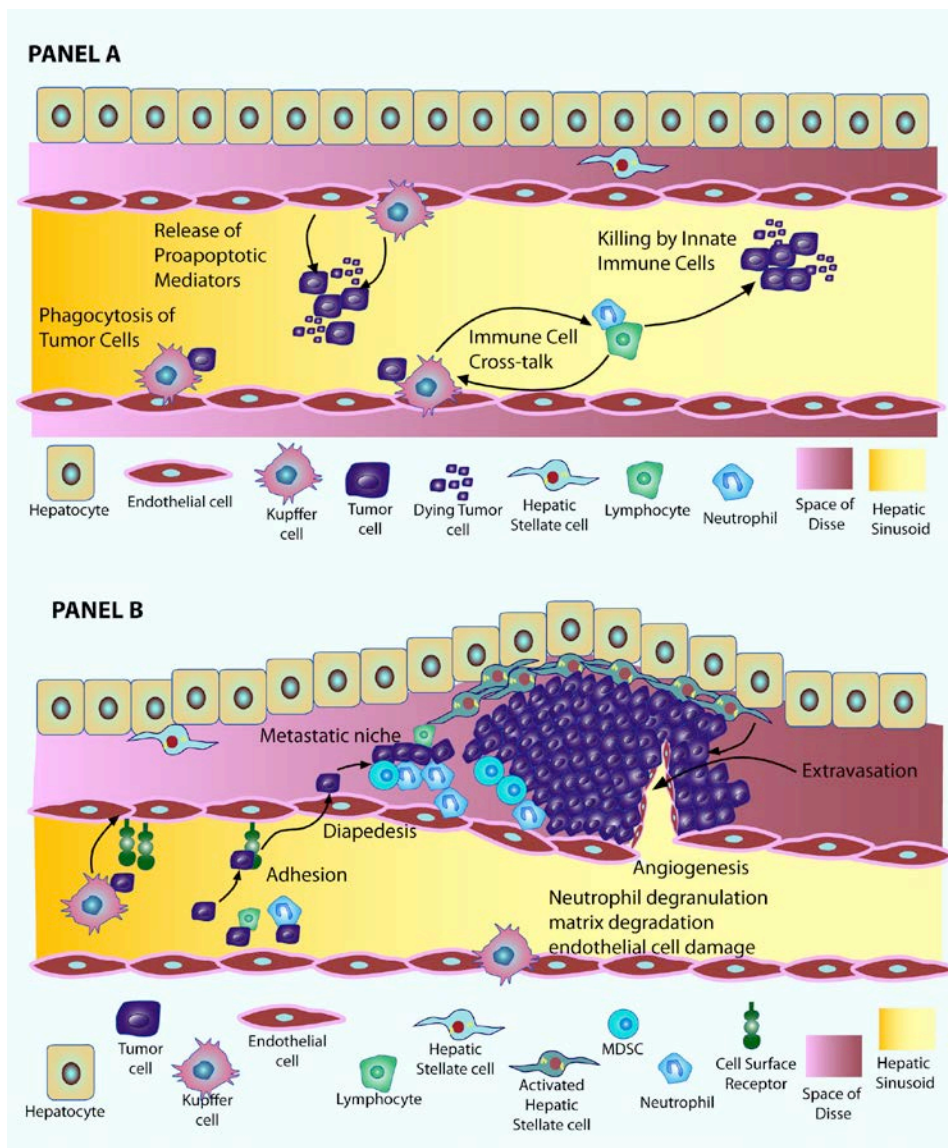


Figure 3. Metastatic seeding and involvement of hepatic non-parenchymal cells (adapted from Van den Eynden et al., 2013). Panel A depicts the body’s natural and uninhibited response to ablating disseminated cancer cells in the hepatic vascular conduits. For example, Kupffer cells perform phagocytosis while liver sinusoidal cells secrete apoptotic signals. Panel B depicts the extravasation process whereby certain carcinoma cells evade the body’s natural response and enable metastatic seeding within the liver microenvironment. This extravasation can trigger the physiologic stress response pathways from the hepatic niche (as depicted in Figure 1) that consequently may trigger dormancy or emergence carcinoma phenotypes.

Carcinoma adhesion to the liver sinusoidal endothelial cells may be important success criteria for metastatic extravasation. Kupffer cells can release cytokines upon being activated by disseminated carcinoma cells which subsequently cross-talk with the LSECs – triggering up-regulation of cell adhesion molecules such as vascular cell adhesion molecule (VCAM-1) or platelet endothelial cell adhesion molecule (PCAM-1). This has been shown to help promote the heterotypic binding of carcinoma cells with the endothelium (Aguste et al., 2007).

1.2.5.1 Mesenchymal-to-epithelial-reverting transition

Clinical examination of primary breast tumors and their associated distant metastases have consistently demonstrated that many of the E-cadherin negative or E-cadherin low primary tumors exhibit membrane-bound E-cadherin positive metastases. This phenomenon is especially true for invasive ductal carcinomas versus the invasive lobular carcinomas where E-cadherin is not membranous, rather, cytosolic (Kowalski et al., 2003). Mesenchymal-to-epithelial-reverting transition (MErT) is characterized by the plasticity of E-cadherin re-expression in the metastatic site from E-cadherin negative primary tumors. MErT can be found in many epithelial-derived cancers (such as prostate) in addition to breast cancer (Yates, 2007). Although the hallmark of MErT is E-cadherin re-expression, the mode of silencing and then re-expressing E-cadherin spans epidermal growth factor receptor activation, transcriptional repression, and epigenetic regulation (Graff et al., 1995; Chaffer et al., 2006; Angelucci et al., 2006).

The highly metastatic and invasive human breast cancer cell line, MDA-MB-231, endogenously expresses very low (to absent) E-cadherin levels and does not form homotypic cell-cell adherens junctions (Benton et al., 2009). The mode of MDA-MB-231 E-cadherin repression is due to hypermethylation of the E-cadherin promoter sequence region; this is an

epigenetic silencing that has since proven to be reversible in co-cultures with primary hepatocytes (Yates, 2007). Additional mechanistic investigations have demonstrated that MErT in MDA-MB-231 cells co-cultured with hepatocytes is a proliferation-dependent process corresponding to the inability to maintain a methylated E-cadherin promoter (Chao et al., 2010). However, the mechanisms driving this process have yet to be discovered.

Molecules that elicit an epithelial phenotype can further characterize MErT. For example, it has been demonstrated that overexpressing profilin-1 in MDA-MB-231 cells induces an epithelial phenotype not through E-cadherin re-expression, but rather through the up-regulation of R-cadherin. This allows for the MDA-MB-231 cells to form adherens junctions through this alternative cadherin family member (Zou et al., 2009).

1.3 BREAST CANCER METASTATIC DORMANCY AND EMERGENCE

The quest for mechanisms that induce metastatic dormancy among disseminated breast cancer cells has been periled with a dearth of direct clinical evidence. Solitary metastatic cells (or micrometastases in sub-angiogenic environments) are not visible by clinical imaging modalities – as these deposits are too small. Common metastatic sites such as the liver, lung, bone and brain are rarely biopsied unless overt metastases are detected. Consequently, catching breast cancer metastases in the act of being dormant in the human condition is not currently feasible, and so the mechanistic study of dormancy is performed through surrogate models.

For those clinical samples where micrometastases were discovered, it has been demonstrated that some of these samples stain low levels of Ki-67 and proliferating cell nuclear

antigen (PCNA) – both markers for proliferation (Reithmuller and Klein, 2001). This implies that those metastases were in a quiescent state of dormancy.

1.3.1 Dormancy mechanisms

The first mechanistic distinction pertains to whether the dormant cells maintain a quiescent state (a G0/G1 cell cycle arrest) or whether they are actively cycling, but are balanced by equal parts proliferation and apoptosis (balanced proliferation). Although balanced proliferation cannot be ruled out, we mathematically modeled the survival probability range in the metastatic niche that would give rise to a dormant phenotype. We discovered that just a one-percentage point survival probability range would invoke dormancy and concluded that dormancy was more likely a consequence of quiescence (Taylor et al., 2013).

A mechanistic explanation for metastatic dormancy is that disseminated breast cancer cells receive signals from the ectopic microenvironment that induce a stress response, subsequently allowing for survival signaling, but failing to permit proliferation. It has been demonstrated in a human epidermoid carcinoma cell line that urokinase type plasminogen activator (uPAR) down-regulation promotes a G0/G1 cell cycle arrest when injected into chick chorioallantoic membranes. The mechanism by which uPAR down-regulation triggers quiescence is through the abrogation of $\alpha 5\beta 1$ signaling which suppresses the extracellular related kinase (ERK) pathway (Aguirre-Ghiso et al., 1999). It has also been shown that the up-regulation of p38 mitogen-activated protein kinase (MAPK) with concurrent reduction in ERK signaling can induce a growth arrest in cancer cells (Ranganathan et al., 2006).

1.3.2 Emergence mechanisms

It is not clear whether emergence from dormancy is a consequence of failing to maintain the dormant mechanism, or whether emergence is initiated by independent mechanisms that overshadow the tonic dormant state.

As discussed herein, the up-regulation of p38 mitogen-activated protein kinase can induce a dormant condition, and it has been previously demonstrated that inhibiting p38 can abrogate the dormant phenotype both within *in vivo* and *in vitro* systems (Aguirre-Ghiso et al., 2004) providing a plausible mechanism and pharmacologic target.

2.0 THE DORMANCY DILEMMA: QUIESCENCE VERSUS BALANCED PROLIFERATION

A Wells^{1,2}, L Griffith⁴, J Wells³, and DP Taylor^{1,2}

Departments of Pathology¹ and Bioengineering², University of Pittsburgh; Taylor Allderdice High School³, Pittsburgh, Pennsylvania; and Department of Biological Engineering⁴, MIT, Cambridge, Massachusetts

Published in Cancer Research. 2013 Jul 1;73(13):3811-6.

2.1 ABSTRACT

Metastatic dissemination with subsequent clinical outgrowth leads to the greatest part of morbidity and mortality from most solid tumors. Even more daunting is that many of these metastatic deposits silently lie undetected, recurring years to decades after primary tumor extirpation by surgery or radiation (termed metastatic dormancy). As primary tumors are frequently curable, a critical focus now turns to preventing the lethal emergence from metastatic dormancy. Current carcinoma treatments include adjuvant therapy intended to kill the cryptic metastatic tumor cells. Because such standard therapies mainly kill cycling cells, this approach carries an implicit assumption that metastatic cells are in the mitogenic cycle. Thus, the pivotal

question arises as to whether clinically occult micrometastases survive in a state of balanced proliferation and death, or whether these cells undergo at least long periods of quiescence marked by cell cycle arrest. The treatment implications are thus obvious—if the carcinoma cells are cycling then therapies should target cycling cells, whereas if cells are quiescent then therapies should either maintain dormancy or be toxic to dormant cells. Because this distinction is paramount to rational therapeutic development and administration, we investigated whether quiescence or balanced proliferation is the most likely etiology underlying metastatic dormancy. We recently published a computer simulation study that determined that balanced proliferation is not the likely driving force and that quiescence most likely participates in metastatic dormancy. As such, a greater emphasis on developing diagnostics and therapeutics for quiescent carcinomas is needed.

2.2 INTRODUCTION TO METASTATIC DORMANCY

Advances in cancer treatment, underpinned by a growing understanding of tumor biology, have rendered the majority of localized solid tumors either curable or controllable. Surgical and radiologic interventions have improved to the point that the initial primary tumor can be extirpated. However, if the primary tumor gives rise to clinically detectable metastatic lesions, current therapies usually only delay mortality and are not curative. Most daunting to patients faced with treatment decisions for disease that is "non-metastatic" at the time of primary tumor diagnosis is that metastatic dissemination may have already occurred despite the primary lesion "being cured" by removal. Many of these metastatic tumors will appear years or more than a decade later, thus termed metastatic dormancy. Although this phenomenon afflicts nearly half of

carcinoma patients that develop metastases (Aguirre-Ghiso, 2007), the cell biology of this remains unknown. Proposed dormancy mechanisms range from cell-cycle arrest, immune function dysregulation, angiogenic insufficiency, stress-related kinase and urokinase receptor imbalance, to tumor/stroma biomechanics (Aguirre-Ghiso et al., 1999; Sosa et al., 2011; Uhr and Panel, 2011; Yu and Ossowski, 1997). Fundamentally, these mechanisms vary between the orthogonally opposed dormancy mechanisms of cellular quiescence or balanced proliferation (mitogenesis equally offset by apoptosis). Spotlighting this difference is critical because therapeutics in the clinic and under development largely target cycling, not quiescent carcinoma cells.

This metastatic dormancy, although present in almost all cancers, is particularly insidious for carcinomas of the mammary gland. For breast cancer, up to one third of small (1 cm or less), noninvasive (or microinvasive) carcinomas with no evidence of metastasis will become evident at distant sites within the decade after diagnosis of the primary tumor (Aguirre-Ghiso, 2007). For this reason, adjuvant chemotherapy, aimed at killing cycling tumor cells, is an option after successful lumpectomy. This adjuvant therapy has been met with limited success for most incarnations of breast carcinoma, as adjuvants reduce metastatic recurrences by only a third (on average) at 10 years (Demicheli et al., 2005). The reasons for this therapeutic failure in breast and other epithelial carcinomas can be summarized by 2 possibilities—the tumors are inherently resistant to the agents used, or the disseminated tumor cells are not cycling (Aguirre-Ghiso, 2007; Brackstone and Townson, 2007).

2.3 PROGNOSTIC ASSAYS FOR METASTATIC DORMANCY

This is the key unknown in metastatic dormancy, whether the clinically silent micrometastases are in a state of balanced proliferation and death or if they exist as mitogenically quiescent (Klein, 2011). The phenotype and genomic fingerprints of the primary tumor often suggest quiescence. Two distinct molecular algorithms are used clinically to predict breast cancer recurrence (<http://www.agendia.com/pages/mammaprint/21.php> and www.oncotypedx.com), and although they do not use the same genes, there is a preponderance of mitosis-related genes that correlate with recurrence consistent with most proposed signatures (Vanet et al., 2011). Furthermore, triple negative (ER-, PR-, HER2 neutral) mammary tumors are generally aggressive, highly proliferative, highly recurrent tumors that are treated with adjuvant chemotherapy but can be considered eliminated (or senescent) if there is no metastatic recurrence after about 3 years. These clinical correlates suggest that the latent tumor cells at the metastatic sites may also have low rates of cycling.

The drawback to these and other current prognostic assays is that the cells examined are from the primary tumor site, where the preponderance of cells likely lacks the necessary traits for successfully seeding, surviving, or expanding in the metastatic microenvironment. Although each step in the metastatic cascade (separation from the primary tumor, intravasation into a conduit, survival in that conduit, extravasation, and finally successful seeding of an ectopic organ) is inefficient, ectopic survival seems to be the most rate-limiting step. Careful enumeration of these stages in animal models shows that it is the establishment of a small number of surviving cells in the metastatic target organ that is the least efficient (Chambers et al., 1995; Kienast et al., 2010). Interestingly, the few cells found weeks after seeding in these animal models were not highly proliferative (Naumov et al., 2002). Still, these are among the few

studies that have examined the early stages of tumor metastasis. Because true human metastatic dormancy (as noted after years to decades) cannot be approached in rodent models (although initial steps of attaining dormancy may be noted in these short-lived animals), it is critical to consider the quiescent behavior of these tumor cells in the human context to direct therapeutic and diagnostic approaches.

2.4 COMPUTER SIMULATION REVEALING QUIESCENCE AS INTEGRAL TO METASTATIC DORMANCY

We recently implemented an *in silico* model to determine the survival probability range that carcinoma micrometastases in a state of balanced proliferation would yield the dormant phenotype (Taylor et al., 2013). Although many other computer simulations have been developed to model metastasis (Haeno and Michor, 2010; Haustein and Schumacher, 2012; Willis et al., 2010), none of these approaches has explored the survival probability requirements of the metastatic niche necessary to confer a dormant phenotype. We used a Markov chain Monte Carlo approach that sampled from a probability distribution to assign either a divide or die condition to each cell in each simulated metastasis. Survival probabilities were assigned ranging from 30% to 70% with an additional stochastic 10-percentage-point probability adjustment at each sampling. So for example, at 40% survival probability, metastatic cells would survive between 30% and 50% of the time, thus providing an additional alignment to the fluxing survival conditions of the metastatic niche. We assumed that any given patient could have 1,000 independent metastatic deposits at the time of primary tumor removal. By defining active cycling as a 3- to 5-day mitogenic window, 1,218 cycles was equated to a 5- to 10-year metastatic

dormancy before the metastases reached the clinically detectable level of one million cells or more. By traversing the survival probability from 30% to 70% during each cycle, we identified the boundary conditions at which any micrometastases might remain in a dormant phenotype over the entire time period (without any metastases in that "peron" clinically emerging). Surprisingly, this survival probability window was narrow, being only about 1 percentage point wide, from a probability of 49.7% to 50.8% (Fig. 4). Even more interesting, the width of this survival probability was independent of the assumed starting size of the micrometastases (1–8 starting cells).

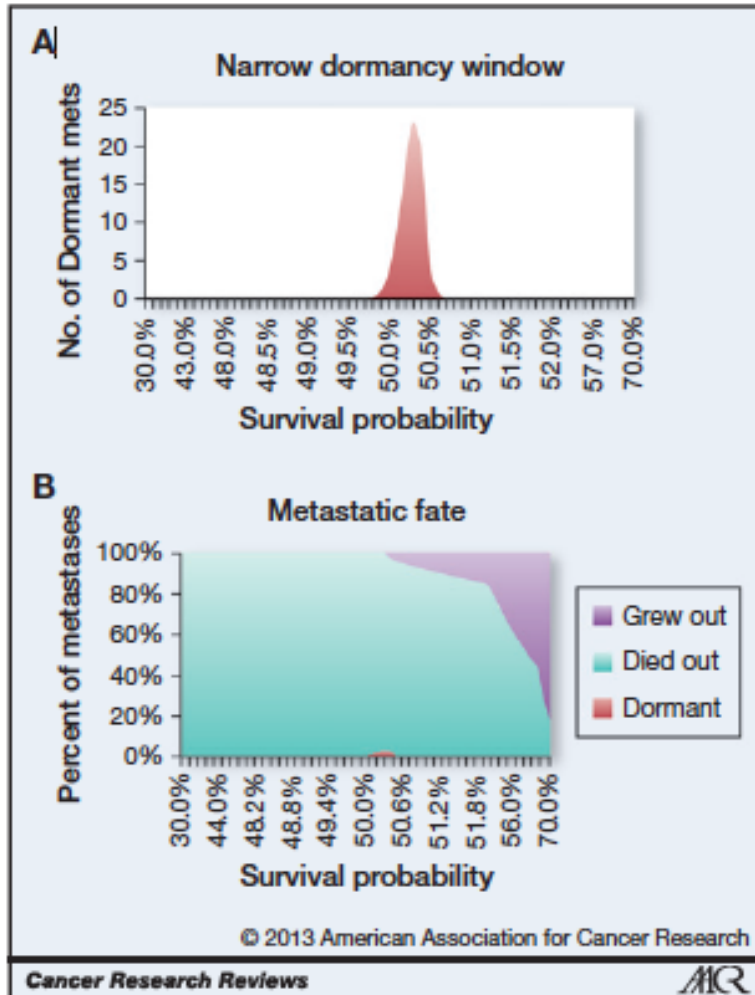


Figure 4. Probability of dormancy from *in silico* simulation. Dormancy is defined by a metastasis achieving 1,218 cycles while having a cell number greater than 0 and below 1 million. The simulated balanced proliferation yields a dormant phenotype for patients harboring 1,000 cryptic micrometastases only between 49.7% and 50.8% survival probability regardless of starting cell number in the micrometastasis. A, the absolute number of dormant metastases at the end of the 1,218 cycles for a starting number of 2 cells per micrometastasis. B, the metastatic fate for each of the survival probabilities showing that same dormancy window (in red). The green area shows that the majority of metastases die out even at survival probabilities approaching 60%. Metastases that become clinically evident (exceed 1 million cells) are shown in purple.

Although it is generally accepted that solitary, extravasated cells initiate metastases and may become quiescent, we also simulated a burst of proliferation before establishment of a micrometastasis by modeling metastases starting at 2,000 cells. Although these larger starting metastases maintained the dormant phenotype, the survival probability window remained the same 1 percentage point. At survival percentages even just slightly lower than 49%, all micrometastases rapidly died out, and by 55% there was rapid outgrowth of clinical metastases (<100 cycles to exceed one million cells) that were more indicative of progressive metastatic disease. This suggested (at least theoretically) that it would be unlikely during extended human clinical dormancy that the tumor cells would exclusively exist in a state of continuous cycling with matched cell death (balanced proliferation).

This analysis assumed a homogenous population behavior (divide or die at each cycle) even though the survival probabilities were stochastic at any given cycle for each metastatic cell. The remarkably small probability window for dormancy in a balanced proliferation/death model holds from at least 1 to 2,000 starting cells. Obviously, if we significantly extended the cycle time beyond 72 hours or introduced intermissions into cycling, the probability window would broaden slightly; however, this would merely reinforce the finding that balanced proliferation and death are not likely the sole mechanism for metastatic dormancy. It should be noted that the model does not account for the processes leading to micrometastatic establishment (escape, transit, extravasation, etc.), nor does it address the starting point for quiescence, nor determine that the quiescent state is uninterrupted. These issues are to be addressed in further modeling studies. Although this model has shortcomings as noted here and in the original article (including that simulated metastases do not spawn secondary metastases), that such a narrow survival probability was defined is highly suggestive of a critical role for quiescence. Although

this model was not designed to statistically reject a null hypothesis that balanced proliferation plays a dominant role in metastatic dormancy, that only a single, narrow, and contiguous survival probability led to metastatic dormancy does not reasonably align with our biologic understanding of the metastable nature of the metastatic niche (unless the cells undergo periods of quiescence). A conceptually different invocation of additional events for metastatic emergence, such as angiogenesis or failure of suppressive events to allow for further metastatic growth (Uhr and Pantel, 2011; Hanahan and Folkman, 1996; Naumov et al., 2008), only invokes the trigger for quiescence but does not alter the idea that for extended tumor dormancy, the micrometastatic cells likely undergo mitogenic quiescence for at least extended periods.

2.5 IN VIVO INVESTIGATIONS INTO METASTATIC DORMANCY

The question arises as to whether dormant metastases that undergo cellular quiescence align with clinical and experimental findings. Studies that directly examine dormant micrometastases are few and hampered by the lack of clinical samples or limitations of experimental systems (Uhr and Pantel, 2011; Brackstone and Townson, 2007). From the experimental side, there have been a number of interventions to regulate cellular quiescence and determine the effects on tumor growth and persistence in host animals (Chatterjee and vanGolen, 2011; Kobayashi et al., 2011; Marshall et al., 2012). The outcomes and correlation of low proliferative rate with metastatic dormancy are consistent with a cellular quiescence hypothesis rather than balanced proliferation. Furthermore, the conversion of micrometastatic cells from a mesenchymal phenotype to a more epithelial one (Chao et al., 2010; Yates et al., 2007; Yates et al., 2007) also is supportive as these epithelioid tumor cells tend to have a reduced mitogenic rate. Additional support comes from

recent *in vivo* work that showed that TGF- β receptor blockade prevents dormancy by microenvironmental bone morphogenetic proteins (Gao et al., 2012). In fact, the authors identified a genetic signature that is predictive of breast cancer organotropism to lung versus other common metastatic sites such as liver and brain.

Another open question concerns that state at which disseminated tumor cells enter dormancy. Although the angiogenic switch model implies a later event after the micrometastasis goes through numerous cell cycles, others suggest a very early event, possibly at the single-cell level (Gao et al., 2012). Work by D.R. Welch and others has investigated single-cell metastatic dormancy *in vivo* and provides insights into mechanisms such as breast cancer metastasis suppressor 1 (BRMS1) and kisspeptin (KISS1; refs. Hurst et al., 2009; Nash et al., 2007; Phadke et al., 2008). These provide mechanistic bases to the earlier work that counted solitary cells surviving in ectopic sites (Chambers et al., 1995). However, in these experiments it is not clear whether these persisting disseminated cancer cells give rise to the later outgrowth. Regardless, the model tested showed the same narrow probability range whether the initially established micrometastatic nodule contained 1 or up to 2,000 cells; only the number of dormant metastases varied based on cell number (Taylor et al., 2013).

The human observations are also consistent with the cellular quiescence model. Disseminated tumor cells isolated from bone marrow even after removal of the primary lesion have been found to have low proliferation rates by mitogenic markers and low to undetectable levels of activated AKT as a key signaling nexus in tumor cell mitogenesis (Pantel et al., 1993; Balz et al., 2012). Still, these singular cells in bone marrow are not the micrometastatic foci one might consider as potentially emergent. Unfortunately, such early small lesions are not often observed and studied in human patients. However, where data have been gathered, it has been

found that such tumor foci are often highly epithelial and morphologically quiescent rather than the mesenchymal-like phenotype displayed by their paired primary lesions (Imai et al., 2004; Kowalski et al., 2003; Chao et al., 2012).

Work on defining metastatic dormancy signatures provides fodder for both cellular quiescence and externally constrained growth (balanced proliferation). For instance, an angiogenic signature predicted tumor outgrowth in a mouse model (Almog et al., 2009), whereas G0-like quiescence was noted in a squamous carcinoma xenograft model (Adam et al., 2009). Combining such mouse model and in vitro networks derived from arrested cells, a 49-gene signature emerged that correlated with clinical dormancy in a retrospective analysis of human mammary carcinomas (Kim et al., 2012). These genetic signatures might be predictive of metastatic dormancy in the human condition and serve as a foundation to explore mechanisms to either maintain metastatic dormancy or induce emergence.

Another data set from which we may draw conclusions relates to the seeming chemoresistance of micrometastases. This can be due to cellular quiescence, inherent chemoresistance, resistance due to the microenvironment (signals or privileged site), or a combination of the preceding; or even simply an artifact of observation. Artifactual observations can arise from the inherent nature of logarithmic doubling in which an impressive 99% reduction in cell number would translate to only a 2-week delay during the emergent phase of tumor cell outgrowth. However, studies have shown that metastatic cells are relatively more chemoresistant than paired primaries when challenged with a range of therapies due to the combination of microenvironmental signals and inherent cell properties (Fridman et al., 1990; Tanaka et al., 2010; Chao et al., 2012; Lin et al., 2010). It also must be noted that non-cycling or quiescent cells are generally more resistant to killing by a variety of insults including chemotherapies, and

although this is not likely the sole reason for the resistance of metastases, mitogenic quiescence would be contributory. Still, the clinical experience suggests that in most carcinomas, chemotherapy rarely cures clinically evident metastases but rather reduces the tumor burden and prolongs life. However, the integration of the experimental and observational findings to date suggest that the cellular quiescence model is consistent with clinical dormancy, but these suggestions fall short of being convincing.

What is needed is a comprehensive approach to metastatic dormancy in which the cellular processes can be evaluated longitudinally, and in real time (Figure 5).

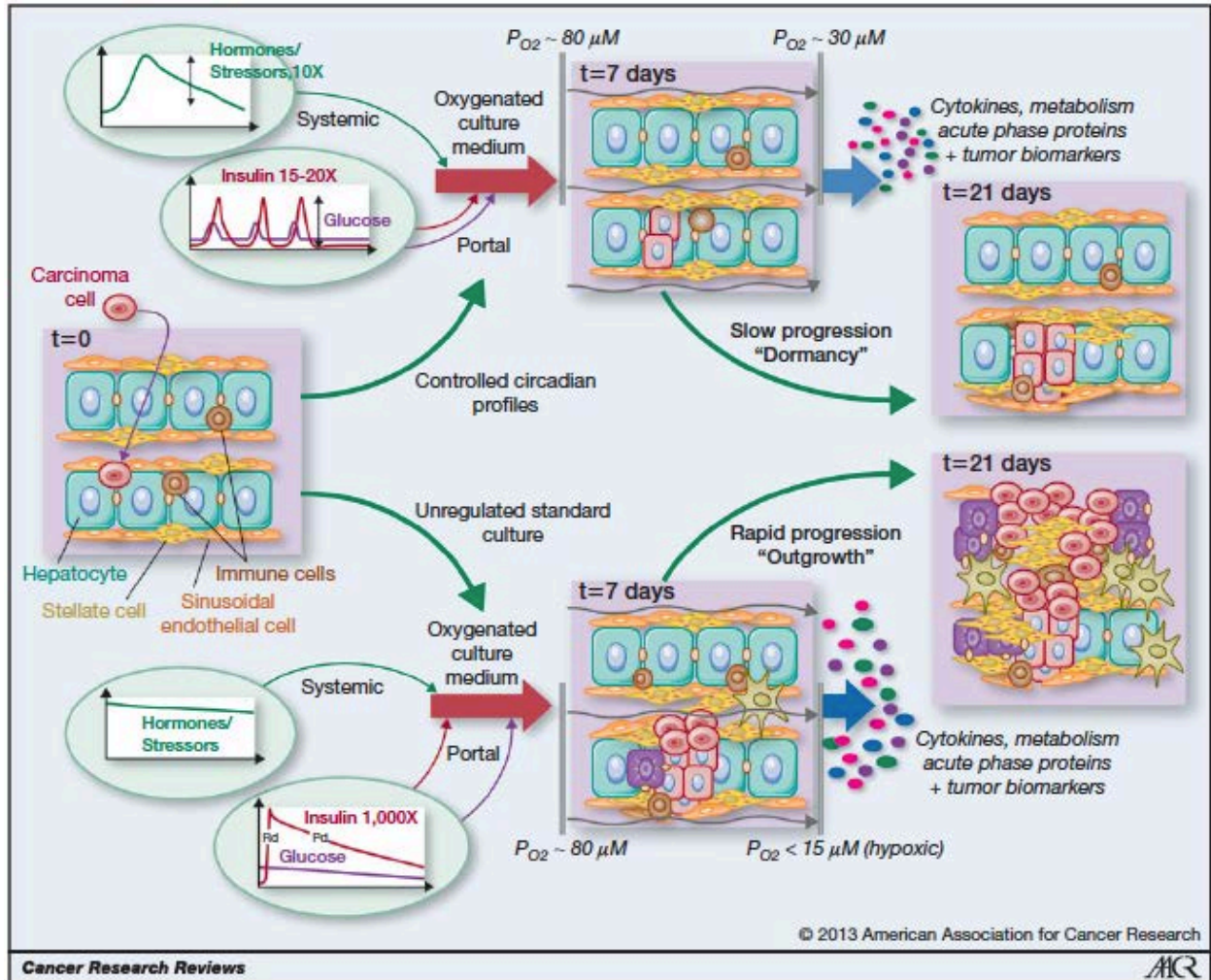


Figure 5. Schematic of an approach to study metastatic dormancy. The development of microphysiologic systems such as organotypic bioreactors allows for the examination of cellular events in metastatic seeding and entry into dormancy or continuous outgrowth for a multiweek period (Griffith & Swartz, 2006). Shown is a cartoon depicting the fate of the micrometastasis following from the host tissue being in a more physiologic state (upper pathway) versus a stressed, inflamed, or fibrotic organ (lower pathway). The stressed pathway prohibits micrometastases from entering dormancy while supporting emergence into frank metastases.

True appreciation of the full span of metastatic dormancy requires human patients due to the time length of the phenomenon and the spontaneous nature of such metastases that confound the existing experimental models (Klein, 2011). However, attempts have been made to use the human patient as an experimental system by examining disseminated tumor cells found in bone marrow and circulation (Uhr and Pantel, 2011). Given the relative abundance of such cells, coupled with the rarity of actual emergent metastases, it is quite possible that the vast majority of these cells are pre-senescent or pre-apoptotic and thus not representative of dormant micrometastases. Rather, one would desire intravital imaging of human micrometastases, a capability for which advances in positron emission tomography and other imaging modalities are striving. However, this is currently not available, and one could envision that the putative cellular quiescence would defeat efficient labeling and detection of such micrometastases.

2.6 MICROPHYSIOLOGIC THREE-DIMENSIONAL BIOREACTORS TO STUDY METASTATIC DORMANCY

We are taking a different approach to examining the early stages of metastatic seeding and dormancy in an all-human microphysiologic bioreactor (ref. Yates et al., 2007; Fig. 2). This *ex vivo* system allows for metastatic seeding and entry into dormancy to be examined at a cellular level for up to several weeks. This approach exceeds the hours-long window possible in animal models (Kienast et al., 2010; Luzzi et al., 1998; Wyckoff et al., 2000) and is beneficial over the random terminal endpoints of long-term metastasis studies in animals and humans. Even with the limitations of having incomplete vascular and immune systems and lacking neural innervation, this system provides for the complex multicellular and matrix interactions within the metastatic

niche comprising human cells. In this manner, one can determine whether tumor cells can enter cellular quiescence. Initial work suggests that cellular quiescence or entry into dormancy is finely regulated and dependent on numerous factors, including tissue rheology, fluid and blood flow, oxygen tension, and nutrient and hormone levels. For instance, a stiff supporting matrix, possibly representative of fibrosis, drives carcinoma cells toward progressive metastatic growth; this may underlie the puzzling phenomenon of cells that attain at least short-term dormancy in vivo growing in 3-dimensional cultures in vitro. Although there are other systems with which to probe dormancy, we are providing this on a template for discussion.

2.7 CONCLUSIONS

The real importance of determining whether the balanced proliferation or cellular quiescence model holds sway is the therapeutic implications of such. Proliferating cells allow for a distinct set of agents and strategies; mainly the routine chemotherapies could be valuable as they target mainly cycling cells. However, if the metastatic cells are quiescent (in a G0 or G1 state), these agents would likely not be efficacious. Therefore, strategies should then be aimed not just at extirpating the cells but also could be designed to keep the cells in a state of indolent dormancy. In fact, generalized toxic therapies might actually be detrimental as the collateral damage to the parenchymal or stromal cells may lead to an inflammatory state; there are suggestions that such an inflammatory milieu may "awaken" the surrounding dormant micrometastases. In such a situation, adjuvant chemotherapy may not only be contraindicated due to toxicity but also due to shortening overall patient survival. Thus, the critical question as to whether the micrometastatic

cells are in a state of quiescence or balanced proliferation is the key to dealing with tumor dormancy and should be at the forefront of new approaches to tumor management.

3.0 MODELING BOUNDARY CONDITIONS FOR BALANCED PROLIFERATION IN METASTATIC LATENCY

Donald P Taylor^{1,2}, Jakob Z Wells⁴, Andrej Savol³, Chakra Chennubhotla³, Alan Wells^{1,2}

Departments of Bioengineering¹, Pathology², and Computational and Systems Biology³,
University of Pittsburgh, Pittsburgh, Pennsylvania, USA and Taylor Allderdice High School⁴,
Pittsburgh, PA, USA

Published in Clinical Cancer Research. 2013 Mar 1;19(5):1063-70.

3.1 ABSTRACT

Purpose: Nearly half of cancer metastases become clinically evident five or more years after primary tumor treatment; thus, metastatic cells survived without emerging for extended periods. This dormancy has been explained by at least two countervailing scenarios: cellular quiescence and balanced proliferation; these entail dichotomous mechanistic etiologies. To examine the boundary parameters for balanced proliferation, we conducted in silico modeling.

Experimental Design: To illuminate the balanced proliferation hypothesis, we explored the specific boundary probabilities under which proliferating micrometastases would remain

dormant. A two-state Markov chain Monte Carlo model simulated micrometastatic proliferation and death according to stochastic survival probabilities. We varied these probabilities across 100 simulated patients each with 1,000 metastatic deposits and documented whether the micrometastases exceeded one million cells, died out, or remained dormant (survived 1,218 generations).

Results: The simulations revealed a narrow survival probability window (49.7–50.8%) that allowed for dormancy across a range of starting cell numbers, and even then for only a small fraction of micrometastases. The majority of micrometastases died out quickly even at survival probabilities that led to rapid emergence of a subset of micrometastases. Within dormant metastases, cell populations depended sensitively on small survival probability increments.

Conclusions: Metastatic dormancy as explained solely by balanced proliferation is bounded by very tight survival probabilities. Considering the far larger survival variability thought to attend fluxing microenvironments, it is more probable that these micrometastatic nodules undergo at least periods of quiescence rather than exclusively being controlled by balanced proliferation.

3.2 TRANSLATIONAL RELEVANCE

Dormancy of metastases constitutes an ominous unknown for cancer patients—should there be adjuvant treatment or not. The call for therapy and selection of type of therapy should rationally depend on the biological properties of metastatic cells. If the cells in these clinically silent micrometastases are in a state of balanced proliferation and death, then agents targeting cycling cells are appropriate. However, if the cells are quiescent, then other approaches, or none, are

appropriate. As clinical data are scarce, and experimental systems are not established to study this directly, we used an unbiased in silico model to identify the boundary condition probabilities that would allow for micrometastases to remain dormant for 5 to 10 years even while undergoing regular cell cycling. The resultant tight one percentage point range suggests that the metastatic cells likely undergo at least periods of quiescence. This would suggest that for longer-term dormancy, novel approaches need to be developed.

3.3 INTRODUCTION

The dormancy dilemma impacts millions of cancer patients worldwide. Certain epithelial carcinomas such as from breast or prostate tissues can recur years or decades after primary tumor ablation (Naumov et al., 2002). This late recurrence afflicts nearly 50% of breast cancer patients that develop metastases; other carcinomas exhibit similar late recurrence rates (Aguirre-Ghiso, 2007). This recurrence is most problematic within metastatic organs such as the liver, lung, bone, and brain where tumor resection may not be possible and chemotherapeutic agents seem to be ineffective in most cases (Fisher et al., 2002; Townson et al., 2006). For instance, aggressive treatment (e.g., adjuvant chemotherapy) of breast cancer after surgical removal of the evident primary tumor may reduce 10-year recurrence by less than one third. Consequently, ostensibly cured cancer patients harbor unseen metastases for decades that eventually emerge into untreatable, lethal tumors. This long period between primary tumor treatment and metastatic appearance is referred to as metastatic latency though the tumor cell behavior during this period is unknown.

Metastatic latency allows disseminated tumor cells to avoid clinical detection and withstand aggressive and toxic neoadjuvant treatment (Aguirre-Ghiso, 2006). How the disseminated carcinoma cells maintained a long-term, clinically undetectable state in an ectopic site such as the liver is unknown (Wells et al., 2008). Although extravasation of carcinoma cells from the primary tumor is common, but most of these cells seem not to establish metastases (Luzzi et al., 1998; Mocellin et al., 2006), it is likely that the pre-metastatic microenvironment contributes to whether carcinoma cells will seed, survive, and either proliferate to prompt tumor formation or exhibit a dormant phenotype.

Because *in vitro* and *in vivo* experimental systems are not sufficiently malleable to consistently and reliably recapitulate the metastatic latency phenotype, *in silico* models have evolved to explore the mechanisms of metastatic competency, dormancy, and emergence (Jiao et al., 2011; Antal et al., 2012; LaPorta et al., 2012). Many of these *in silico* models predominately simulate metastatic latency according to the theory of balanced proliferation among micrometastases of greater than one million cells. Therefore, they introduce various biological factors such as angiogenesis, immune response, hypoxia, and growth factor availability and deduce through partial differential equations what impact these have on the ability for the micrometastases to emerge or maintain a dormant state. A major limitation to this approach is that little empirical biological data are available to make these models translatable to the *in vivo* response. Moreover, such studies often assume that latent metastases experience balanced proliferation, meaning additional biological data, even if available, would not resolve latency as being due to balanced proliferation, cellular quiescence, or a combination of both.

Notwithstanding these limitations, *in silico* models are becoming increasingly important to offering insights in prioritizing the landscape of contributing metastatic factors. By using an

Approximate Bayesian Computation model applied to empirical patient data Willis and colleagues inferred that metastatic breast cancer late relapse evolved from just 1 to 6 micrometastases that escape from dormancy (Willis et al., 2010). Other approaches used the Gompertzian growth function to calculate periods of metastatic growth and growth arrest to fit clinical data as presented in the Munich Cancer Registry (Haustein and Schumacher, 2012). These results predicted that metastatic seeding occurred before the clinical detectability of the primary tumors. Computational models have also been used to predict the metastatic response according to primary tumor removal and front line chemotherapy (Haeno and Michor, 2010).

Biologically, the issue of metastatic dormancy has been approached as balanced proliferation and death, quiescence, or a combination of both. In arguing for balanced proliferation and death, investigators invoke various constraints, such as the "angiogenic switch," before which the metastatic nodule is constrained to a certain mass in the absence of a vascular supply (Aguirre-Ghiso, 2007; Naumov et al., 2006). In other considerations, multiple feedback mechanisms are invoked to maintain a small, but cycling cell population (Marshall et al., 2012). The cellular and/or molecular mechanisms behind tumor dormancy present with an absence of solid clinical data, although emerging evidence of phenotypic plasticity suggests some other possible routes to dormancy and may suggest quiescence of the disseminated tumor cells.

Thus, the situation remains unsettled as to which behavior predominates during these latent periods. To take an unbiased approach, we modeled metastatic growth dynamics by invoking a 2 state, Markov chain Monte Carlo (MCMC) simulation where only cell-survival probability and starting metastasis populations were varied. As depicted in Fig. 6, the MCMC method assigns a survival probability for each cell in each metastasis during each replication cycle.

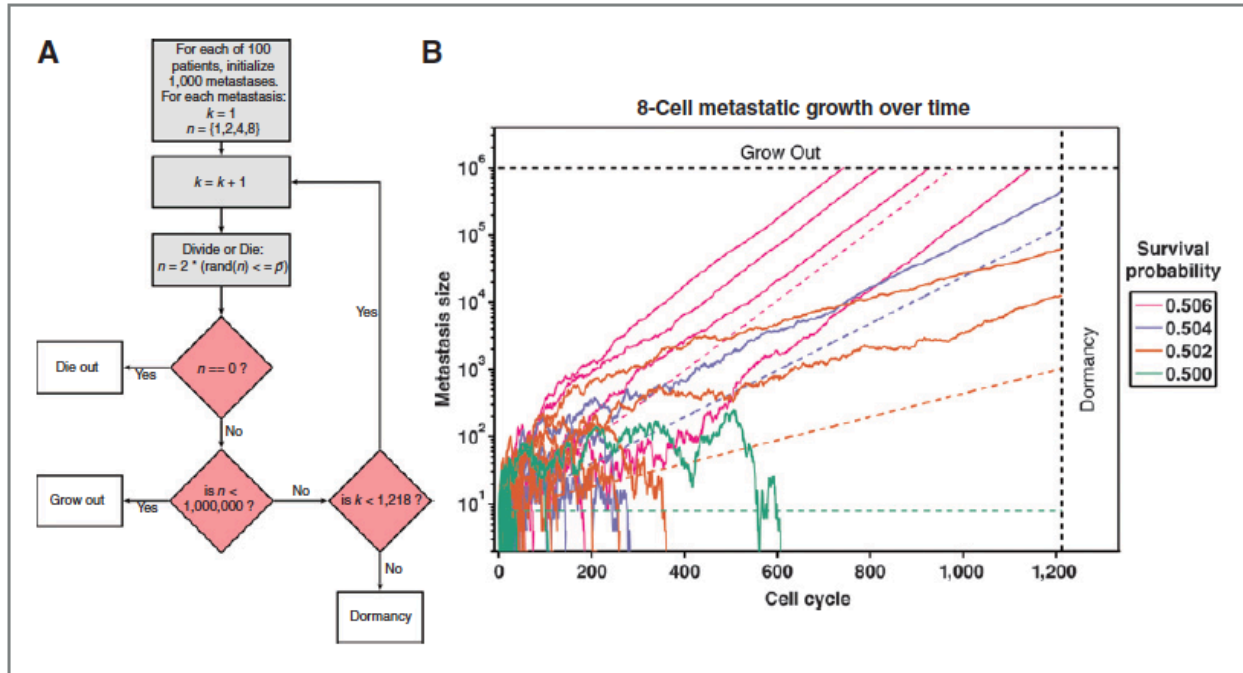


Figure 6. Metastatic cell fates are determined via a Markov chain Monte Carlo method developed in the Matlab programming environment. A, the simulation's progression starting with 1,000 metastases initialized for each of the 100 patients. Within each simulation, there exists a starting cell number denoted by n (1, 2, 4, or 8) across survival probabilities ranging from 30% to 70%. Starting with the first cell cycle (denoted by k) a random number is generated and compared with the survival probability. If n is equal to 0, the metastasis dies out, and the next metastasis simulation (up to 1,000) begins. If n reaches 1 million, the metastasis is assumed to grow out to be clinically evident. If k reaches 1,218 while n is greater than 0, the metastasis goes dormant. B, traces the fate of 100 individual metastases across 4 survival probabilities, showing the variability in metastatic progression. Once metastases reach approximately 1,000 cells, the growth rate equals the expected growth rate as depicted by the dotted lines.

Cells will then either proliferate or die as statistically influenced by the survival probabilities allowing for metastases to exhibit a range of outcomes not predetermined. If metastatic dormancy can emerge across a wide spectrum of survival probabilities then balanced proliferation may be the dominant contributor. However, if the latent phenotype via balanced proliferation is only manifest within a narrow probability window we propose that cellular quiescence would likely participate nontrivially in protracted metastatic survival.

3.4 MATERIALS AND METHODS

3.4.1 MCMC model overview

MCMC simulation is a computational method that samples from a probability distribution to assign system outcomes commensurate with the underlying distribution (Dodds et al., 2004). This model is described as a branching process whereby each cell in cell cycle k will randomly give rise to 0 or 2 cells in the $k + 1$ cell cycle. We applied MCMC simulation as a means to model the fate of extravasated circulating tumor cells into the metastatic site. We developed 2 MCMC approaches to assign cell fates (Fig. 6). The first, a fixed probability model, assigned static survival probabilities to every cell in each metastatic nodule; the probability of survival for each individual cell was not dependent on the other cells in that metastatic nodule (Fig. 6).

The second approach incorporated a stochastic element where the survival probability for any given cell was sampled randomly between 10 percentage points around the specified mean survival probability for the group. We refer to this variable probability as P where appropriate to distinguish it from the assigned probability P . All results herein were developed from the second,

stochastic model, diagrammed in Fig. 1A. Both formulations, however, are examples of branching processes, which allow for convenient analytic expressions for some aspects of tumor behavior. In our 2-state MCMC system, every cell in each metastasis could either divide or die per cell cycle, thus mimicking the balanced proliferation phenotype. Notably, cells were individually assigned a new survival probability at each cycle with the stochastically assigned probability adjustment within 10 percentage points above or below the initially assigned survival probability. For example, simulations at a fixed 60% survival probability will allow for random fluctuations between 50% and 70% survival. Although these survival probabilities coalesced to the expected means, this additional percentage point adjustment further imitated the dynamic survival conditions of the metastatic niche.

These simulated micrometastases could devolve to 0 cells (died out), exceed 1 million cells (clinical metastasis) or exceed 1,218 cycles with fewer than 1 million cells (dormant). Our data represent 100 compiled patient trials (100,000 micrometastases) for each combination of cell survival rate and starting cell number. For the progressive clinical metastases, we capture the range of cycles at which this occurred. For the dormant metastases we document the mean cell numbers at the time of dormancy. Although this model does not achieve pseudo-equilibrium given all simulated metastases terminate under one of 3 conditions, dormancy is nonetheless modeled by means of achieving neither the 0 or 1 million cell boundary before reaching 1,218 cycles; although it is likely that should there be no cycle limit, the cell boundaries will be reached.

3.4.2 Assumptions

We simulated patients in groups of 100 person cohorts across a matrix of cell survival probabilities (0.3 to 0.7, given as percentages) and number of initially extravasated cells. For each patient we modeled 1,000 carcinoma deposits to the metastatic organ at the time of primary tumor resection. The probability of an outgrowth is based on individual micrometastasis and not on patient load of total micrometastases. Each deposit started with 1, 2, 4, or 8 cells (later at 1,000 and 4,000 cells for boundary validation) to separate initial extravasation and seeding from subsequent metastatic behavior. We also assumed a one-and-one-half to 3-day cell cycle so that 1,218 cell cycles represented 5 to ten person years (dormancy) at a cycle time of 1.5 to 3 days per mitosis. Micrometastases that grew beyond 1 million cells were classified as approaching clinically evident and were not simulated further. Finally, we assumed that the initial 1,000 micrometastatic deposits did not give rise to additional deposits and were free to either die out, grow out to greater than 1 million cells, or become dormant. Representative traces of micrometastatic-tumor growth for 4 survival probabilities (0.500, 0.502, 0.504, and 0.506) are shown in Fig. 6B.

3.5 RESULTS

3.5.1 Survival after metastatic extravasation is rate limiting

The metastatic fate across all simulated patient trials for 1, 2, 4, and 8 cell starting metastases revealed that the majority of metastases died out until the survival probability exceeded 60%

(Fig. 7). Sampled time courses of metastatic tumor growth illustrate this phenomenon, even for probabilities above 50% (Fig. 6B).

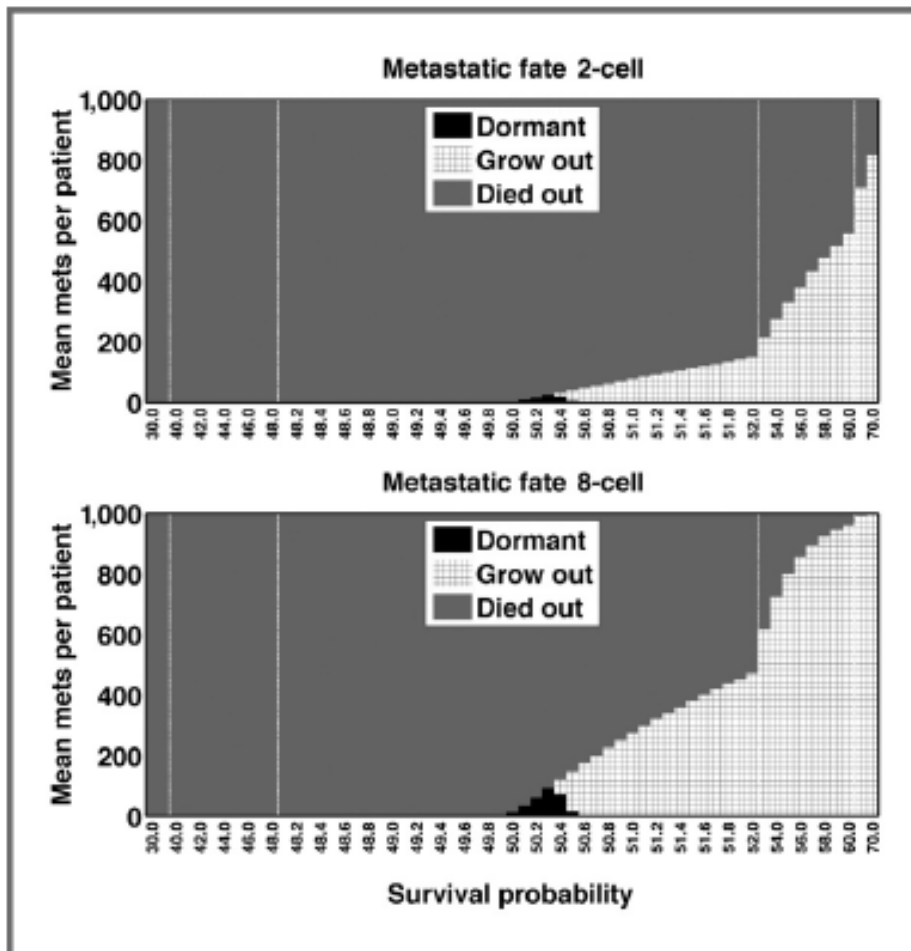


Figure 7. Metastatic fate for 2-cell Metastatic fate for 2-cell (top) and 8-cell (bottom) starting metastases followed identical trends with the majority of metastases dying out. The metastatic fate is coded with black designating the metastases that remained dormant, gray the ones that died out, and patterned those that grew out. X-axis represents survival probability from 30% to 70% with vertical bars representing incremental probability rate changes. Shown are stochastic models; the fixed survival percentages exhibited similar fates (data not shown).

Eight-cell starting metastases conferred a grow-out advantage particularly above the 60% survival probability whereas 1-cell starting metastases still exhibited metastatic abatement in that range. Of those metastases that die out, they do so quickly in fewer than 60 cycles (Fig. 8). Dormant metastases represented a small fraction and were tightly bounded by a small survival probability.

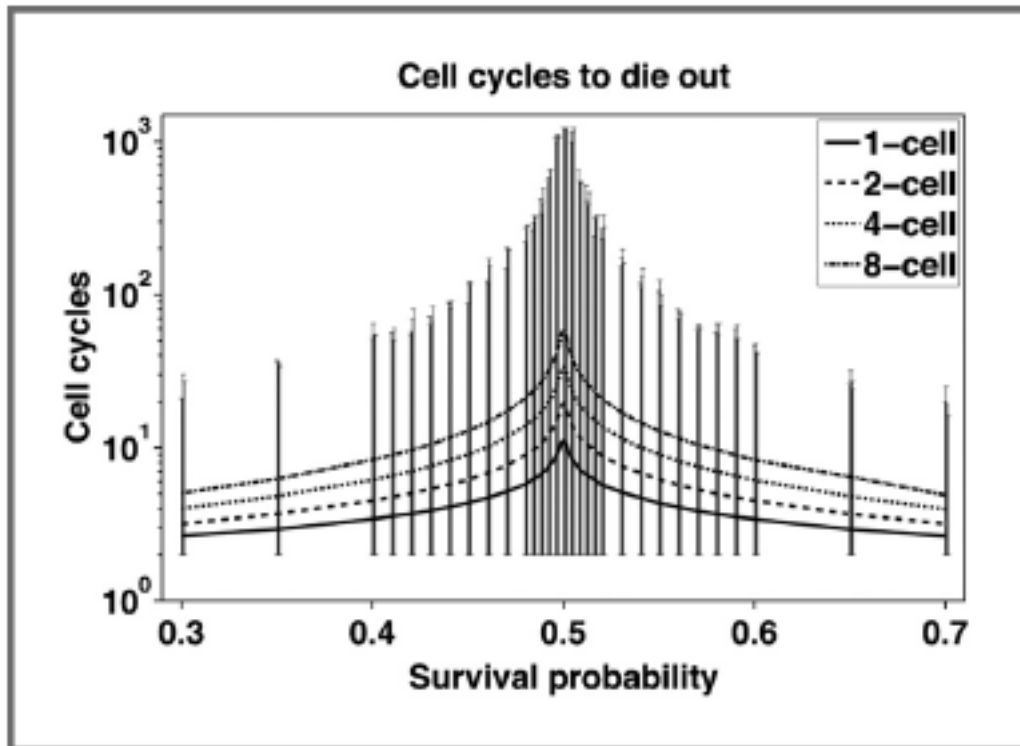


Figure 8. Micrometastases that die do so quickly when survival probability is low or high. As P increases mets are, on average, surviving longer, even though most still die. The symmetric, decreasing curves capture results from the increased likelihood of cell survival, meaning that those that do die out must converge to that fate quickly. Vertical bars indicate cell survival maxima and minima for non-surviving metastases. Only near the dormancy survival ranges do micrometastases have marked increases in cell cycles to die out, but still well below 1,218 cycles.

3.5.2 Dormant metastases arise only for survival probabilities proximal to 50 percent

Metastatic dormancy was a rare outcome that manifested only between 49.7% and 50.8% survival probability (Fig. 9, top). Starting with 1 versus 8 cells in the micrometastases did not impact this survival probability range. However, the mean number of dormant metastases increased as the starting cell number increased, up to a maximum of 80 mean dormant metastases per patient (still less than 10%) for 8-cell simulations (Fig. 9, bottom). In a small series of 1000- or 4000-cell micrometastases, the boundary percentages were within the same narrow survival probability range.

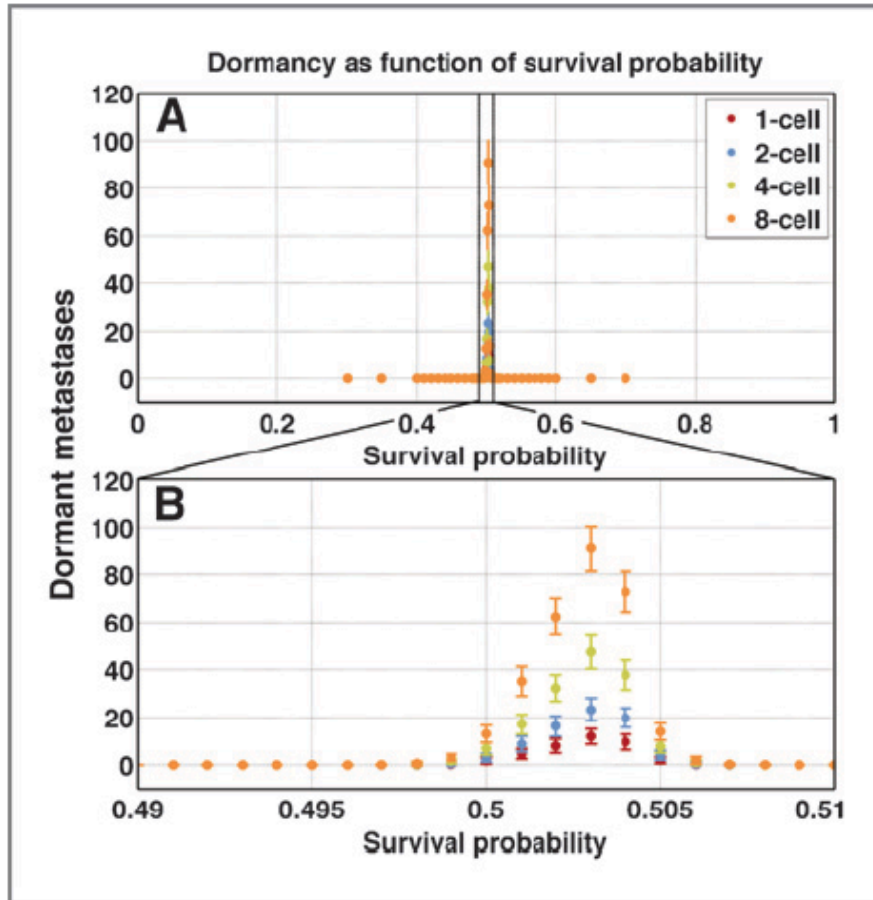


Figure 9. Dormancy only manifests between 49.7% and 50.8% survival probability. Mean number of dormant metastases per 1,000 initial nodules (ordinate) increases as starting cell number increases, although they remain bounded by the same restraints in terms of survival probabilities (abscissa). B, an enlarged view of the narrow probability window indicated in A.

3.5.3 Dormant metastases exhibited a large range in cell numbers

Although dormancy was tightly bounded proximal to the 50% survival probability, a dramatic variance of the mean dormant metastatic size was highly sensitive to small changes in survival probability (Fig. 10). Half of the survival range (between 49.7% and 50.2%) yielded dormant metastases composed of fewer than a few thousand cells. Interestingly, between 50.3% and 50.7% survival probabilities the populations peaked at around 500,000 cells. Not until the 50.8% survival probability did the dormant metastases (a single metastasis for 2-cell initialization, 3 metastases for the 8-cell case) approach the outgrowth condition—reaching nearly 1 million cells.

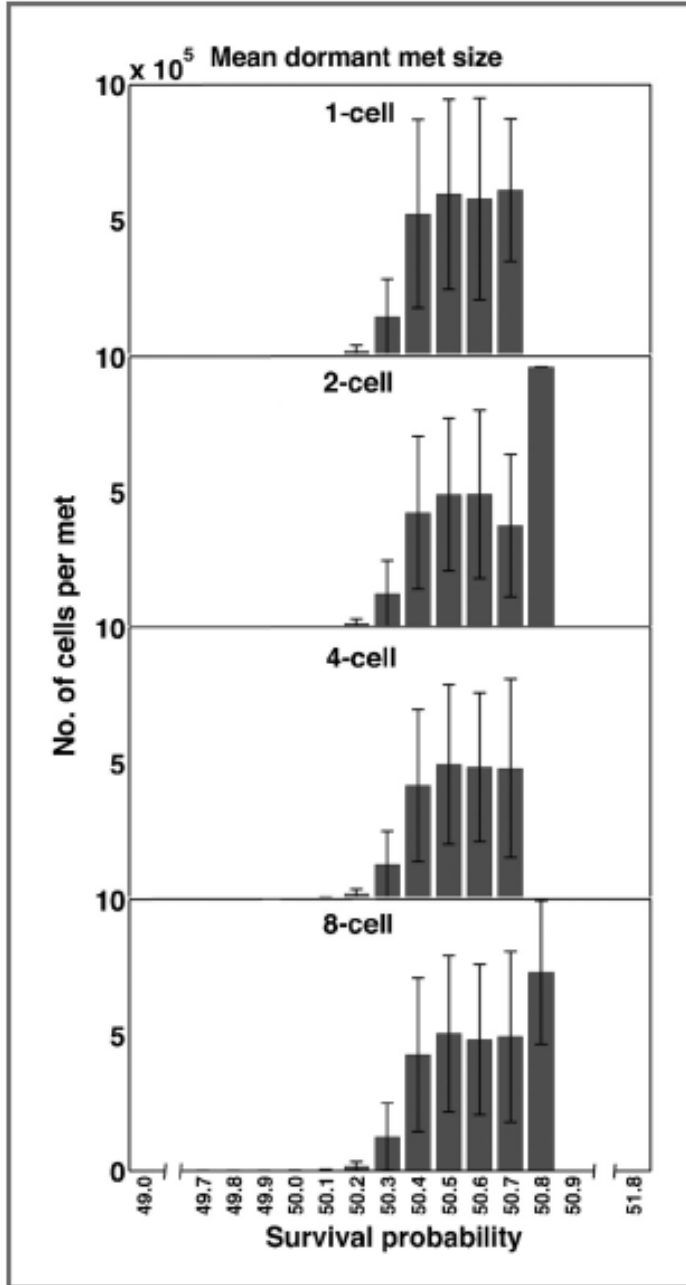


Figure 10. Dormant metastases exhibit a wide range of cell numbers per metastasis. The number of cells in each dormant nodule (ordinate) spanned from hundreds to nearly one million cells, with similar results between 1-cell to 8-cell starting metastases across the survival percentages. This range is highly sensitive to small changes in survival probability.

3.5.4 Metastatic outgrowth was highly sensitive to small changes to survival probability

The cumulative density function in Fig. 11 compares 1-cell versus 8-cell starting metastases to the outgrowth condition. At the 70% survival probability, all of the metastases that grew out did so in less than 50 cycles. In contrast, half the metastases grew out in approximately 400 cycles for the 51.5% survival probability. Interestingly, at just above the 50% survival probability, a one-percentage point increase in survival probability resulted in the required number of cycles for the surviving metastases to achieve outgrowth being reduced by two thirds.

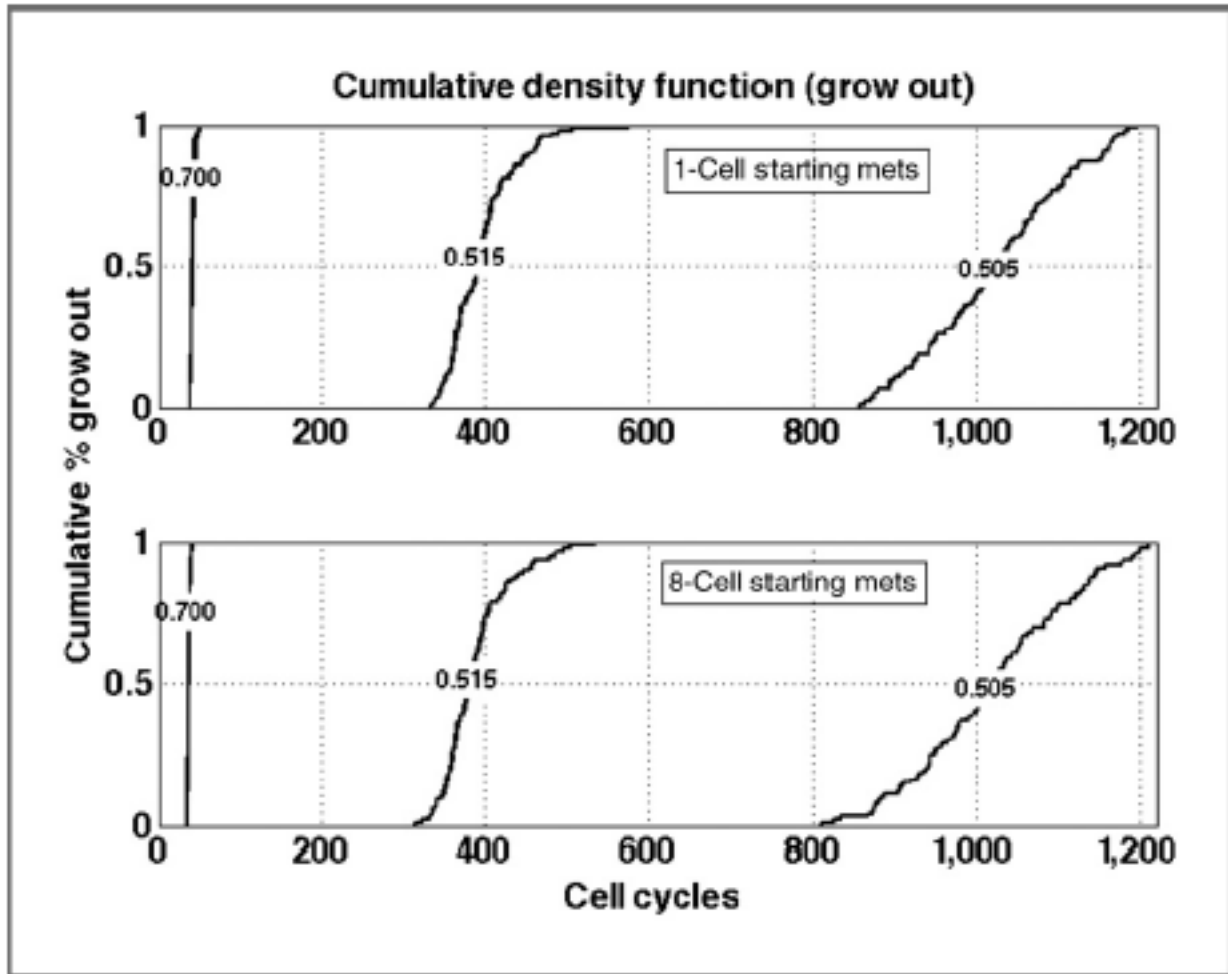


Figure 11. Cycles to outgrowth between 1- and 8-cell metastases. The cumulative fraction (ordinate) of micrometastases that grow out as a function of survival probability leads to fewer cycles (abscissa) with even a one percentage point increase in cell survival reducing outgrowth time by nearly two thirds.

3.6 DISCUSSION

Research into metastatic latency has rapidly evolved over the past decade given the high prevalence of this condition and the lack of effective clinical interventions. Unfortunately, this phenomenon is difficult to recapitulate across *in vitro* and *in vivo* experimental systems. Moreover, it is not certain whether metastatic latency results from small deposits of quiescent carcinoma cells that had recently extravasated into the metastatic site or whether small- to mid-sized micrometastases maintain clinically undetectable sizes based on balanced proliferation and cell death (or a combination of explanations). This distinction is critical as therapeutic approaches would be different for either condition: that of targeting proliferating or quiescent cells.

Because of the metastatic latency prevalence, patients are confronted with the dilemma of undergoing extensive and toxic systemic treatments for putative metastases based on the characteristics of the primary nodule and statistical considerations of similar patients that experienced metastatic latency. Although the ability to predict which patients will suffer metastatic recurrence has improved (Kamiya et al., 2012), the current approach to these dreaded sequelae only reduces the rate by a third, while evoking untoward toxicity including hair loss, neurological impairments, opportunistic infections, bleeding, and death. As most of the therapy is ineffective, we need to characterize the status of the disseminated tumor cells before their frank metastatic emergence so as to more effectively target them. What is not known is whether these few surviving cells exist in cellular quiescence or undergo balanced proliferation to engage

the dormant phenomenon. This distinction has immense implications, as predominantly only cycling cells are susceptible to chemotherapy, and is therefore the focus of this article.

Given these limitations, many *in silico* models have been developed that may help prioritize or frame the metastatic etiology (Berman et al., 1992; Ycart, 2012). For example, Michor and colleagues computed the probability of metastatic dissemination from primary tumors based on oncogenic mutations in RAS, ERBB2/NEU, or MYC (Michor et al., 2006). Implementing a stochastic Moran process the authors simulated a single genetic mutation that gave rise to neutral, advantageous, or disadvantageous metastatic potential. These simulations computed the temporal accumulation of metastases as a function of primary tumor size. Further model development eventually may help clinicians validate whether to treat more aggressively with adjuvant therapy. Another study implemented a Voronoi tessellation approach to model the impact heterogeneous or homogenous extracellular matrix (ECM) stiffness had on metastatic and primary tumor growth kinetics (Jiao et al., 2011). Whereas non-rigid, homogenous ECM gave rise to isotropic tumors and rigid homogenous ECM invoked anisotropic morphologies, a heterogeneous ECM stiffness exhibited both properties, but in a predictable manner. Consequently this modeling if matured may assist clinicians in determining which metastatic tumor-adjacent tissue (in critical metastatic organs such as the brain) may likely harbor disseminated tumor cells—leading to either more or less aggressive tissue resection. Although these models have promise to improve clinical treatments there is a dearth of modeling within the very early stages of metastatic extravasation.

The model presented here invokes explicit representation of each cell and leverages repeated computed trials to sample the distributions of die out, grow out, and dormancy phenotypes exactly. However, analytic formulations called branching processes can also be

applied to derive convenient predictions for this type of growth (Watson et al., 1875). These models exploit the fact that daughter cells are independent from one another and thus behave as if individual metastases (branching processes) themselves, lending to a compact, recursive formulation: $h_n(t) = [f^n(t)]^N$. Here, $h(t)$ is the "probability generating function" (pgf) at cell cycle n , and is computed as the product of N identical pgf's (for N starting cells in the micrometastatic tumor; ref. 23). The pgf allows us to quickly compute the expected cell population after n cell cycles $\left(N[(2p)^n]\right)$, the expected variance, $\left(\frac{(2p)^{2n} - 1}{(2p)^2 - 1} - N(2p)^n\right)$, and the probability of eventual extinction, $\left(\frac{p}{1-p}\right)^N$. In all expressions, the inputs are the number of starting cells, N , the survival probability, p , and the number of cell cycles, n , just as in our stochastic simulation model. The recursive formula above cannot yield the exact population distribution for any large n (Harris, 1964), such as our cell cycle limit of 1,218. That is, although we can predict dying out and survival, we cannot exactly predict dormancy with the model, for which simulations are required.

Metastatic lesions are visible through imaging modalities such as MRI when they approach 0.1 cm³. A tumor of this small size actually consists of approximately 100 million cells (Klein et al., 2006). Therefore, disseminated tumor cell deposits of less than this cannot be detected without invasive biopsy and subsequent analyses such as immunohistochemistry. Because metastatic latency can be explained by 2 very different mechanisms—that of cellular quiescence or proliferation offset by cell death (or a combination of both), we sought to model the second hypothesis and determine what survival probability range would give rise to the dormant phenotype. We simulated 100 patients each with 1,000 metastatic deposits (1-, 2-, 4-, and 8-cell starting sizes) across stochastic survival probabilities discontinuous between 30% and

70%. The modeling revealed a very narrow survival probability range between 49.7% and 50.8% that gave rise to dormant metastases. The reason why this dormancy probability window is so small is based upon how sensitive simulated metastases are to small changes in survival probability. If the probability of survival is less than 50%, the metastases all die out with the exception of the few dormant clusters because the probability favors the boundary condition of dying out. Only a rare escape from this tendency will therefore evoke a dormant metastasis. Once the probability of survival exceeds 50.8%, the grow-out condition of reaching 1 million cells begins to dominate. Thus, we conclude that it is unlikely that metastatic dormancy is governed predominantly by internally balanced proliferation and cell death. As shown in Fig. 3, it may seem unexpected that micrometastases will die out even at survival probabilities exceeding 70%. The reason for this phenomenon is closely related to the number of starting cells in the metastases. It is difficult for a simulated metastasis to live through its first few generations especially when it has 2 starting cells; because when a cell dies the metastasis evolves closer to the boundary of dying out.

As Fig. 7 shows, the chance of a metastasis dying out is reduced when there are 8 starting cells versus 2 starting cells. Of the metastases that die out, they do so in a short time (Fig. 3) as this relates to the fact that the metastases start near the null boundary and thus are easy to involute early before attaining a greater cell number. An often suggested model involves micrometastases growing and then being constrained at a subclinical size by the need for external supports; this is the basis of the postulated "angiogenic switch" (Naumov et al., 2008). However, even here the constraints must be tightly controlled; in an initial series of examining metastases of 1,000 or 4,000 starting cells, the range for staying dormant remained constrained similarly to the smaller micrometastases at between 49.5% and 51% survival probabilities; if the survival

percentage drops below this, the metastatic nodules quickly die out (data not shown). Thus, even this tumor extrinsic constraint would need to be tightly controlled or frequently vacillate between outgrowth and involution. In the spirit of Occam's razor, we propose that extended periods of cellular quiescence most likely accounts for this dormant period.

Although there are numerous models for dormancy these suffer from significant differences in the animal hosts, such as life-span and time-scale to development, and a lack of information about the micrometastatic state in actual cancer patients. This approach does not account for the richness of interactions and signals that may constrain or support micrometastatic nodules. For instance, it is possible that an "angiogenic switch" is required for outgrowth once these nodules reach a certain size. However, the experimental data are lacking currently to build models incorporating such inputs. Rather, such models would presuppose these constraints and be built to account for the limitations and interventions (Divoli et al., 2011). Herein, we chose an a priori unbiased calculation to simply define the boundary conditions of metastatic outgrowth regardless of the actual biological and physiological networks.

The value of mathematical models lies in their ability to suggest avenues for investigation. Recent findings of tumor cells in circulation or bone marrow despite no evidence of metastases may provide some insights into the behavior of the early metastatic cells. Interestingly, ongoing proliferation is evident only in few of these cells (Bednarz-Knoll et al., 2011) consistent with quiescence of these cells. If these cells were truly quiescent then therapies targeted to killing growing cells would not be effective and may even cause outgrowth if the dormant microenvironment is perturbed. Still such findings are only suggestive, and highlight the need to examine human micrometastases with innovative technologies to determine the actual proliferative rates in these hidden metastases. As our currently available chemotherapy mainly

attacks cycling cells, the mode of quiescence would make this treatment less effective and necessitate new approaches to the problem of metastatic dormancy.

4.0 HEPATIC NON-PARENCHYMAL CELLS DRIVE BREAST CANCER PROLIFERATION AND PARTIAL EPITHELIAL-TO-MESENCHYMAL TRANSITION

Donald P Taylor^{1,2}, Amanda Clark², Sarah Wheeler², Alan Wells^{1,2}

Departments of Bioengineering¹ and Pathology², University of Pittsburgh

Manuscript under development

4.1 ABSTRACT

Purpose: Nearly half of carcinoma metastases will become clinically evident only 5 or more years after the primary tumor was seemingly ablated. This implies that metastatic cancer cells survived over this extended timeframe without emerging as detectable nodules. The liver is a common metastatic target, whose parenchymal hepatocytes have been shown to impart a less malignant, dormant phenotype on metastatic cancer cells. To explore emergence from metastatic dormancy we investigated whether hepatic non-parenchymal cells (NPCs) contributed to metastatic breast cancer cell outgrowth and a mesenchymal phenotypic shift indicative of emergence.

Experimental Design: Co-culture experiments of NPCs and breast cancer cells were conducted to investigate the role that NPCs play in metastatic emergence from dormancy. Human microvascular endothelial cells (HMEC-1) were co-cultured with a DsRed-transfected

human immortalized non-invasive breast cancer cell line (MCF-7) for up to seven days. Flow cytometry and immunofluorescence were performed in order to quantify MCF-7 outgrowth and phenotype respectively. Additional 2D co-culture experiments were performed with primary human or rat NPCs and hepatocytes, including investigating the outgrowth response of MDA-MB-231 cells.

Results: MCF-7 cells co-cultured with the NPC types grew out at rates nearing their growth-medium controls. Co-cultured MCF-7 cells underwent a mesenchymal shift as indicated by spindle morphology, membrane delocalization of E-cadherin, and p38 translocation to the nucleus. The NPC co-cultured invasive MDA-MB-231 cells exhibited similar characteristics. Outgrowth of the MDA-MB-231 cells among NPCs was substantially greater than in hepatocyte co-cultures.

Conclusions: We conclude that NPCs impart a partial mesenchymal shift to the MCF-7 cells thus conferring a grow-out advantage. These data suggest that perturbations of the parenchymal and NPC ratios (or activation status) in the liver metastatic microenvironment may contribute to emergence from metastatic dormancy.

4.2 INTRODUCTION

Breast cancer metastatic dormancy is a state in which cancer cells avoid clinical detection over many years or decades – as these cancer cells remain as microscopic foci or single cells versus detectable masses undergoing continual growth (Demicheli, 2001; Naumov, 2002). Dormancy requires a combination of cell survival or escape from apoptotic signaling pathways, coupled

with a phenotype suitable for avoiding the body's immune response (Aguirre-Ghiso, 2006; Townson and Chambers, 2006). Thus, metastatic breast cancer dormancy is likely not sustainable by the invasive, mesenchymal phenotype but rather through a partial epithelial reversion (Yates et al., 2007; Chao and Wells, 2010; Gunasinghe, 2012). Many of the human metastatic breast cancer lesions are E-cadherin positive but are thought to be derived from E-cadherin negative primary tumors (Wells, 2008 CEM review). Consequently dormancy may require this reverted epithelial phenotype, while a subsequent outgrowth may require a phenotypic switch back to an E-cadherin negative mesenchymal phenotype (Gunasinghe, 2012). Although studying the conditions by which the dormant metastatic phenotype can be maintained is a critical topic, it's the emergence from dormancy that ultimately takes lives. Therefore, we have explored a pathophysiologic aspect of the metastatic niche (specifically the NPCs) that may prompt this secondary mesenchymal reversion allowing metastatic breast cancer cells to escape from dormancy.

In addition to providing for the structure and microvasculature in the liver, the liver sinusoidal endothelial cells (LSEC), kupffer cells, and stellate cells play critical roles in mitigating acute or chronic liver injury (Michalopoulos et al., 1982). As such, these NPCs are involved in a tightly orchestrated extracellular signaling cascade that regulates functions including immune response, angiogenesis, and hepatocyte proliferation (Michalopoulos, 2007). The establishment of breast cancer micrometastases would certainly disrupt the parenchymal and non-parenchymal balance with consequences that may direct metastatic dormancy, retreat, or emergence from dormancy. The acquisition of an epithelial versus mesenchymal phenotype may direct whether metastatic breast cancer cells establish clinically evident metastases, form dormant sub-clinical metastases, or even fail to initiate metastatic seeding. In early stages,

localized carcinoma cells transform into a more invasive mesenchymal phenotype characterized by loss (or down-regulation) of E-cadherin in order to escape from the primary site and metastasize (Onder et al., 2008). Clinical evidence suggests that many of the recently extravasated breast cancer cells partially revert their mesenchymal phenotype (MErT) to an epithelial phenotype (Chao et al., 2012). This coincides with dormancy and resistance to chemotherapy (Chao et al., 2012). Consequently it is theorized that cells failing to undergo MErT perish, while those that engage the epithelial shift quiesce until such time they are prompted to undergo proliferation. Herein we investigated whether the hepatic NPCs trigger such a proliferative and mesenchymal shift in otherwise non-metastatic, epithelial breast cancer cells.

4.3 RESULTS

4.3.1 Endothelial cell lines confer a grow-out and survival advantage to breast cancer cells

As micrometastases form in the sub-endothelial space (Vlodavsky et al., 1983), we investigated whether active endothelial cells alter the phenotype of epithelial breast cancer cells. For this we used the non-invasive breast cancer line MCF-7, and two different types of endothelial cells: a human microvascular cell line (HMEC-1) to represent vessels, and an immortalized human liver sinusoidal cell (TMNK-1) line. MCF-7 cells were seeded under three culture conditions: 1) co-cultured with HMEC-1 cells in hepatocyte maintenance medium (HMM), 2) mono-cultured MCF-7 in HMM, and 3) mono-cultured MCF-7 in their growth medium (RPMI). MCF-7 cells in

HMM medium (serum free) mostly expire throughout this four-day experimental timeframe, while they experience exponential growth in RPMI (as expected). Notably the MCF-7 cells outgrow during this timeframe in co-culture with the HMEC-1 cells, suggesting that the HMEC-1 cells are providing a survival and grow-out advantage (Figure 12A).

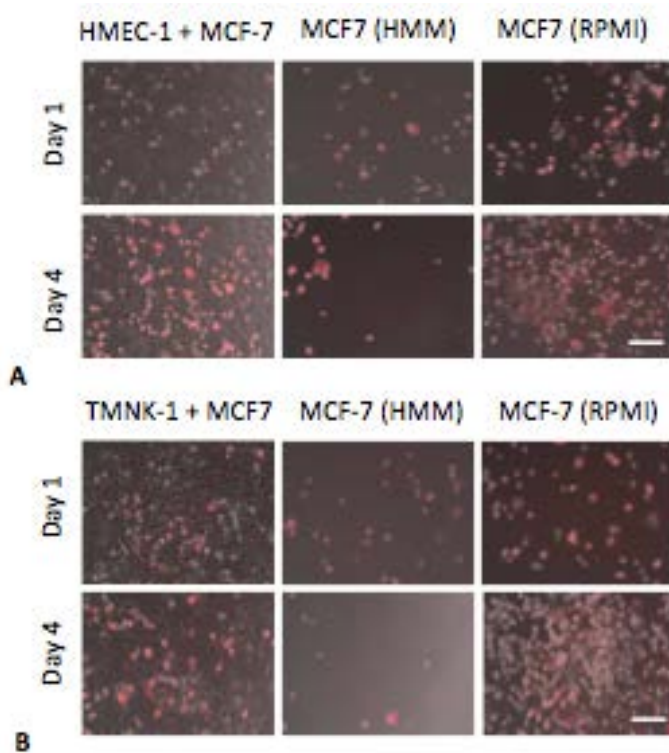


Figure 12. Non-parenchymal cell lines co-cultured with MCF-7-RFP cells confer carcinoma outgrowth. A) Phase contrast imaging with a fluorescence overlay (Red: MCF-7 cells) are representative images on Day 1 and Day 4 across 3 conditions: HMEC-1 co-culture in HMM, MCF-7-RFP in HMM, and MCF-7-RFP in RPMI. MCF-7 cells in HMM fail to outgrow, while outgrowing exponentially in the RPMI controls as expected. The MCF-7 cells experience outgrowth in the presence of HMEC-1 cells. B) Same conditions as in Panel A but with TMNK-1 cells. Day 1 is 24 hours after MCF-7-RFP cell seeding. Greater than 95% of the MCF-7-RFP cells expressed RFP on Day 4. Scale bar 250 micrometers.

To quantify the number of MCF-7 cells we performed flow cytometry (Figure 13) in a separate biological replicate counting the viable MCF-7-RFP cells (Annexin V negative and DsRed positive) supporting the outgrowth trends as seen in Figure 12. Although the HMEC-1 cells exhibit endothelial characteristics, we chose to also explore another endothelial cell line more closely associated with the hepatic microenvironment. Immortalized liver sinusoidal endothelial cells (TMNK-1) were established in 2004 (Matsumura et al., 2004). TMNK-1 co-cultured MCF-7 cells undergo a grow out phenotype (Figure 13), but less so than the HMEC-1 cultured cells, possibly due to TMNK-1 cell health degrading over the 4-day culture period in hepatocyte maintenance medium (HMM).

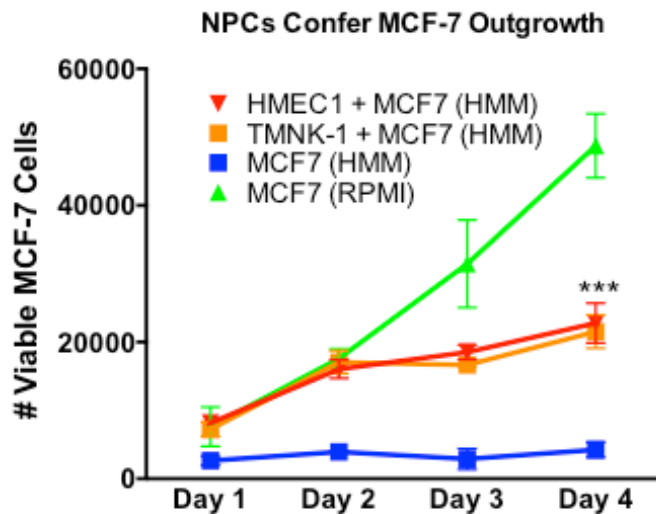


Figure 13. Flow cytometry for Annexin V negative, RFP positive cells (MCF-7-RFP) used to quantify cell counts in a separate biological replicate than in Figures 12A and 12B. HMEC-1 co-culture MCF-7 cells grew out at rates similar to the MCF-7 growth medium controls. Technical replicates performed in triplicate; p value < .001.

4.3.2 Primary human non-parenchymal cells confer a grow-out advantage to breast cancer cells

Although cell lines such as HMEC-1 and TMNK-1 reasonably function as endothelial cells according to the literature, we aimed to conduct these same proliferation experiments using primary non-parenchymal cell fractions enriched for liver sinusoidal endothelial cells. In addition to using the ER/PR+ MCF-7 cells, we also co-cultured the triple negative MDA-MB-231 cells as an invasive and metastatic line. Carcinoma outgrowth between the two breast cancer cell lines was similar in co-culture conditions (Figure 14) while they did not experience expansion in HMM-only controls as quantified on day 4 using the same methods described in Figure 12. This demonstrates a breast cancer cell grow-out advantage with primary NPCs, though to a lesser extent than in growth medium.

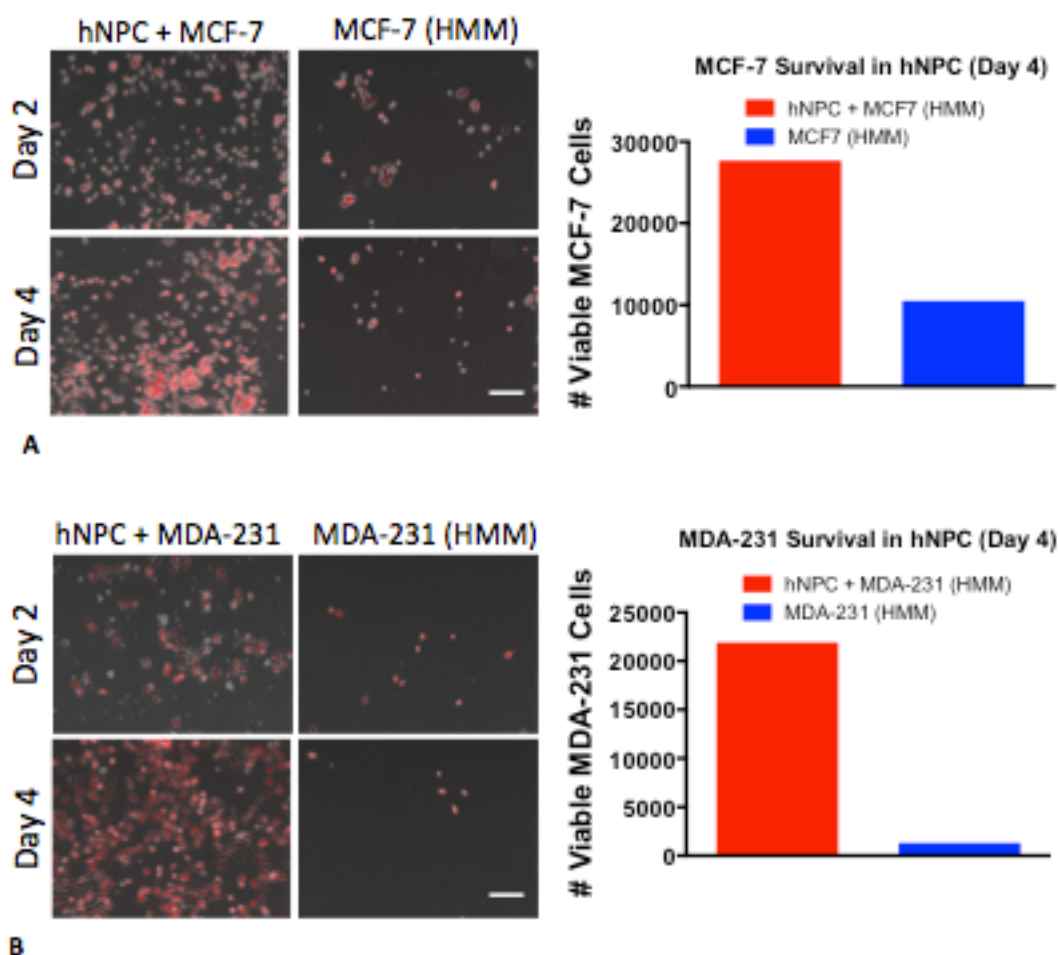


Figure 14. Human primary non-parenchymal liver cells (NPCs) confer carcinoma outgrowth. A) Representative images of MCF-7-RFP and B) MDA-MB-231-RFP cells in co-culture with primary NPCs compared to their HMM controls demonstrating carcinoma outgrowth in the presence of NPCs. Flow cytometry quantification for Annexin V negative, RFP positive breast cancer cells. One well of a single biologic sample. Scale bar 250 micrometers.

4.3.3 Breast cancer cell outgrowth is increased in primary rat NPC co-culture versus hepatocyte co-culture

We have previously published that both MCF-7 cells and MDA-MB-231 cells proliferate in hepatocyte co-cultures while the MDA-231 cells also undergo a partial mesenchymal-to-epithelial reversion (MER_T) in part characterized by the re-expression of E-cadherin (Chao and Wells, 2010). Herein we investigated whether the primary rat NPC cells or the primary rat hepatocytes in co-culture with the breast cancer cells would confer differential outgrowth (Figures 15 and 16).

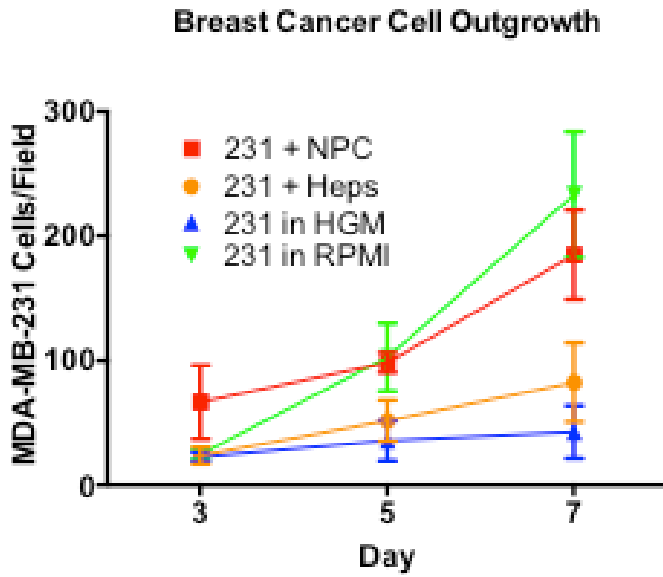


Figure 15. Hepatocytes confer MDA-MB-231 outgrowth but less than non-parenchymal liver cells. Flow cytometry quantifying MDA-MB-231-RFP cell count for Annexin V negative, RFP positive cells in co-culture conditions versus positive and negative controls. Technical replicates performed in triplicate.

MDA-231 cells experienced outgrowth in excess of their HMM-only controls demonstrating that both hepatocytes and NPC cells individually contribute to breast cancer cell proliferation. Interestingly the breast cancer cells outgrew significantly greater in the NPC co-cultures versus the hepatocyte co-cultures suggesting an imbalance of the non-parenchymal hepatic niche may induce an emergent phenotype.

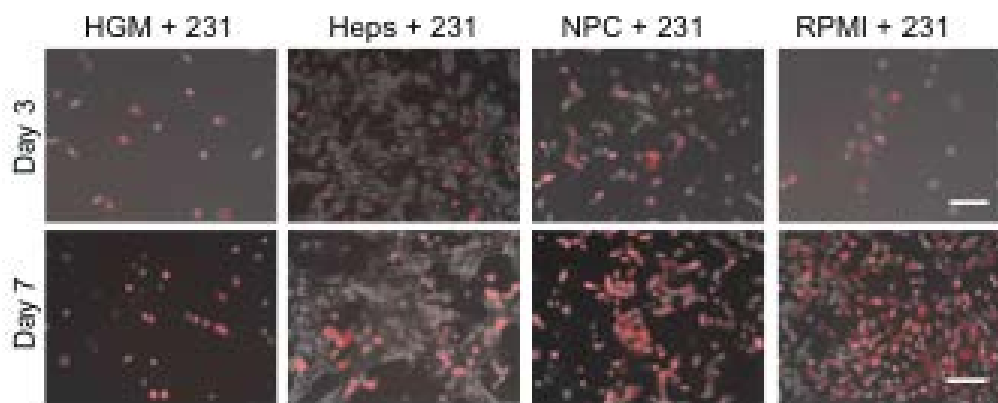


Figure 16. Representative phase contrast images with fluorescence overlay of MDA-MB-231 cells across four culture conditions: hepatocyte growth medium alone, hepatocyte co-cultures, non-parenchymal hepatic cell co-cultures, and RPMI MDA-231 growth medium alone. Scale bar 250 micrometers.

4.3.4 NPC cells confer a partial mesenchymal phenotypic shift to E-cadherin positive breast cancer cells

To investigate the effect of NPCs on breast cancer cell phenotype, we challenged the epithelial MCF-7 cells with HMEC-1 co-cultures in HMM. MCF-7 cells in standard growth medium are

characterized by a cobblestone appearance and tight cell-cell contacts (Figure 17, left column). In the presence of HMEC-1 co-cultures a sub-population of the MCF-7 cells have become spindle-shaped and are not readily forming cell-cell contacts (Figure 17, right column). Thus, a partial mesenchymal shift has been imparted to the MCF-7 cells in co-culture with the HMEC-1 cells indicative of the metastatically invasive, highly proliferative MDA-MB-231 cells.

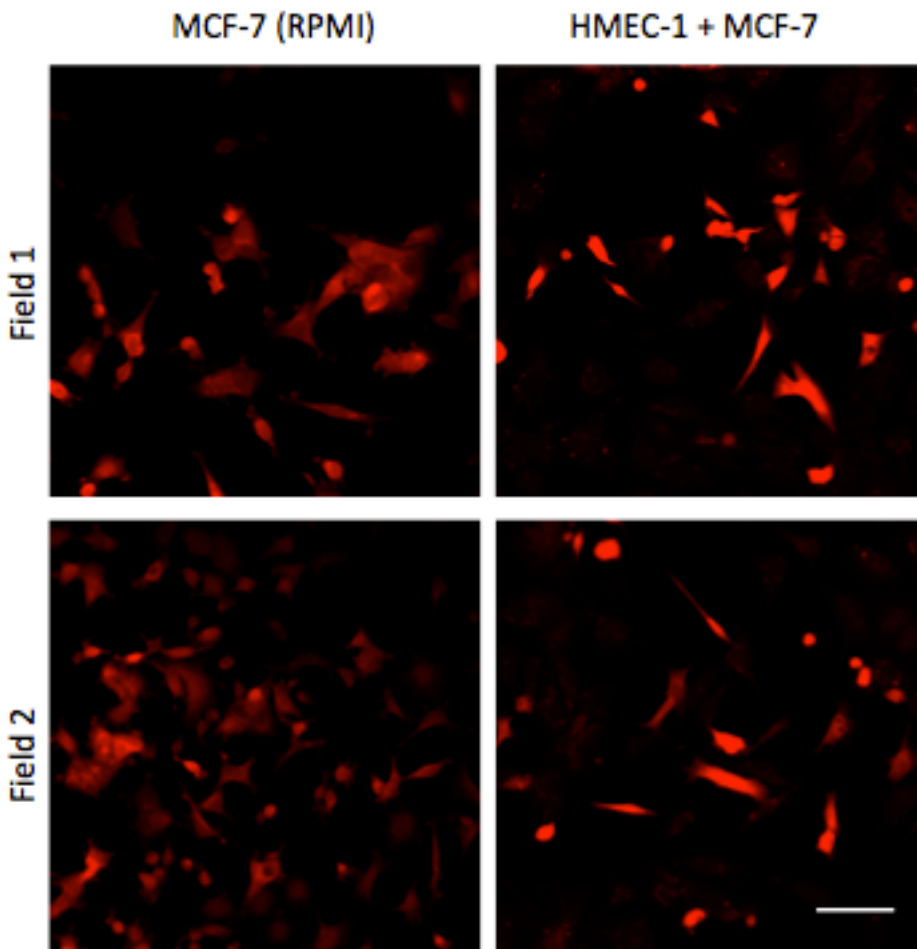


Figure 17. HMEC-1 co-culture confers a mesenchymal phenotype to MCF-7 cells. Representative fluorescent images on Day 4 of MCF-7 cells (in red) co-cultured with HMEC-1 cells. Fluorescent imaging depicts MCF-7-RFP cells in growth medium (left column) versus in HMEC-1 co-culture in HMM (right column). Scale bar 50 micrometers.

Epithelial cell phenotype is predominately determined by whether the cells form E-cadherin-mediated cell-cell adherens junctions. As expected, the MCF-7 cells concentrate E-cadherin expression to the membrane in the RPMI controls (Figure 18, panel 1). Notably in the HMEC-1 co-cultures, a sub-population of MCF-7 cells fail to maintain membrane E-cadherin expression with E-cadherin being internalized, similar to the situation that occurs in response to growth factor receptor activation.

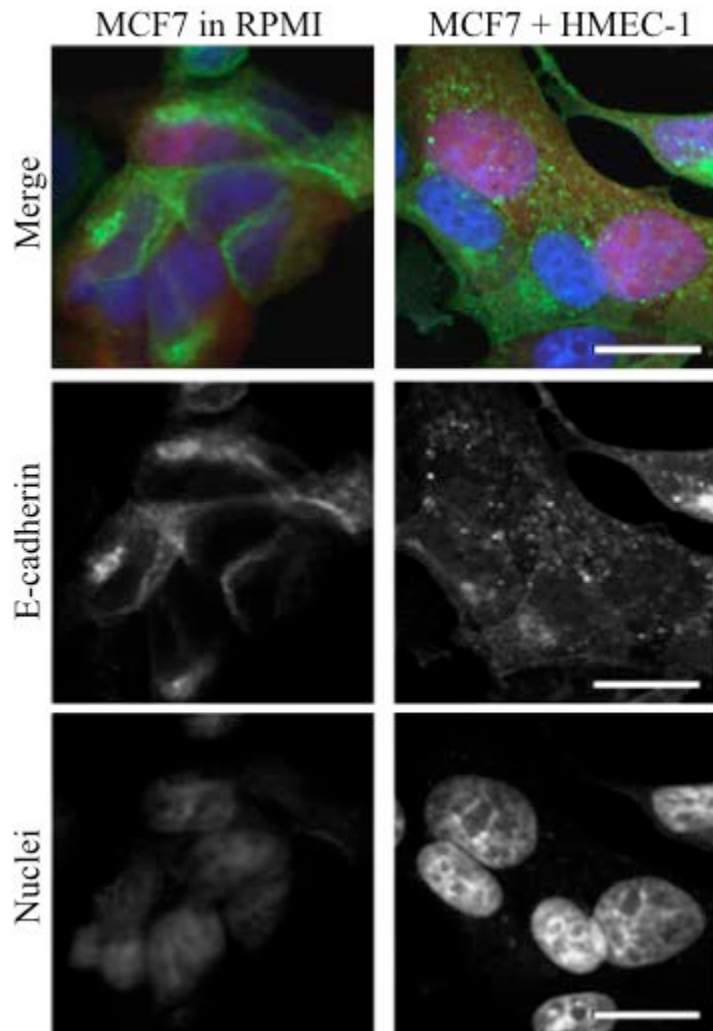


Figure 18. HMEC-1 cells induce a partial mesenchymal shift to MCF-7-RFP cells. Confocal imaging for E-cadherin (green) shows membrane-bound staining in RPMI controls while co-cultured MCF-7 cells (red) internalize E-cadherin within the cytoplasm. Scale bar 50 micrometers. Nuclei indicated in blue.

Total cell E-cadherin protein levels remain constant (Figure 19) throughout the HMEC-1 co-cultures suggesting that E-cadherin is readily available for membrane re-localization to potentially establish a secondary MErT.

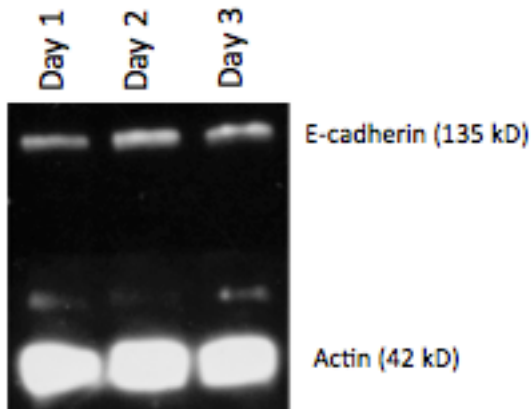


Figure 19. Immunoblot for E-cadherin in MCF-7 cells co-cultured with HMEC-1 cells (not expressing E-cadherin).

4.3.5 NPC cells initiate p38 nuclear translocation in MCF-7 cells

It has been previously been demonstrated that the stress kinase, p38, is involved with pathways supporting cell cycle arrest in the G0/G1 checkpoints, as it forms complexes in the cytoplasm. (Coulthard et al., 2009). Further studies have shown that p38 to ERK ratios contribute to metastatic dormancy (Ranganathan et al., 2006) or emergence. However, the effects of p38 nuclear translocation are understudied. MCF-7 cells co-cultured with HMEC-1 cells exhibit p38

localization from the cytosol to the nuclei (Figure 20). Further investigation will be required to determine whether p38 nuclear translocation plays a role in emergence from metastatic dormancy.

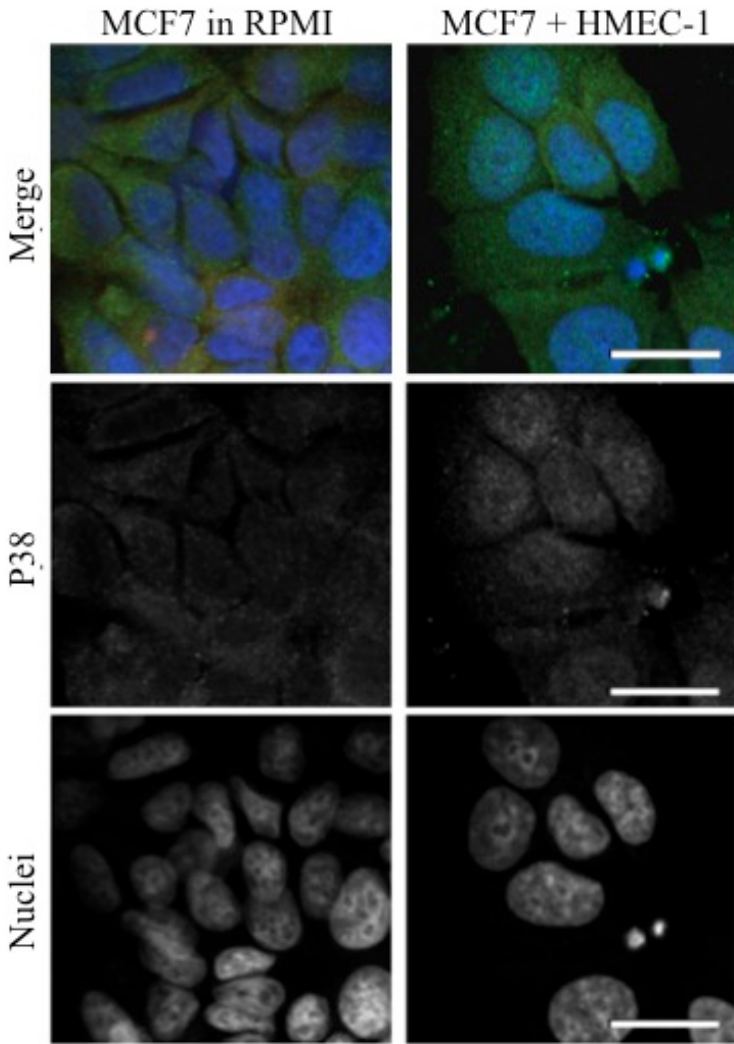
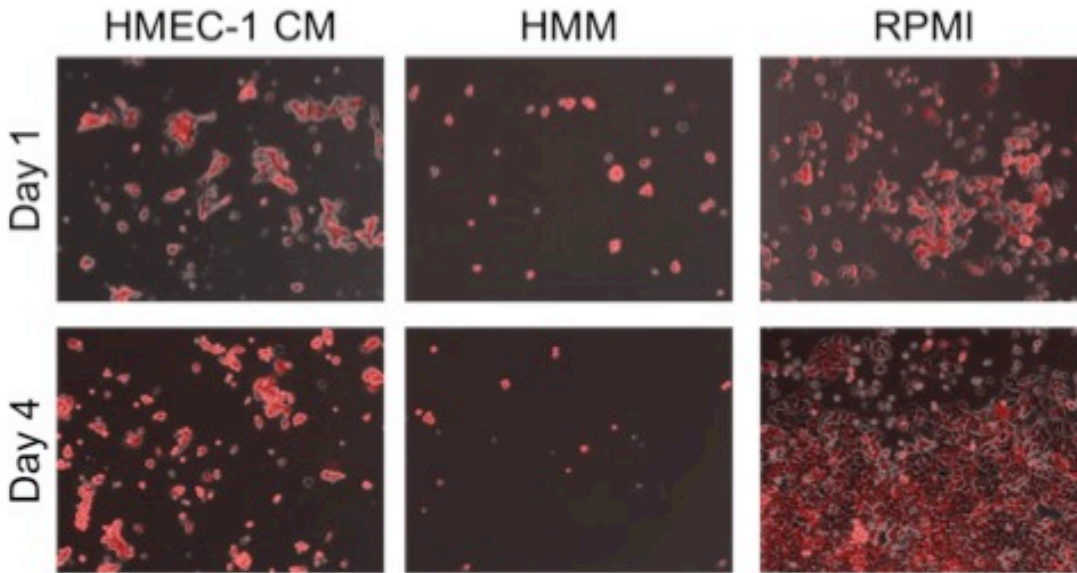


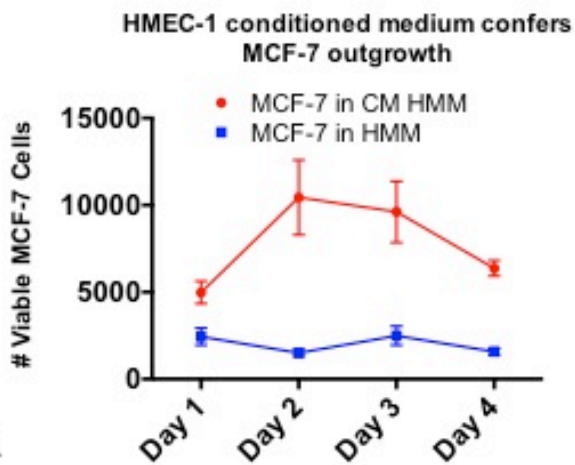
Figure 20. HMEC-1 cells induce a stress response in MCF-7 cells. Confocal imaging for phosphorylated p38 (Green) shows a nuclear translocation in HMEC-1 co-cultures versus the RPMI control. Scale bar 50 micrometers.

4.3.6 NPC-induced MCF-7 outgrowth is at least partially mediated by soluble factor secretion through epidermal growth factor receptor activation

We investigated whether paracrine soluble factor signaling from the HMEC-1 cells to the MCF-7 cells was at least in part responsible for the breast cancer cell outgrowth phenotype. HMEC-1 conditioned medium cultures (in HMM) were collected on days 1 through 4 and used to seed and incubate the MCF-7 cells. The HMEC-1 conditioned medium prompted an outgrowth phenotype as we saw in the HMEC-1 co-cultures but to a lesser extent (Figure 21).



A.



B.

Figure 21. HMEC-1 conditioned medium supports MCF-7 outgrowth. Phase contrast images of MCF-7-RFP cells with fluorescent overlay (Panel A) across three culture conditions: 1) HMEC-1 conditioned medium, 2) HMM, and 3) RPMI growth medium. MCF-7 cells in conditioned medium exhibited a grow-out advantage over MCF-7 cells cultured in the HMM controls (Panel B). Technical replicates performed in triplicate.

We then investigated whether the mechanism of HMEC-1 signaling involved the epidermal growth factor receptor (EGFR) pathway. We inoculated an HMEC-1 and MCF-7 treatment group with an EGFR receptor blocking antibody and performed the same co-culture experiments as described in Figure 13. We found that EGFR inhibition significantly blunted MCF-7 cell outgrowth while the positive control of EGFR inhibition in MCF-7 RPMI cultures promoted outgrowth (Figure 22). These data suggest that the breast cancer cell outgrowth phenotype triggered by NPC cells at least involves the EGFR activation pathway.

EGFR-I Blunts MCF-7 Outgrowth in HMEC-1 Cultures

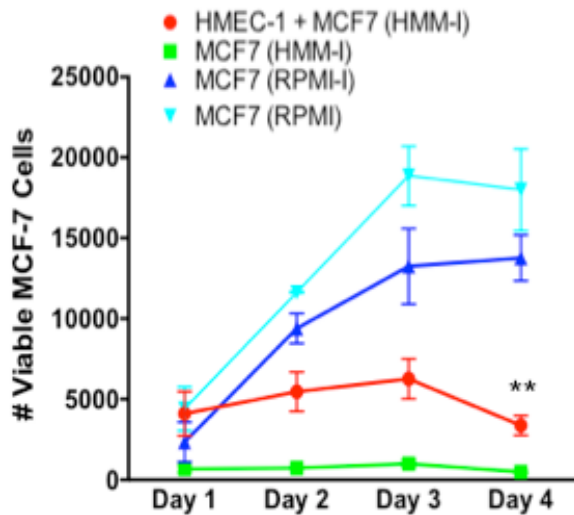


Figure 22. EGFR inhibition blunts MCF-7 outgrowth in HMEC-1 cultures. Co-cultures were administered as described in Figure 13. 500 nM of EGFR inhibitor was introduced into the three treatment groups while MCF-7 positive growth controls in RPMI were free from inhibitor. Technical replicates were performed in triplicate; $p < .001$.

4.4 DISCUSSION

Breast cancer has the insidious propensity to recur many years or decades after primary tumor diagnosis. This recurrence is typically refractory to current treatments including radiation, chemotherapy and surgical resection. The long latency period between primary tumor diagnosis and clinical metastatic presentation is termed metastatic dormancy. This dormancy can be largely explained by two theories: 1) disseminated cancer cells become quiescent, or 2) they have a balance of apoptosis and proliferation. Although investigations are underway to help resolve this distinction, developing a dormant metastatic phenotype has been a significant challenge. So instead of studying dormancy directly, we aimed to study physiologic perturbations in the liver metastatic microenvironment that might be responsible for emergence from dormancy. The principle being that if we can uncover metastatic breast cancer proliferation inducers we might be able to backwards integrate into what might prompt the precursor dormancy period. We therefore directed our attention to the hepatic stromal cells with particular emphasis on the endothelial cells.

Cancer-associated EMT cells are capable of extravasation into the liver parenchyma from the pre-capillary constriction sites in which they may become arrested. Although EMT cell migration deeper into the liver parenchyma may not be required for survival, proliferation, or further systemic invasion, we posited that a favorable microenvironment is necessary for maintaining metastatic dormancy or prompting emergence from dormancy. We investigated

emergence from metastatic dormancy based on the assumption that cancer-associated EMT cells must extravasate within a protective sheath of hepatocytes and partially revert to an epithelial phenotype.

We found that liver non-parenchymal cells drive E-cadherin positive breast cancer cells to a mesenchymal phenotype, while conferring a substantial grow-out advantage, at least in part through EGFR activation. These data suggest that perturbations of the parenchymal and non-parenchymal cell ratios in the liver metastatic microenvironment may differentially contribute to metastatic dormancy, stability, or emergence. Therefore dormancy and emergence from dormancy may hinge upon the inactivated or activated status of the hepatic non-parenchymal cells, thus making the metastatic niche a potential therapeutic target to combat metastatic disease.

4.5 MATERIALS AND METHODS

4.5.1 Cells and cell culture

RFP expressing MDA-MB-231 and MCF-7 cell lines were transfected as previously described (Chao et al., 2010). To maintain selection for RFP positive breast cancer cells, MCF-7 cells were cultured with 900 ug/ml G418 and MDA-MB-231 were cultured with 5 ug/ml puromycin in RPMI-1640 (Life Technologies, Carlsbad, CA) supplemented with 10% FBS until used in the experiments. HMEC-1 cells were a kind gift from Dr. Richard Bodnar of the Pittsburgh Veterans Affairs (Pittsburgh, PA). HMEC-1 cells were cultured in MCDB 131 medium (Life Technologies, Carlsbad, CA) with 10% FBS, 10 ng/ml EGF, 1 ug/ml hydrocortisone, and 10 mM

L-glutamine until used for experiments. TMNK-1 cells were a kind gift from Dr. Alex Soto-Gutierrez of the University of Pittsburgh. TMNK-1 cells were cultured in DMEM (Life Technologies, Carlsbad, CA) with 4.5 g/ml glucose, 1% Penicillin-Streptomycin, and 10% FBS until used for experiments. HMEC-1 and TMNK-1 co-cultures with MCF-7 or MDA-MB-231 cells were performed in serum free hepatocyte maintenance medium (HMM) (Lonza, Anaheim, CA) supplemented with SingleQuots® (Lonza, Anaheim, CA). HMEC-1 conditioned medium was prepared by incubating 70% confluent HMEC-1 cells in HMM for 24 hours. The supernatant was collected and spun for 5 minutes at 1,000 g to remove any particulate. Samples were stored at -80 until used in experimentation.

4.5.2 Co-culture

TMNK-1 or HMEC-1 cells (NPC cell lines) were trypsinized from T75 flasks at 80% confluence and resuspended in their respective growth medium with 10% FBS to inactivate the trypsin. NPC cell lines were spun into pellets, their growth medium aspirated, and resuspended in HMM. 20,000 NPC cell line cells/cm² were seeded into 12-well polystyrene plates and allowed to attach for 3-4 hours before breast cancer cell co-culture. Breast cancer cell lines were prepared the same way as the NPC cell lines but seeded at 1,000 cells/cm² after the NPC cell line attachment period.

4.5.3 Imaging

Phase contrast images were captured by an Olympus inverted scope and digitally captured using Spot Advanced™ software (Diagnostics Instruments, Macomb, Michigan). Confocal images

were captured on an Olympus Fluoview 1000 scope (Olympus, Center Valley, PA) and captured using Fluoview Viewer™. Immunofluorescence was performed by 24-hour primary antibody incubation against E-cadherin Cat# 610182 (BD Biosciences) and phospho p38 Cat# 4631S (Cell Signaling, Danvers, MA) each at 1:200 dilution. Alexa Fluor® 488 rabbit anti-mouse (Life Technologies) secondary antibody was incubated for 45 minutes at room temperature at 1:500 dilution. Hoechst was incubated for 10 minutes at 1:500 dilution at room temperature.

4.5.4 Immunoblotting

A 7.5% SDS-PAGE gel resolved cell lysates and subsequently transferred to a PVDF membrane. Membranes were blocked with 1% serum albumin for 1 hour and incubated overnight with E-cadherin primary antibody Cat# 3195 (Cell Signaling, Danvers, MA) or Actin (Abcam, Cambridge, MA). Chemiluminescence was detected on film following incubation with peroxidase-conjugated secondary antibodies.

4.5.5 Flow cytometry

Cell cultures in each well were incubated in trypsin for 30 minutes until dissociated. 2 mL of PBS with 2% FBS were added to each well, transferred to flow tubes, and pelleted. The media was aspirated and cell pellets incubated with the reconstituted components of the Alexa Fluor® 488 Annexin V/Dead Cell Apoptosis Kit (Life Technologies, Carlsbad, CA) for 15 minutes. The reaction was terminated by adding 100 ul of the Annexin binding buffer to each tube. 10 uL of CountBright™ Absolute Counting Beads (Life Technologies, Carlsbad, CA) were added to each tube in order to compute the number of RFP positive, Annexin V negative breast cancer cells.

Cell suspensions were run on the BD LSRFortessa™ flow cytometer and BD FACSDiva Software (BD Biosciences, Franklin Lakes, NJ).

4.5.6 EGFR inhibition

PD 153035 hydrochloride Cat# 1037 (Tocris Bioscience, Minneapolis, MN) was incubated in EGFR inhibition treatment cultures at a 500 nM concentration throughout the experiment. HMEC-1 cells were plated and seeded with MCF-7 cells as described above except that the MCF-7 cells were resuspended in the EGFR inhibitor media where applied.

4.5.7 Statistical Analysis

Graphical data are provided as mean +/- standard deviation from three independent technical replicates. P-value significance was evaluated using ANOVA and Tukey method and set at a minimum 0.05. Images were representative of at least three independent fields per well.

5.0 THE PRE-STRESSED HEPATIC NICHE PROMOTES BREAST CANCER METASTATIC COMPETENCY

Donald P Taylor^{1,2}, Amanda Clark², Sarah Wheeler², Alan Wells^{1,2}

Departments of Bioengineering¹ and Pathology², University of Pittsburgh

Manuscript under development

5.1 ABSTRACT

Purpose: As seeding and subsequent survival in the ectopic metastatic target organ is the most rate-limiting step, the purpose of this study was to determine key elements in enabling this. Based on the concepts of matching phenotypic status of the parenchyma with the disseminated tumor cell we investigated whether a pre-stressed metastatic niche would better accommodate metastatic seeding and survival. We focused on breast cancer metastasis to the liver, as this is the second most diagnosed cancer in women with liver being a common metastatic site.

Experimental Design: We pre-stressed the primary rat or human hepatocytes in 2D and 3D cultures through biochemical challenges such as EGF, a growth factor secreted by most carcinomas. Two human immortalized breast cancer cells lines (MDA-MB-231 and MCF-7) expressing RFP were inoculated into the hepatocyte cultures directly following the removal of

the stressors. MDA-MB-231 cells with exogenously modulated E-cadherin were intrasplenically injected into NOD/scid gamma mice in order to investigate E-cadherin's role in establishing liver metastases.

Results: Breast cancer cells formed greater numbers of metastatic deposits in the pre-stressed hepatic cultures in 2D and 3D. Mean breast cancer cell RFP intensity and flow cytometry revealed increased numbers of breast cancer cells in pre-stressed hepatocyte cultures on Day 6. Confocal immunofluorescent imaging and immunoblots for proliferation and epithelial markers revealed that E-cadherin was increased in the pre-stressed co-cultures. *In vivo* the E-cadherin negative MDA-MB-231 cells partially reverted their mesenchymal phenotype and re-expressed E-cadherin. Compared to the paired ectopic primary tumors in the spleens, the partially reverted MDA-MB-231 cells in the liver exhibited lower expression of Vimentin and Ki-67 suggesting this partial reversion is more indicative of a dormant phenotype.

Conclusions: We conclude that the pre-stressed liver microenvironment confers a metastatic seeding advantage to the breast cancer cells at least in part by promoting a more pronounced epithelial reversion marked by E-cadherin up-regulation. *In vivo* studies confirmed that E-cadherin correlates to metastatic proliferation and outgrowth. This suggests that the metastatic microenvironment plays a role in metastatic competency through modulating the tumor cell EMT/MErT plasticity and should be considered as a potential target for ablating disseminated tumor cells.

5.2 INTRODUCTION

As dissemination of EMT cells from the primary tumor is common as noted by tumor cells in circulation (Aleamar and Schuur, 2013), but few progressive metastases follow (Chambers et al., 1995; Brackstone et al., 2007), we posit that conditions of the pre-metastatic microenvironment largely dictate whether breast cancer cells will seed, survive, and become either proliferative or dormant. Focusing on the hepatic metastatic niche we hypothesize that biochemical and biophysical stress particularly primes the liver for metastatic seeding and triggers a hepatic compensatory response fostering dormant conditions for metastatic cancer cells. Clinically this stress may be triggered by hematogenous shear forces surrounding the disseminated cancer cells at the ectopic site, systemic pre-signaling from the primary tumor, tumor-independent liver stress (such as localized infection), secreted factors from the disseminated cancer cells (or resident hepatic cells), or a combination of the above.

It is generally argued that it is the subpopulation of cancer cells in the primary tumor that acquire mesenchymal properties that then disseminate. This epithelial-to-mesenchymal transition (EMT) provides for invasiveness to gain access to conduits for spread. However, micrometastases often present an epithelial phenotype. We have previously found that normal parenchymal cells of certain metastatic organs cause a partial reversion of the EMT cells to a more epithelial phenotype termed Mesenchymal to Epithelial Reverting Transition, or MErT (Wells et al., 2008). Compared to carcinoma cells in the primary breast tumor, MErT cells are characterized by increased E-cadherin expression, MAPK and AKT signaling, and chemoresistance (Chao et al., 2011). MErT provides not only survival signals to the breast cancer cells but may also drive differentiation and limit autocrine signaling (or extracellular factors) that otherwise may prompt the breast cancer cells to initiate metastatic outgrowth.

However, this occurs only after carcinoma cell proliferation in the case of breast cancer. Thus, it is likely that the metastatic niche needs to provide for a hospitable environment at least temporarily for the mesenchymal-like disseminated cells.

Therefore we aimed to determine whether pre-stressed hepatocytes would impart a metastatic seeding advantage and confer a stronger MERT response to the breast cancer cells. Our experiments focused on two signals extant during metastasis to the liver, EGF given the high degree of EGF secretion by metastatic breast cancer cells and lipopolysaccharide given the drainage conduits from the gut to the liver. We found that EGF-stimulated hepatocytes (challenged prior to breast cancer cell inoculation) increased the breast cancer cell clustering morphology indicative of an epithelial reversion. In addition, we found epithelial markers including E-cadherin increased thus demonstrating an enhanced mesenchymal-to-epithelial reversion over standard hepatocyte cultures.

5.3 RESULTS

5.3.1 Pre-stressing hepatocytes does not significantly damage the cells while causing homotypic E-cadherin membrane delocalization

We challenged rat or human hepatocytes with EGF for 6 hours; the hepatocytes had a prior 24 hours to recover from plating. We aspirated the treatment medium and rinsed gently with PBS prior to seeding the breast cancer cells. We confirmed that pre-stressed hepatic cultures were similar in blood urea nitrogen (BUN) and Aspartate aminotransferase (AST) to untreated controls (Figure 23), demonstrating that the challenges did not significantly damage the cells.

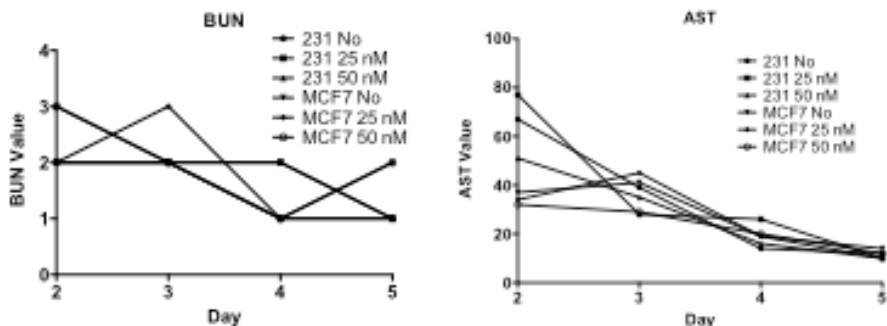


Figure 23. BUN and AST levels in 2D cultures are similar between pre-stressed and non-stressed hepatic cultures with either MDA-MB-231 or MCF-7 cells. EGF was incubated for 6 hours prior to aspiration and PBS washes. 231 No and MCF7 No categories reflect cultures not incubated with EGF.

It has been demonstrated that breast cancer cells can re-express E-cadherin and form heterotypic connections with hepatocytes but not mesenchymal cells such as fibroblasts (Chao et al., 2012). However, for tumor cells to intercalate among cells in an epithelial sheet, those cells need to separate. Thus, we asked whether pre-stressed hepatocytes would down-regulate their E-cadherin. The 6-hour EGF pre-stressed human hepatocytes experienced pronounced E-cadherin cytosolic internalization and cell-cell physical disruption compared to the non-EGF controls (Figure 24, left panel). A 24-hour EGF pre-stress at the same 20nM concentration demonstrated that this process is reversible by E-cadherin reverting to its membrane-bound state (Figure 24, right panel). These data support that the pre-stressed hepatic niche can be minimally damaging to the hepatic function while being substantially disruptive to their interconnections.

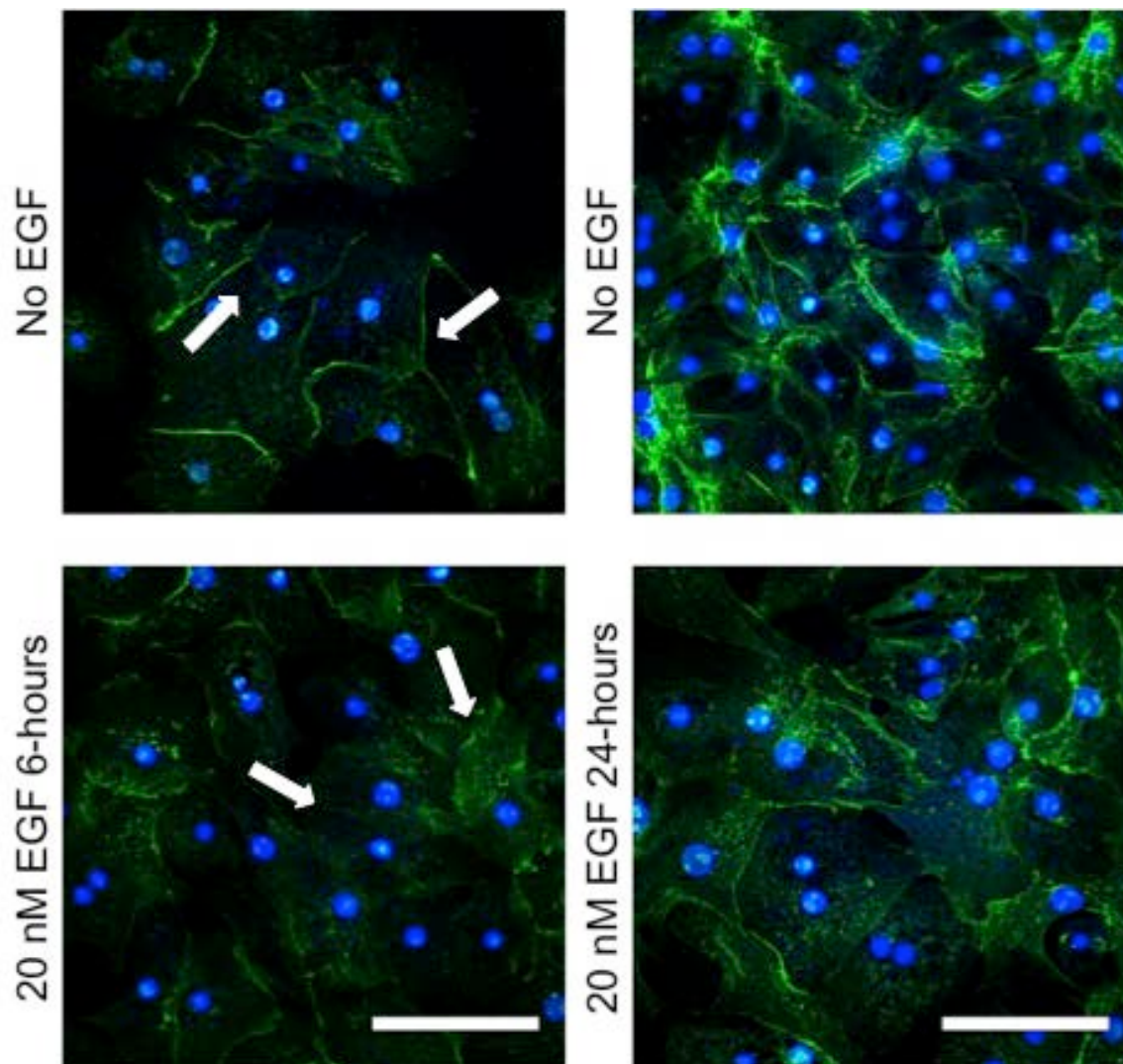


Figure 24. Human hepatocytes fail to maintain membrane-bound E-cadherin in pre-stressed cultures during the 6 hour EGF incubation period. E-cadherin (shown in green) delocalizes from the hepatocyte membranes at the 6-hour timepoint (versus the No EGF controls). After 24 hours of EGF incubation the hepatocytes begin to restore membrane-bound E-cadherin suggesting that the pre-stress EGF condition provides an opportunity for breast cancer cells to intercalate for seeding, and then become incorporated into the restored heterotypic E-cadherin connections. Scale bars 50 micrometers.

5.3.2 Pre-stressed hepatocytes induce an epithelial-like clustering morphology in breast cancer cells and prompt E-cadherin up-regulation.

We hypothesized that breast cancer cells in pre-stressed hepatic cultures would experience a metastatic seeding advantage among the disrupted hepatocytes. We found that breast cancer cells in the pre-stressed hepatocyte cultures formed greater numbers of metastatic clusters (Figure 25a) as quantified by contiguous 4-cell or greater metastases (Figures 25c) indicative of a more epithelial phenotype. However, cluster size was not significantly different between the pre-stress versus no-stress cultures (Figure 25b).

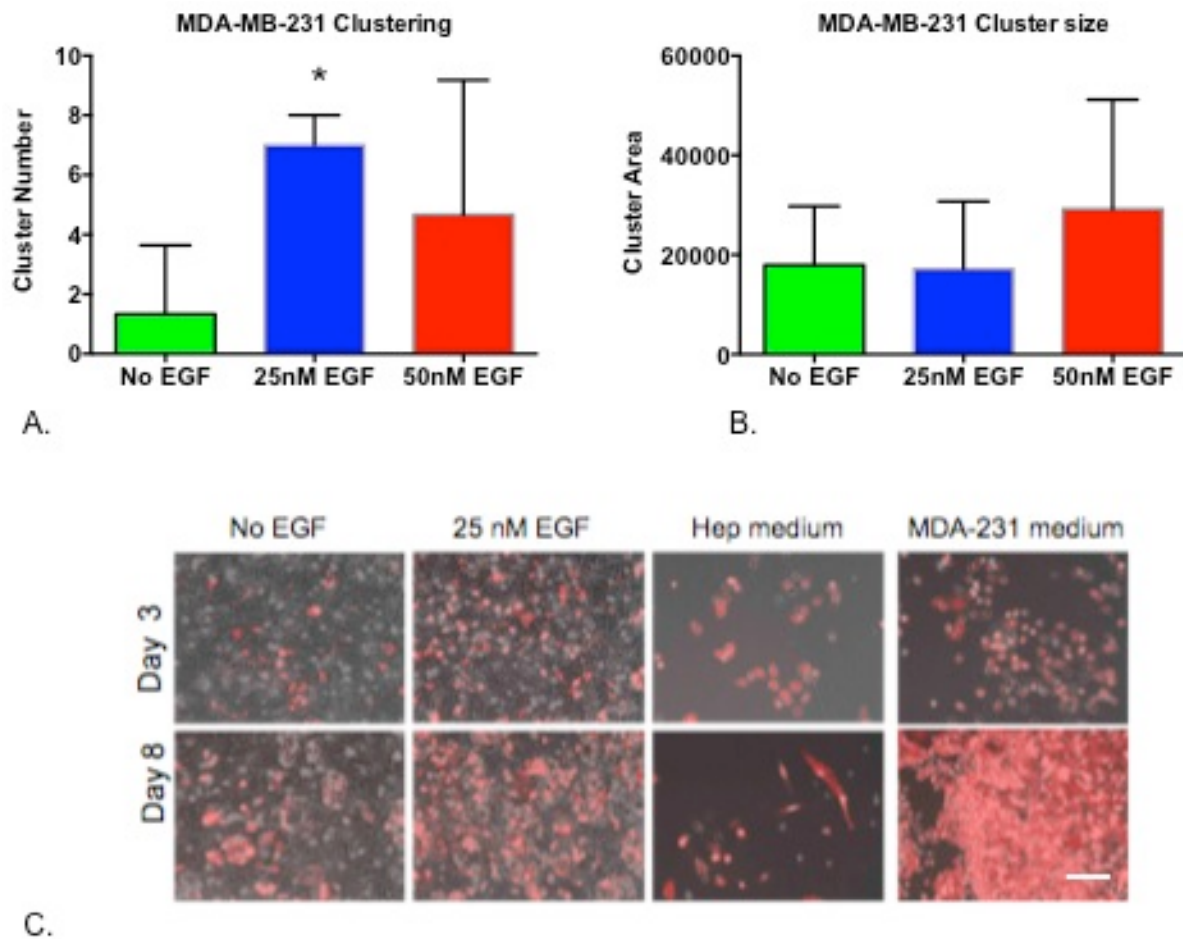


Figure 25. MDA-MB-231 cells form greater numbers of epithelial-like clusters in pre-stressed versus non-stressed co-cultures (Panel A) for 20nM EGF cultures (incubated for 6 hours prior to breast cancer cell inoculation). There was no significant difference in cluster area across the pre-stress conditions (Panel B). Clusters were defined as 4 or more contiguous MDA-MB-231 cells across 9 fields per well in duplicate. Scale bar 200 micrometers.

5.3.3 Pre-stressed hepatocytes impart a grow-out advantage to breast cancer cells.

The functional significance of a pre-stressed hepatic niche was investigated. Flow cytometry revealed that EGF pre-stressed hepatic cultures contained significantly greater numbers of MDA-MB-231-RFP cells by Day 5 of hepatocyte co-culture (Figure 26).

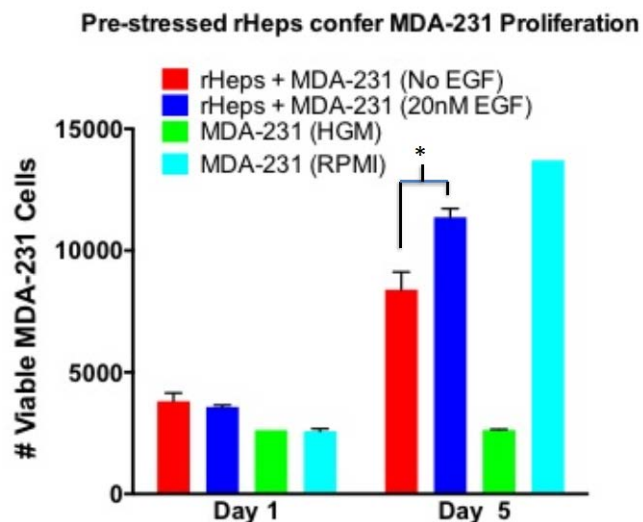


Figure 26. Pre-stressing promotes cancer cell proliferation. By day 5 of co-cultures, there were 35% more MDA-MB-231 cells in the pre-stressed hepatic cultures versus the non-stressed controls as quantified by flow cytometry for Annexin V negative, RFP-positive MDA-MB-231 cells. Error bars represent the standard deviation from the mean of three technical replicate samples. P value < .01

Mean RFP intensity quantification from 2D images corroborated this same finding (data not shown).

5.3.4 MErT is enhanced in the pre-stressed hepatocyte cultures

We have previously demonstrated that human or rat primary hepatocyte co-cultures in 2D and 3D promote passive loss of E-cadherin promoter methylation and subsequent re-expression in MDA-MB-231 breast cancer cells (MErT). This phenomenon confers survival advantages to the breast cancer cells including chemoresistance and survival signaling such as ERK/MAPK up-regulation.

Confocal immunofluorescent imaging revealed that breast cancer cells within the pre-stressed hepatic cultures more strongly reverted their epithelial phenotype as defined by E-cadherin expression (Figure 27).

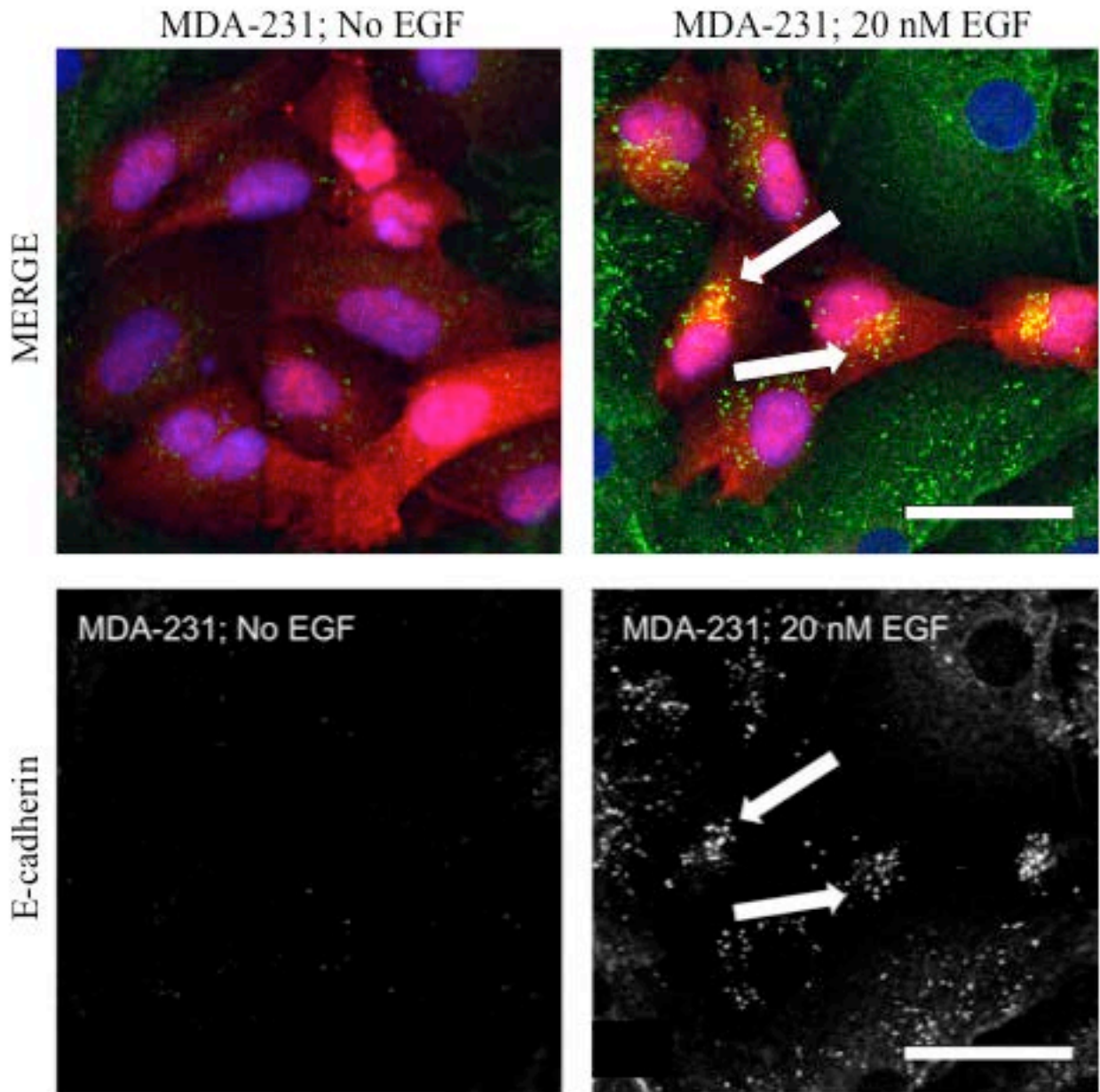


Figure 27. E-cadherin is more strongly expressed among breast cancer cells co-cultured in pre-stressed hepatocytes. MDA-MB-231 breast cancer cells (red) weakly re-express E-cadherin (green) in no press hepatic cultures (left panel). Pre-stressed cultures (20nM EGF) elicit a stronger E-cadherin re-expression (right panel). Scale bar 50 micrometers.

As the re-expression of E-cadherin in the 2D hepatic niche was realized we wanted to investigate whether MERT would occur *in vivo* and to determine whether a dormant or emergent phenotype would ensue. We therefore performed intrasplenic injections of MDA-MB-231 E-cadherin expression variants in order to establish primary ectopic breast tumors that would give rise to liver metastases.

5.3.5 MDA-MB-231 cells undergo mesenchymal to epithelial reversion in spontaneous metastases derived from ectopic primary tumors in mouse models

Splenic injections of breast cancer cells into NOD/scid gamma mice were performed to determine whether spontaneous metastases to the liver revert E-cadherin *in vivo*. Three cell injection groups were performed: 1) wild-type MDA-MB-231, 2) MDA-MB-231 cells exogenously expressing E-cadherin, and 3) MDA-MB-231 cells with shRNA to E-cadherin. Five hundred thousand cells of each treatment group were injected into the spleen and the mice were sacrificed 30 days later. Livers and spleens from all three injection groups exhibited macroscopic ectopic primary tumor and metastasis formation (Figure 28).



Figure 28. Spleens and livers were harvested from the three MDA-MB-231 variants across 18 NOD/scid gamma mice. Metastases were macroscopically apparent in all injections from their cognate ectopic primary tumors in the spleens.

Histological analysis of these organs revealed that the MDA-MB-231 injections exhibited more differentiated metastases than their cognate ectopic primary tumors (Figure 29).

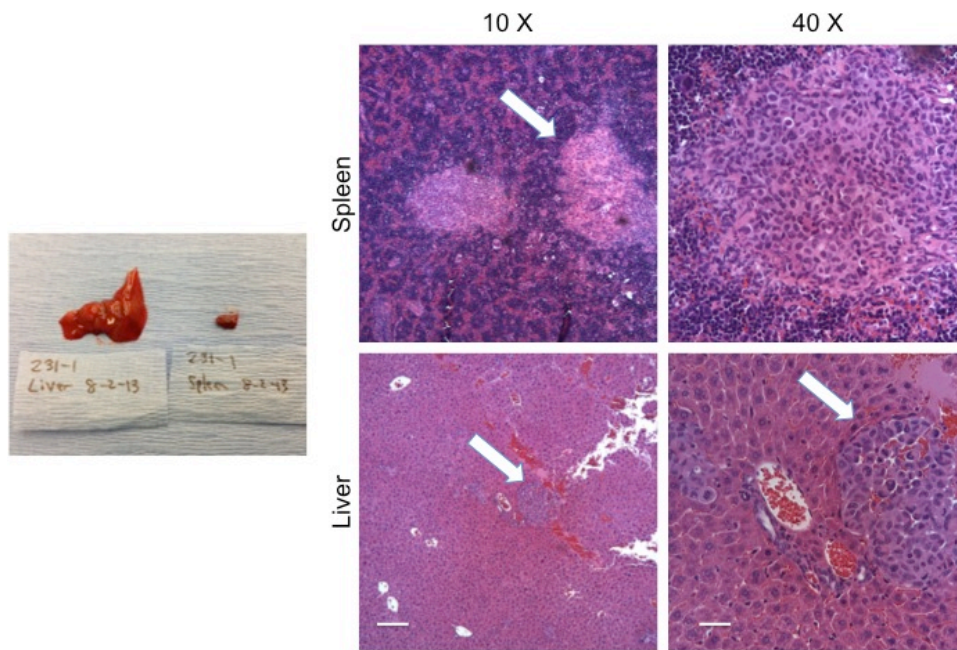


Figure 29. MDA-MB-231 cells injected into mouse spleens formed irregular and disorganized ectopic primary tumors while the paired liver metastases exhibited a more organized and clustered phenotype. This demonstrates that the metastases histologically appear more differentiated than their primary tumor cognates. Scale bars – 10x 200 micrometers, 40x 50 micrometers.

The E-cadherin knock down injections exhibited a de-differentiated morphology for both the ectopic primary tumors and metastases (Figure 30).

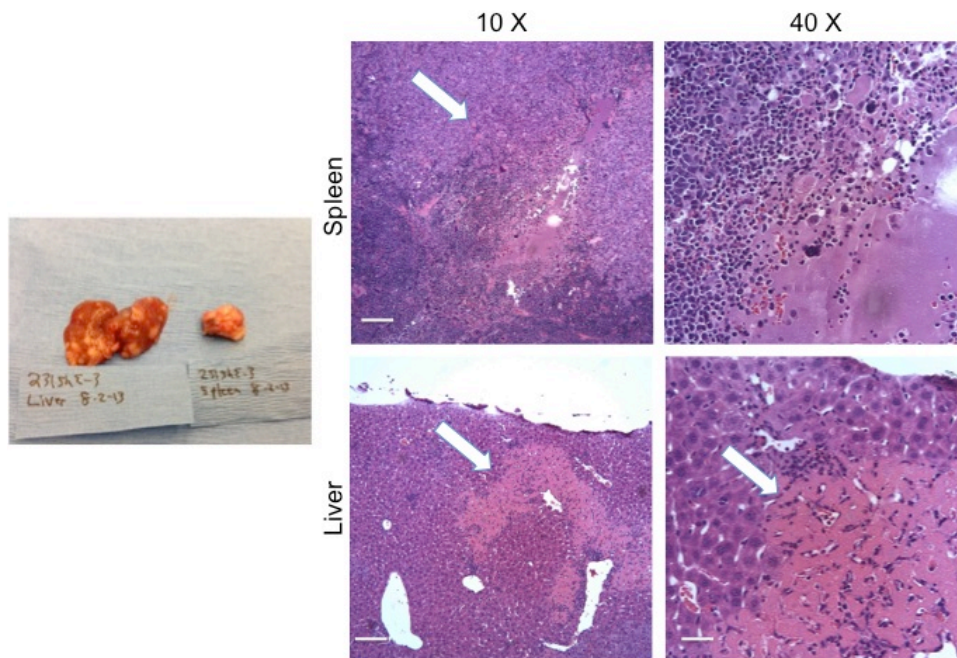


Figure 30. The MDA-MB-231 E-cadherin knock-down cell injections maintain a de-differentiated and irregular morphology in both the ectopic primary tumors and paired liver metastases. Scale bars – 10x 200 micrometers, 40x 50 micrometers.

We next investigated whether E-cadherin was re-expressed in the liver metastases first by immunohistochemistry. Immunoperoxidase staining against a human specific primary E-cadherin antibody was performed on sections of the formalin fixed, paraffin embedded tissues. The MDA-MB-231 wild type injections were E-cadherin negative in the spleen while their liver metastases stained positive for E-cadherin (Figure 31).

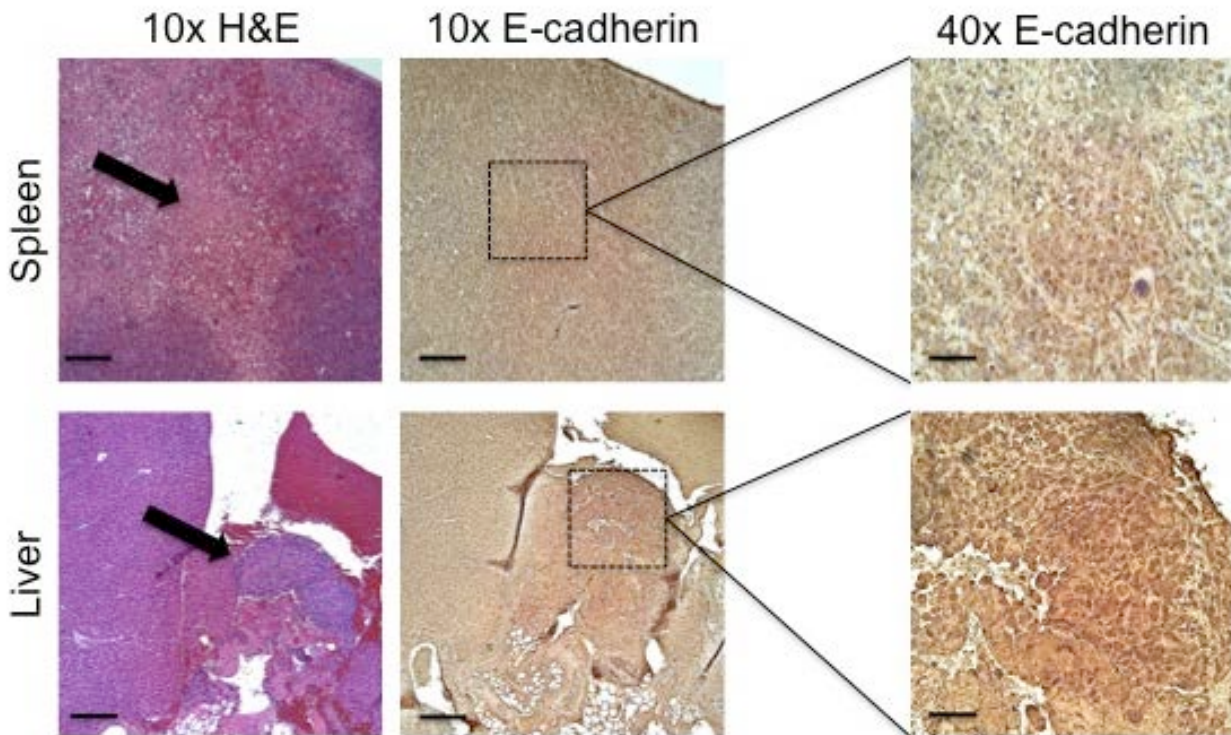


Figure 31. MDA-MB-231 injections into NOD/scid Gamma mice. Spleens are E-cadherin negative while their cognate liver metastases stain positive for E-cadherin. Scale bars – 10x 200 micrometers, 40x 50 micrometers.

The MDA-MB-231 cells exogenously expressing E-cadherin were E-cadherin positive in the spleen while their liver metastases stained positive for E-cadherin (Figure 32).

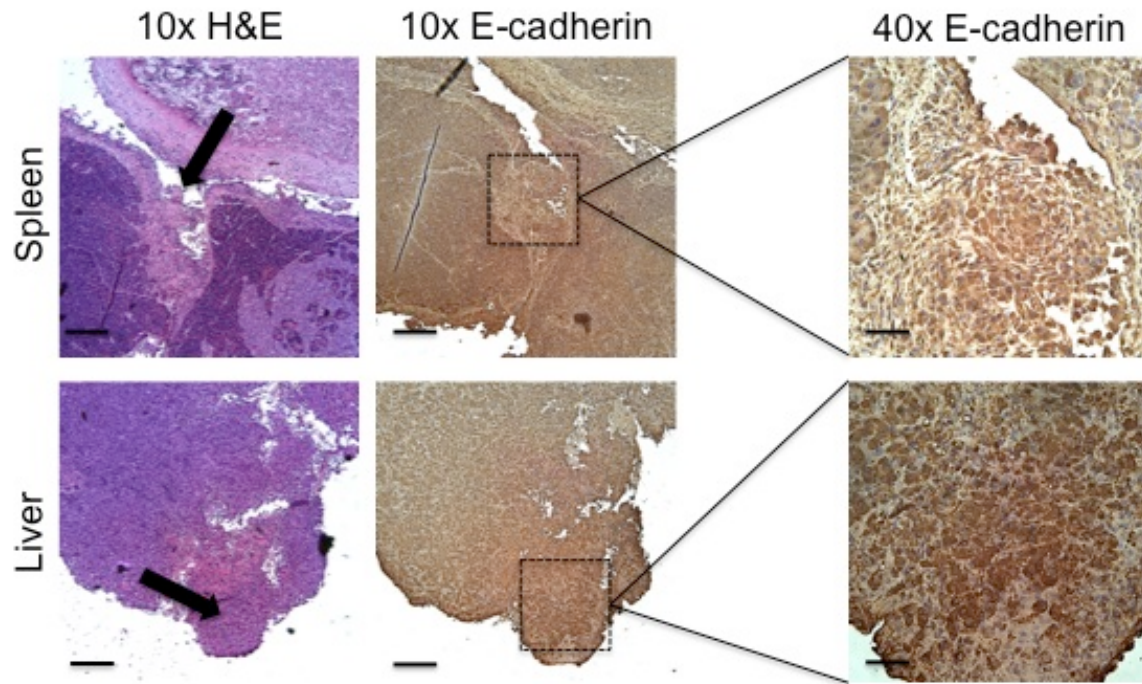


Figure 32. MDA-231Ecad cells injected into NOD/scid gamma mice. Scale bars – 10x 200 micrometers, 40x 50 micrometers.

The MDA-MB-231 cells exogenously repressing E-cadherin were E-cadherin negative in the spleen while their liver metastases were also E-cadherin negative (Figure 33).

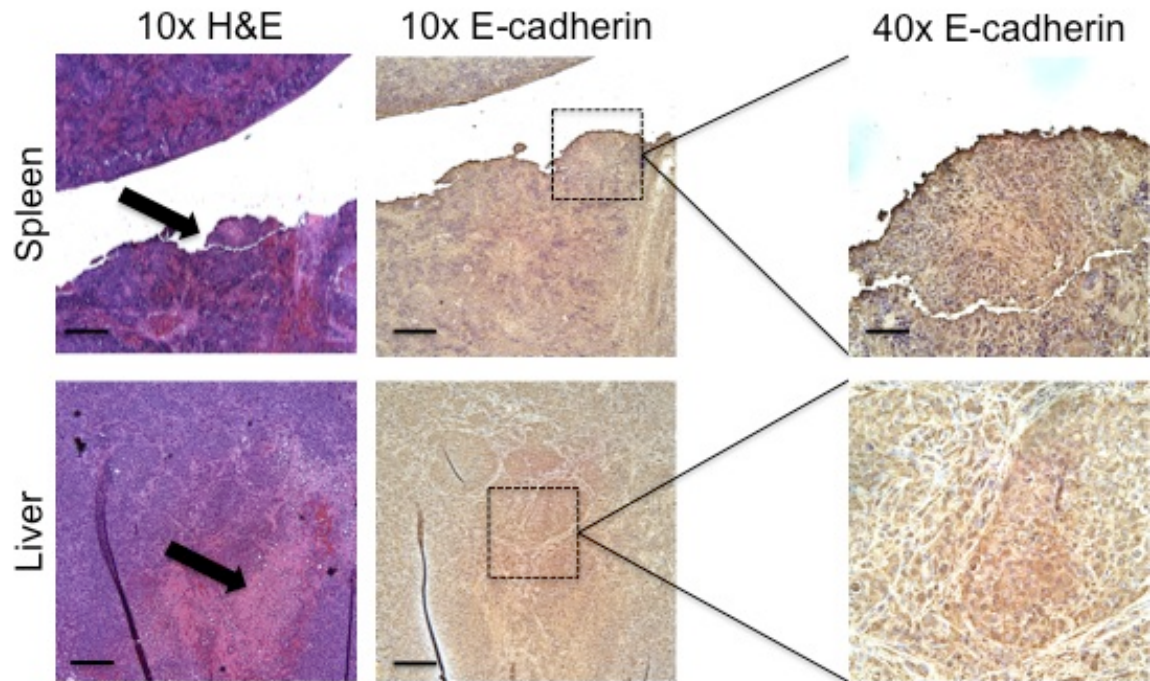


Figure 33. MDA-231shEcad injections into NOD/scid gamma mice. Scale bars – 10x 200 micrometers, 40x 50 micrometers.

To further validate the E-cadherin status of each injection group for the paired organ samples we performed reverse transcriptase quantitative polymerase chain reaction (qRT-PCR) from the flash frozen tissue samples. E-cadherin expression levels in spleens normalized to the MDA-MB-231 wild type spleen samples showed no expression except for in the exogenously expressing E-cadherin lines (data not shown). The qRT-PCR results confirmed that E-cadherin is re-expressed in the MDA-MB-231 wild type samples (Figure 34).

E-cadherin levels in paired organs

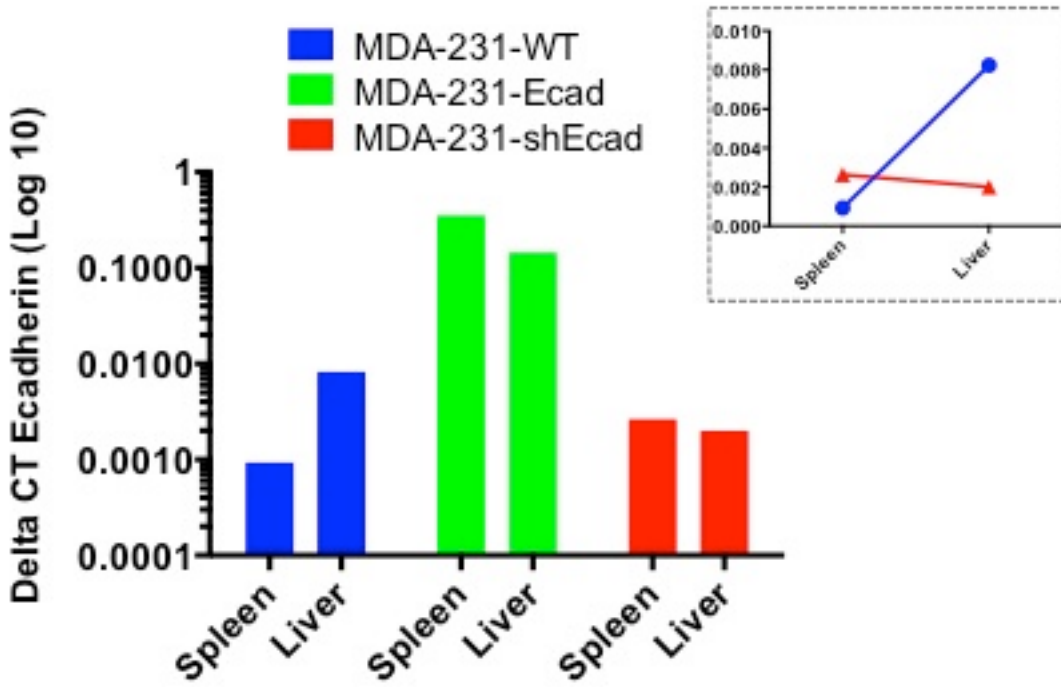


Figure 34. E-cadherin increases in MDA-MB-231-WT spontaneous metastases to the liver (MErT). In the main graph the y-axis represents E-cadherin normalized to GAPDH with the delta CT transformation ($1/2^x$) where x = mean E-cadherin CT normalized to GAPDH CT within 3 samples of each tissue. Inset – represents the same E-cadherin quantification as in the main graph, but depicts the MDA-MB-231-WT (blue) and shEcad (red) on a linear scale. Human E-cadherin and GAPDH primers.

5.3.6 E-cadherin expression in the metastatic niche correlates with proliferation and outgrowth

We next investigated whether the liver metastases of MDA-MB-231 wild type injections differentially expressed markers for a dormant or emergent phenotype. We performed immunohistochemistry on the samples and discovered that the E-cadherin reverting metastases were lower in Vimentin and Ki-67 expression suggesting that a more dormant phenotype correlates with E-cadherin re-expression in the metastatic niche (Figure 35).

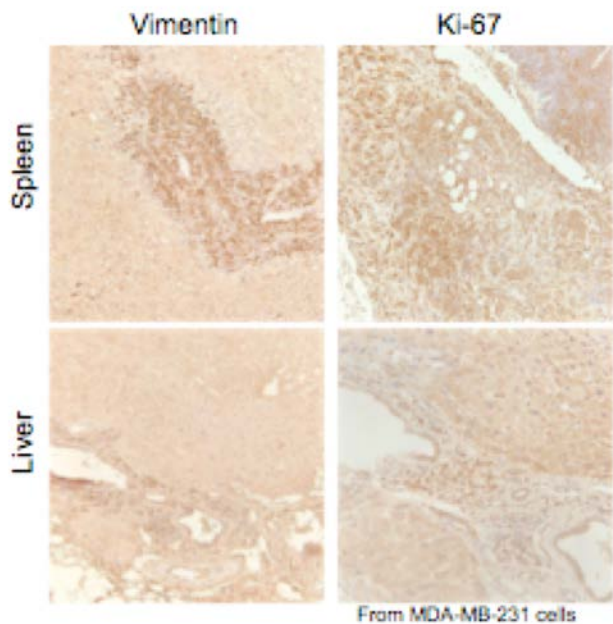


Figure 35. Spleens strongly stain for Vimentin and Ki-67 versus their paired liver metastases.

5.4 DISCUSSION

Cancer-associated EMT cells are capable of extravasation into the liver parenchyma from the pre-capillary constriction sites in which they may become arrested. Although EMT cell migration deeper into the liver parenchyma may not be required for survival, proliferation, or further systemic invasion, we posited that a favorable microenvironment is necessary for either inducing a grow-out phenotype or metastatic dormancy. Therefore we hypothesized that as part of the dormant transition, cancer-associated EMT cells must extravasate within a protective sheath of hepatocytes. Thus, we investigated whether a pre-stressed hepatic niche was more accommodating to the E-cadherin re-expression and heterotypic binding between the hepatic parenchyma and the cancer-associated EMT cells.

The liver is a highly regenerative organ that can recover from substantial injury and even two-thirds partial resection (Taub, 2004). While remodeling from injury the liver can simultaneously carry out its hepatic functions through a tightly orchestrated signaling cascade resembling wound healing across the entire organ (Michalopoulos and DeFrances, 1997). This hepatic remodeling hierarchy has been studied most closely in partial hepatectomy (PHx) – serving as a surrogate model system for behavior expected from the pre-stressed hepatic niche (Figure 1). The signaling cascade following PHx begins as soon as five minutes and lasts up to approximately 15 days – providing a sufficient window for EMT cell extravasation into the liver parenchyma to be caught in this process. Within 24 hours of PHx the hepatocytes begin DNA synthesis and eventually recreate the original liver mass, with at least one interesting exception.

In the remodeled liver the hepatic plates are thicker and the liver lobules are larger (Michalopoulos, 2007). This may reasonably result in a superior microenvironment for breast cancer cells to undergo a more pronounced MErT phenotype. Hepatocyte proliferation often exceeds the original hepatic mass but a wave of apoptosis attenuates such overgrowth (Sakamoto et al., 2009). Further, hepatic lobules continually remodel even weeks after PHx (Wagenaar et al., 1993). Taken together, these stress signaling cascades optimized for balancing liver growth and atrophy may trigger dormancy in disseminated breast cancer cells whereas an unchallenged liver microenvironment would only support MErT with continued proliferation.

Tumor dormancy in primary and secondary cancers may be described as a state in which cancer cells avoid clinical detection over a period of many years or decades – as these cancer cells remain as microscopic foci or single cells versus detectable masses undergoing continual growth. Metastatic dormancy may be characterized by cell cycle arrest and a quiescent state in which metabolic function is diminished to the lowest survival maintenance levels. Dormancy would likely require a combination of normal and abhorrent cell survival and apoptotic signaling pathways, coupled with a phenotype suitable for avoiding the body's immune response and harnessing a microenvironment appropriate for survival. Thus, tumor dormancy defined in this way is likely not sustainable by the invasive, metastatic cancer cells and so we propose a reversion to a more epithelial phenotype is at least partially required for tumor cell dormancy (Chao et al., 2010; Yates et al., 2007). However, another prevailing theory cites a balance of apoptosis and proliferation among cancer cells in which exponential cellular growth is inhibited. This theory would support a cancerous mesenchymal phenotype without requiring a Mesenchymal to Epithelial Reversion Transition. In prior work we published that computer simulations of metastatic proliferation reveal quiescence as the more likely contributor to

dormancy (Taylor et al, 2013). The narrow probability range we identified for dormancy or late outgrowth makes it unlikely that for extended periods the micrometastases are actively proliferating and dying. Rather the cells are likely to be in a quiescent state. This is a critical distinction therapeutics targeting the cancer cells or even the metastatic niche would need to consider this difference.

Breast cancer has the insidious propensity to recur many years or decades after primary tumor diagnosis. This recurrence is typically refractory to current treatments including radiation, chemotherapy and surgical resection. Once compelling evidence establishes that dormant metastatic phenotypes can exist, the next logical step is to demonstrate how they can emerge from dormancy into invasive secondary carcinomas. From here drug-screening tools can be designed to select for those compounds (or biologics) that maintain cancer dormancy even in the presence of endogenous proliferation signals.

The same pre-stress conditions driving the seeding advantage may also participate in the dormancy phenotype. For example, a stressed hepatic niche may disrupt the normal functioning and ratios of non-parenchymal cells (such as liver sinusoidal endothelial cells) that may subsequently act upon the breast cancer cells triggering either a dormant or emergent phenotype. Epithelial versus mesenchymal phenotype may direct whether metastatic breast cancer cells establish clinically evident metastases, form dormant sub-clinical metastases, or even fail to initiate metastatic seeding. We have previously demonstrated that mesenchymal-to-epithelial-reverting transition confers chemo-resistance and survival signaling to breast cancer cells in the metastatic niche and herein we investigated whether E-cadherin re-expression is a likely precursor to metastatic dormancy. We discovered that a stressed metastatic niche confers a growth advantage and a stronger epithelial reversion in the highly metastatic breast cancer cell

line MDA-MB-231. We also found that liver non-parenchymal cells drive E-cadherin positive breast cancer cells to a mesenchymal phenotype. These data suggest that perturbations of the parenchymal and non-parenchymal cell ratios in the liver metastatic microenvironment may differentially contribute to metastatic dormancy, stability, or emergence. Therefore dormancy and emergence from dormancy may hinge upon the inactivated or activated status of the hepatic non-parenchymal cells, thus making the metastatic niche a potential therapeutic target to combat metastatic disease.

5.5 MATERIALS AND METHODS

5.5.1 Cells and cell culture

MDA-MB-231E (exogenously expressing E-cadherin) and MDA-MB-231shE (E-cadherin known-down) variants were transfected as previously described (Chao et al., 2010). To maintain selection cells were cultured with 900 ug/ml G418 (MDA-MB-231E) or 5 ug/ml puromycin (MDA-MB-231shE) in RPMI-1640 (Life Technologies, Carlsbad, CA) supplemented with 10% FBS until used in the experiments.

5.5.2 Animal procurement and care

Four-week-old female NOD/scid gamma mice (The Jackson Laboratory, Bar Harbor, ME) Cat# 005557 were ordered through the Pittsburgh VA Healthcare center and acclimated for at least 7

days prior to experimentation. Mice were injected with approximately .05 mL of Ketamine and Xylazine to anesthetize the animals. Following surgery the mice were observed until they were independently walking and showing no signs of distress. To minimize distress mice recovered on a heating pad, with a heating gel pack placed in their cage following recovery. For any mice showing distress on subsequent days, approximately .05 mL of Buprenorphine was injected to relieve pain. Euthanasia was performed using a carbon dioxide chamber consistent with the recommendations of the American Veterinary Medical Association (AVMA) Guidelines on Euthanasia.

5.5.3 Imaging

Phase contrast images were captured by an Olympus inverted scope and digitally captured using Spot Advanced™ software (Diagnostics Instruments, Macomb, Michigan). Confocal images were captured on an Olympus Fluoview 1000 scope (Olympus, Center Valley, PA) and captured using Fluoview Viewer™. Immunofluorescence was performed by 24-hour primary antibody incubation against E-cadherin Cat# 610182 (BD Biosciences) at 1:200 dilution. Alexa Fluor® 488 rabbit anti-mouse (Life Technologies) secondary antibody was incubated for 45 minutes at room temperature at 1:500 dilution. Hoechst was incubated for 10 minutes at 1:500 dilution at room temperature.

5.5.4 Flow cytometry

Cell cultures in each were incubated in trypsin for 30 minutes until dissociated. 2 mL of PBS with 2% FBS were added to each well, transferred to flow tubes, and pelleted. The media were

aspirated and cell pellets incubated with the reconstituted components of the Alexa Fluor® 488 Annexin V/Dead Cell Apoptosis Kit (Life Technologies, Carlsbad, CA) for 15 minutes. The reaction was terminated by adding 100 ul of the Annexin binding buffer to each tube. 10 uL of CountBright™ Absolute Counting Beads (Life Technologies, Carlsbad, CA) in order to compute the number of RFP positive, Annexin V negative breast cancer cells. Cell suspensions were run on the BD LSRFortessa™ flow cytometer and BD FACSDiva Software (BD Biosciences, Franklin Lakes, NJ).

5.5.5 Quantitative real-time PCR

Flash frozen liver and spleen tissues were thawed and mechanically digested to release RNA into solution. The RNEasy Kit (Qiagen, Valencia, CA) was used to extra total RNA from the digested tissue. QuantiTect (Qiagen, Valencia, CA) was used to reverse-transcribe 1µg of each RNA sample into cDNA. We then performed quantitative PCR using SYBR Green (Agilent, Santa Clara, CA) on 1µL of each cDNA sample with the following primers: E-cadherin: forward 5'-ATCCCAAGTGCCTGCTTTT-3'; reverse 5'-ACCCCTCAACTAACCCCTT-3' GAPDH: forward 5'-GAGTCAACGGATTTGGTCGT-3'; reverse 5'-TTGATTTTGGAGGGATCTCG-3'. All primers were ordered from idtDNA. Quantification was performed by the delta CT method and normalized to either paired spleen GAPDH or wild-type MDA-MB-231 spleens.

5.5.6 Immunohistochemistry

Harvested tissues were fixed in formalin, processed and then paraffin embedded. Samples were cut and mounted on glass slides and stained under normal procedures for hematoxylin & eosin.

5.5.7 Statistical Analysis

Except where otherwise noted, graphical data are provided as mean +/- standard deviation from three independent technical replicates. P-value significance was evaluated using ANOVA and Tukey method and set at a minimum 0.05. Images were representative of at least three independent fields per well.

6.0 3D ORGANOTYPIC BIOREACTOR SYSTEMS HOLD PROMISE TO UNCOVER METASTATIC DORMANCY AND EMERGENCE MECHANISMS

6.1 BIOREACTOR OVERVIEW

Limitations to traditional tissue culture have inspired a new generation of *in vitro* systems that more deftly recapitulate the *in vivo* microenvironment. One such system is the now commercialized LiverChip™ system (licensed by Zyoxel, LTD, based in Oxfordshire, UK) jointly developed between the Massachusetts Institute of Technology in Cambridge, MA and the University of Pittsburgh in Pittsburgh, PA.

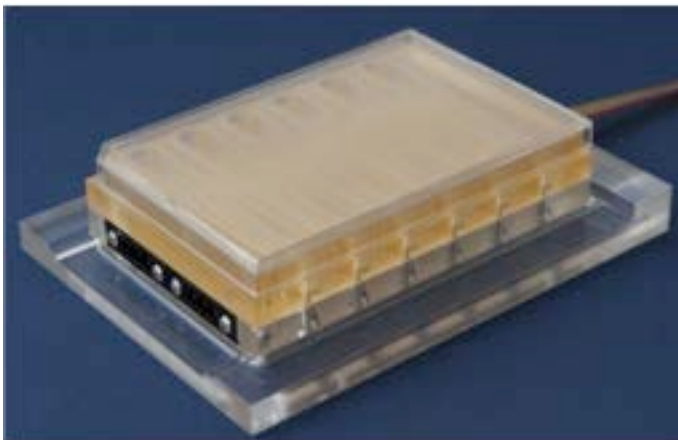


Figure 36. LiverChip bioreactor plate positioned within the pneumatic pump docking station.

The LiverChip™ functional unit is placed within a pneumatic docking station (Figure 36). Within this system are 12 hermetically sealed scaffold and reservoir chambers allowing for 12 independent tissue constructs.

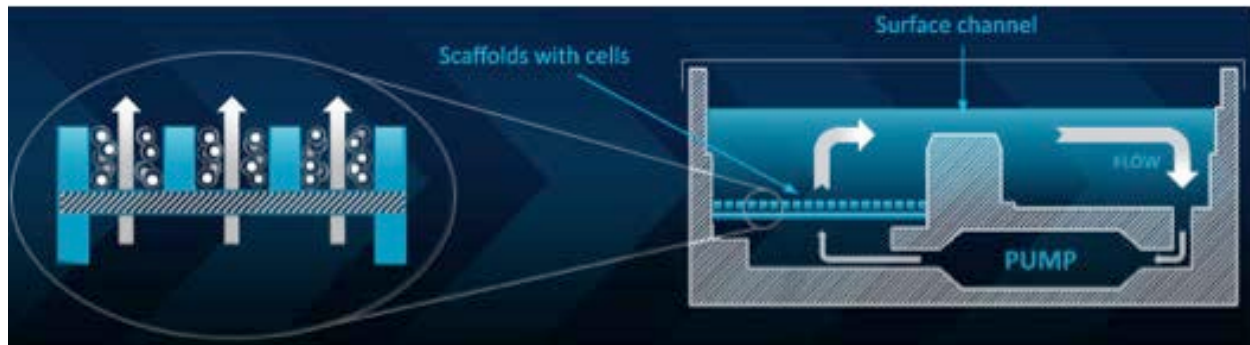


Figure 37. Cross sectional schematic of the LiverChips' reactor and reservoir system (Linda Griffith lab diagram).

Alternating vacuum and air pressure pneumatically drives the medium in a clockwise fashion up through the tissue scaffold (Figure 37), across the surface channel (in order to replenish dissolved oxygen) and down through the reservoir channel. Thus, the micro-tissue is under constant flow receiving re-oxygenated medium (typically at a rate of 2 microliters per second).

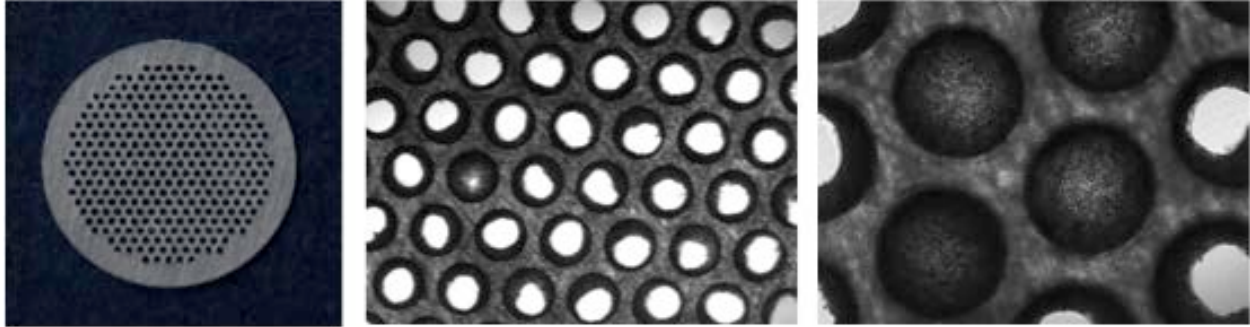


Figure 38. LiverChip scaffold

The hepatic tissues are formed in three dimensions within the channels of the polystyrene scaffolds. Phase contrast imaging at 4x and 10x (Figure 38 middle panel and right panel respectively) demonstrate hepatic tissue formation as indicated by the occluded channels.

6.2 REACTOR EQUATIONS FOR OXYGEN MASS TRANSPORT

Proper tissue oxygenation within the hepatic tissue constructs is a critical parameter for which to optimize in the bioreactor design. Improper oxygenation in the tissues can lead to necrotic lesions that can release cytokines and damage associated proteins into the system, thus compromising a normal hepatic microenvironment. Further, sub- or supra-physiologic oxygen concentrations can dramatically affect the pH of the bioreactor medium further compromising the hepatic tissues. So bioreactor design characteristics such as scaffold volume, well geometry, scaffold-to-air interface distance, and fluid flow rate must be optimized for proper oxygen consumption by hepatic tissues.

Therefore, in the bioreactor design and optimization, custom oxygen probes were employed to measure the scaffolds' inlet and outlet oxygen parameters. The convection

diffusion equation, $\frac{\partial c}{\partial t} = -v\nabla C + D_{O_2}\nabla^2 C - R$ can be used as a foundation to calculate

oxygen consumption through the tissue within the bioreactor scaffolds where v is fluid velocity, C is the concentration of oxygen, D_{O_2} is oxygen's diffusion coefficient, and R is the local rate of consumption. By transforming this mass transport equation into a dimensionless form (Inman, 2011) and using Michaelis-Menten kinetics, the equation becomes,

$$\frac{\partial c}{\partial t} = -v \nabla C + Pe^{-1}\nabla^2 C - Da \frac{c}{k_m + c}$$

where transport processes such as oxygen consumption can be derived.

6.3 FUNCTIONAL TISSUE CONSTRUCTS

Of critical importance in applying such a bioreactor technology to these *in vitro* investigations of metastatic dormancy is to ensure that the hepatic tissue constructs maintain hepatic functions.

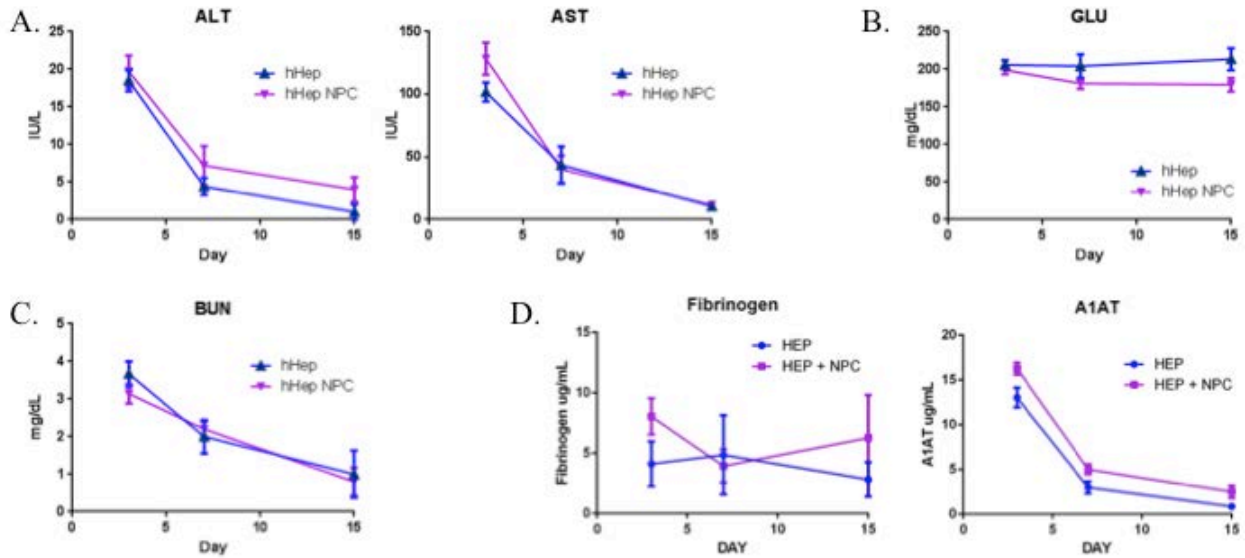


Figure 39. Evaluating LiverChip hepatic injury and function through extended culture periods.

Hepatic injury and function markers in hepatocyte-only versus hepatocytes plus non-parenchymal cells (NPCs) were evaluated in the LiverChip system over a 15-day culture period. Alanine aminotransferase (ALT) and aspartate aminotransferase (AST) decrease from an initial high level of Day 3 throughout the culture period (Figure 39a). We expected the elevated ALT and AST levels in the early culture period because the hepatic cultures are inherently injured during the bioreactor seeding process. The lower injury levels throughout the remaining period suggest that these hepatic cultures recover from the initial stress. Clinical tests for glucose concentration show no statistically significant difference in glucose consumption from the baseline of 200mg/dl as well as no difference between the two culture formats (Figure 39b). Hepatocyte protein catabolism function as measured by blood urea nitrogen (BUN) steadily declines over the culture period, but is still active on Day 15 (Figure 39c). Again, there was no difference between the hepatocyte-only and the hepatocyte + NPC cultures. We performed

ELIZA assays for alpha-1 anti-trypsin (A1AT) and fibrinogen (Figure 39d) to further measure hepatic tissue function. Fibrinogen maintained a steady level while we noted a decline in A1AT.

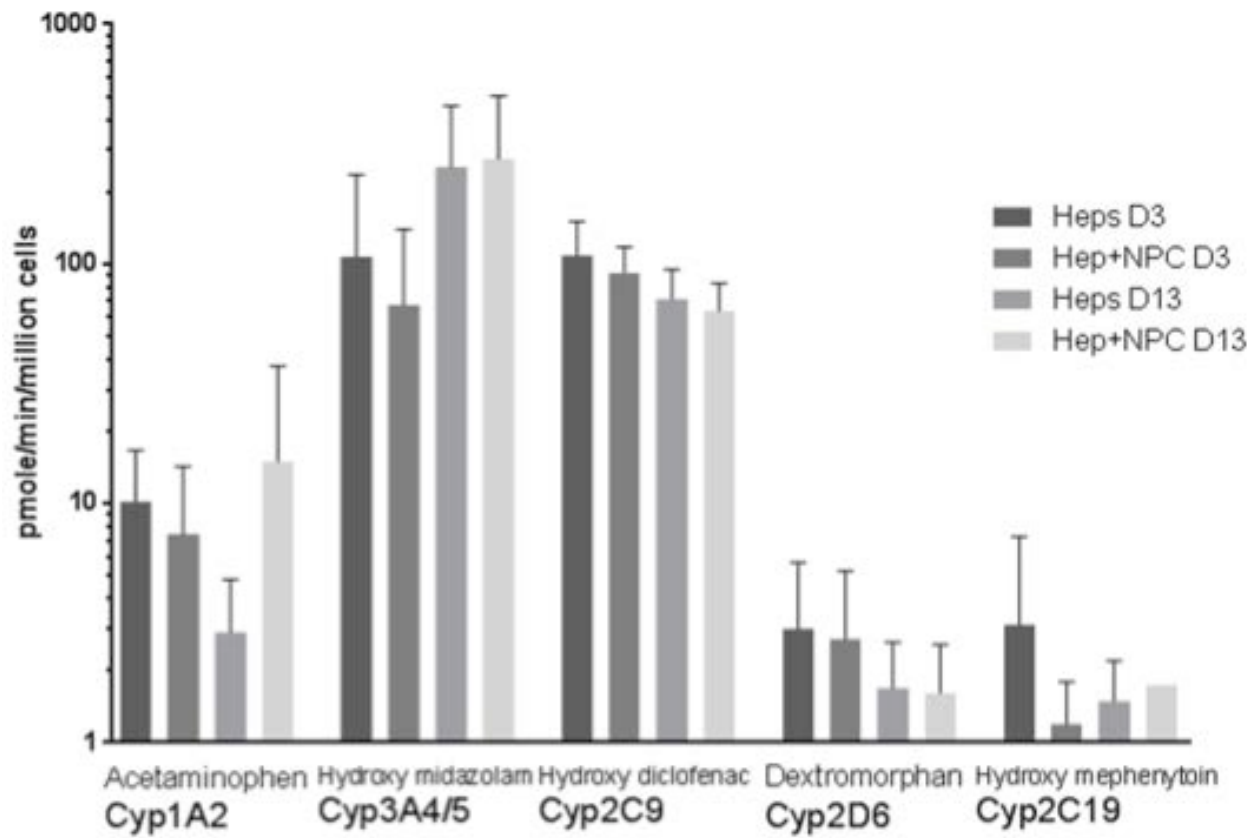


Figure 40. Cytochrome P450 activity in 13-day LiverChip cultures with and without non-parenchymal cells.

A primary characteristic of the liver is xenobiotic metabolism. The cytochrome P450 proteins in the liver perform these functions – with a handful of these P450's performing the majority of the metabolism. Therefore we assayed for the most common P450's to determine whether our hepatic tissue constructs were P450 functional on Day 13 versus Day 3. There was no significant difference between P450 functions on Day 13 versus Day 3, or between hepatocyte-only and hepatocyte + NPC cultures (Figure 40).

Together these hepatic health and injury markers demonstrate that the 3D hepatic tissue cultures maintain sufficient *in vitro* hepatic functions while having no marked difference with the inclusion of the non-parenchymal cells. These are encouraging results because a major concern of using 3D micro tissue cultures is having necrotic, non-functional tissue due to inadequate oxygen, nutrient, and waste diffusion through the tissues.

Now that we had determined from clinical chemistry and tandem LC mass spectrometry that the 3D hepatic tissue cultures were reasonably functioning as we'd expect, we imaged the reactor scaffolds to identify the cell types present.

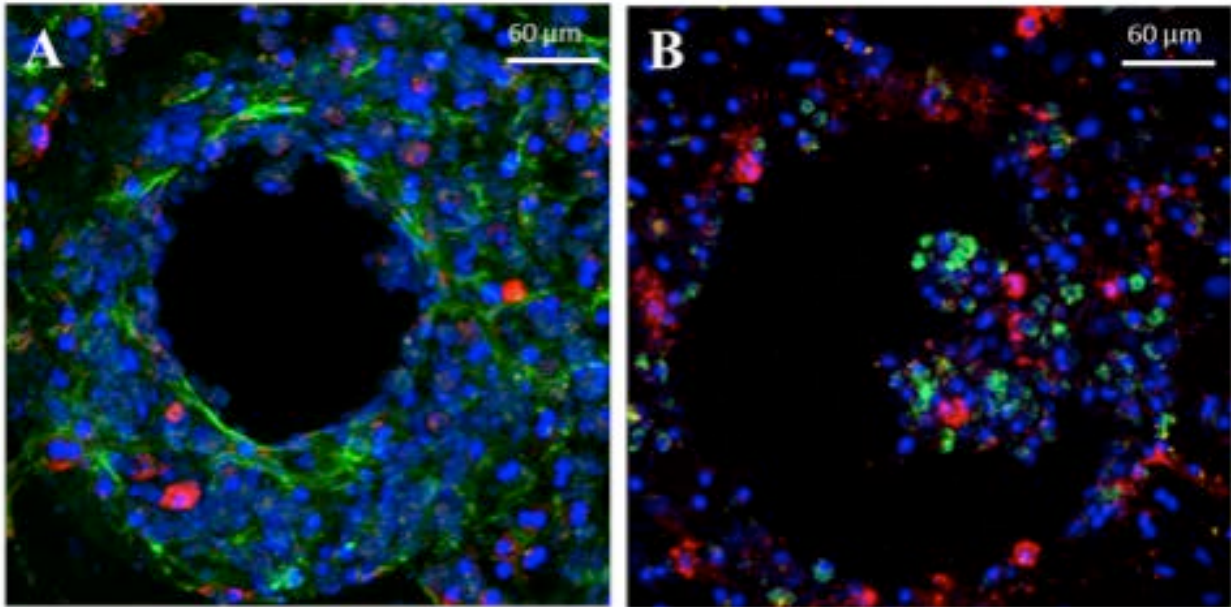


Figure 41. Day 15 of cryopreserved hepatic cultures (A) and freshly-harvested hepatic cultures (B). F-actin in green, kupffer cells in red (for CD68). Nuclei are stained blue (DAPI). Red is stained with CF45 which is a pan-leukocyte marker while green represents the liver sinusoidal endothelial cells (stained for Lyve-1). The nuclei are stained in blue (DAPI).

The non-parenchymal cells and hepatocytes form viable tissue through Day 15 further suggesting the liver bioreactor system is capable of supporting functional hepatic tissue constructs (Figure 41).

6.4 BREAST CANCER CELL INOCULATION

Next we investigated whether these 3D hepatic tissue constructs could support the intercalation of breast cancer cells.

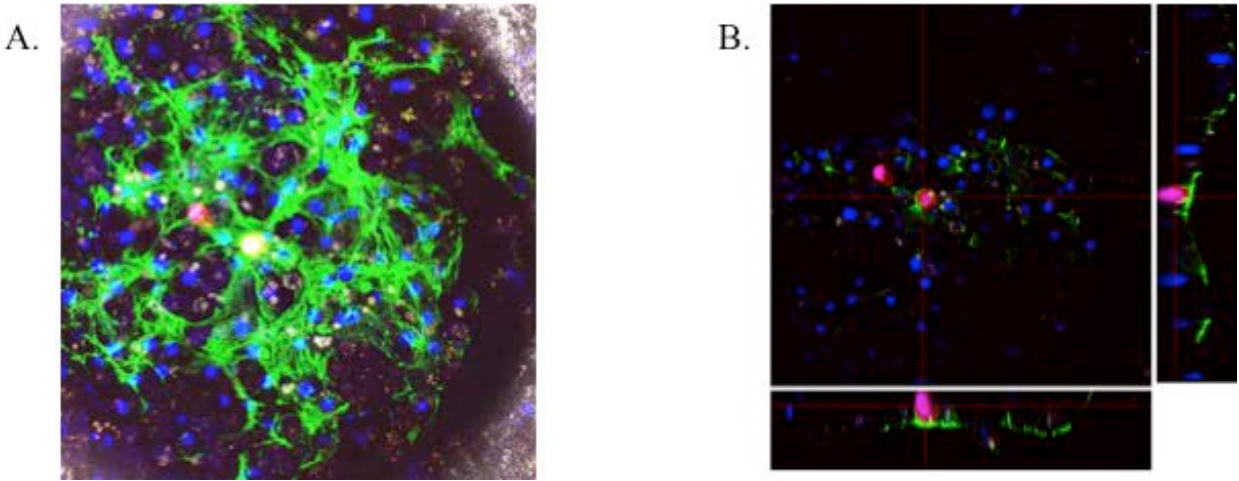


Figure 42. MCF-7 cells intercalating in the hepatic niche. A representative scaffold on Day 15 of the metastatic culture system. Actin is labeled in green, nuclei in blue (DAPI), and the MCF-7 cells are exogenously expressing dsRED (in red). B) is an orthogonal plan composite from A).

Freshly harvested human hepatocytes and matched non-parenchymal cells were inoculated in the LiverChip system on Day 1 and allowed to form stable tissue by Day 3. MCF-7 cells were inoculated in the bioreactor scaffolds on Day 3 and allowed to incubate through Day 15 when the scaffolds were sacrificed, fixed and stained. MCF-7 cells persist in the hepatic scaffolds on Day 15 (Figure 42a), embed and intercalate among the hepatic tissue constructs (Figure 42b). These data suggest that the micro hepatic tissues accommodate metastatic seeding and survival over these extended culture timeframes.

Next we aimed to investigate how the highly invasive MDA-MB-231 human immortalized breast cancer cell line would behave in this 3D reactor system.

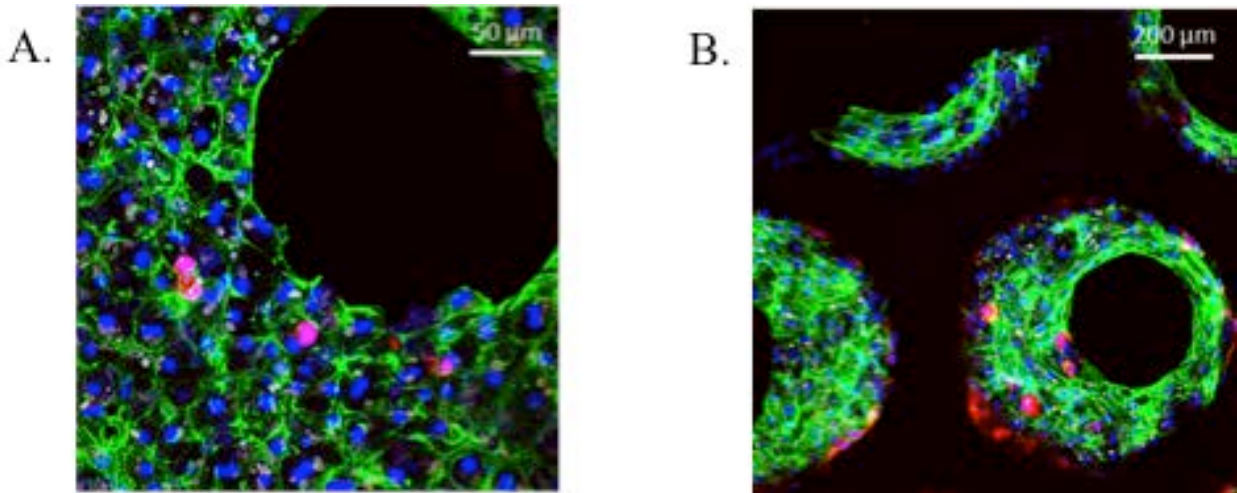


Figure 43. Spontaneous growth attenuation among sub-populations of human immortalized breast cancer cells. MCF-7 cells (Red) on Day 15 of co-culture in the LiverChip system. MCF-7 cells seeded Day 3 (1,000 cells per scaffold). B) MDA-MB-231 cells Day 15.

By Day 15 the MCF-7 cells did not experience exponential outgrowth as we've seen in our standard 2D co-cultures (Figure 43a). A sub-population of the highly invasive and metastatic cells (MDA-MB-231) attenuated their growth (Figure 43b). Further investigations are underway to assess the degree to which these breast cancer cells are characteristic of dormancy through assaying for the proliferation markers Ki-67 and BrdU. However, these are encouraging images suggesting that this 3D perfused microwell bioreactor system is capable of recapitulating a dormant metastatic microenvironment.

7.0 DISCUSSION

Despite advances in successfully treating breast cancer within the primary site (including new surgical techniques, improved radiological extirpation, and administration of targeted therapeutics) treating disseminated disease remains woefully unsatisfactory. As breast cancer (among other cancers) typically involves a serial progression of genetic aberrations from carcinoma *in situ* to widespread disseminated disease, most investigations have heretofore aimed to overcome the cancer's genetic abnormalities. Thus, we now have new drugs in our armament targeting malignant growth receptor activation (Trastuzumab) or hormone receptor over-expressers (Tamoxafen) ostensibly stemming from genetic abnormalities. These drugs can be quite successful in treating the appropriate patient sub-populations in the primary site, but are oftentimes only palliative for even those same patient populations for disseminated disease. Certainly one explanation may be that significant additional genetic degradation has occurred in those metastatic cells as a function of either time or being surrounded by a foreign microenvironment. However, there is another contributing factor that has been largely overlooked in comparison – that of the metastatic microenvironment itself conferring dormancy and emergence (as well as drug resistance). Therefore we have focused our investigations on the metastatic niche that may one day illuminate new drugs and therapies that perhaps could be effective against larger patient sub-populations independent of the carcinoma's genetic nuances.

We first sought to identify whether dormant breast cancer metastases were more likely to be in a state of cellular quiescence or active cycling, but equally offset by apoptosis (balanced proliferation). This is a critical distinction because the mechanism of action for existing drugs and therapies (such as radiation) are largely directed to cycling cells – as a consequence they would fail to eliminate cryptic quiescent cells. Unfortunately (as discussed in Chapter 6) traditional *in vivo* and *in vitro* model systems to resolve this distinction lack the ability to adequately recapitulate a dormant metastatic niche (although advances are being made via the implementation of 3D bioreactors). Therefore we developed a computational simulation of metastatic balanced proliferation and investigated at what survival probabilities the metastatic niche would need to confer to the carcinoma cells in order to invoke the dormant phenotype. We found that only a 1.1 percentage point survival probability range existed and therefore concluded that it's more likely that quiescence drives metastatic dormancy as the fluxing metastatic microenvironment is not conducive to such a narrow probability window. This finding (although not sufficient in itself to reject balanced proliferation completely) will hopefully be a catalyst for researchers to invest more resources toward the study of quiescence in order to help diagnose and/or treat dormant metastases.

Next we focused our attention to biochemical and biophysical aspects of the liver that could impart dormant or emergent phenotypes to metastatic breast cancer independent of the carcinomas' genetic makeup. Because the liver is a highly regenerative organ that is in a constant state of defense and offense in order to ensure its health and ability to function, we investigated the effect of the stressed hepatic microenvironment on breast cancer cells. Our hypothesis was that a stressed hepatic niche would more efficiently accommodate carcinoma cell intercalation and through the stress-response remodeling confer a more dormant phenotype. We

found that otherwise E-cadherin negative breast cancer cells more strongly re-expressed E-cadherin in pre-stressed hepatocytes but we noted increased breast cancer cell outgrowth – contrary to a dormant phenotype. However, the two dimensional *in vitro* system we initially employed may not be sufficient to capture the stress response dynamics that otherwise would have been imparted in a three dimensional culture system. Further investigations have been underway in the 3D perfused microwell bioreactor system (discussed in Section 6) in order to further investigate the role of a pre-stressed hepatic niche in breast cancer metastatic dormancy.

We further probed the hepatic niche driving the carcinoma dormancy and emergence phenotype by investigating the role of the non-parenchymal cells (NPCs). The oft-studied hepatic cells have been the parenchymal hepatocytes given they comprise greater than 70 percent of the liver's volume – and are the primary functional cell in hepatic metabolism. However, the non-parenchymal cells comprise nearly half of the liver by cell number but have received much less scientific investigation. Through co-culturing both primary non-parenchymal hepatic cells and NPC cell lines we discovered that the NPCs confer an outgrowth phenotype and a partial mesenchymal reversion to the otherwise epithelial and weakly metastatic human immortalized breast cancer MCF-7 cells. This finding has significant implication to new therapies directed to exogenously modify the non-parenchymal cell activation/in-activation status in order to maintain metastatic dormancy as a cryptic, indolent disease.

Finally we sought to illuminate the role that a known tumor suppressor protein (E-cadherin) plays in metastatic dormancy and emergence. E-cadherin is an adherens junction protein that's normally expressed by breast epithelial cells and is down-regulated in the majority of transformed carcinomas. Our lab has previously investigated the plasticity of this protein in the metastatic microenvironment and discovered that a proliferation dependent inability to

maintain E-cadherin promoter methylation drives E-cadherin re-expression in hepatocyte 2D and 3D culture systems. This discovery was a critical achievement because it demonstrated that at least *in vitro* the metastatic microenvironment could revert the mesenchymal E-cadherin negative breast cancer phenotype to a less aggressive epithelial phenotype – that our lab termed mesenchymal-to-epithelial reverting transition (MErT). However, this reversion in the liver had never been recapitulated through experimental systems *in vivo* – and so had not been ruled out as an artifact of *in vitro* culture systems. Therefore we sought to investigate whether those same E-cadherin negative breast carcinoma cells (MDA-MB-231) could undergo MErT in a spontaneous mouse model of metastasis to the liver. We intrasplenically injected three MDA-231 variants (MDA-231 wild type, MDA-231 E-cadherin knock-in, and MDA-231 E-cadherin knock-down) into groups of mice and performed immunohistochemistry and quantitative real time polymerase chain reaction to measure both E-cadherin levels and related markers of dormancy or emergence. Our findings uncovered for the first time that the MDA-231 wild type cells re-expressed E-cadherin in the mouse liver metastases thus validating the ability of the metastatic niche to revert the aggressive mesenchymal phenotype to a less aggressive epithelial phenotype. We further uncovered that those reverted metastases were less proliferative than the matched ectopic primary tumors as indicated by their Ki-67 expression.

Together these findings mark an incremental but important step in demonstrating the role that the metastatic microenvironment plays in directing metastatic dormancy and emergence. However, the majority of this investigation relied upon the implementation of 2D culture systems and *in vivo* models that suffer from limitations that introduce experimental variables that can misrepresent or cloud the actual human *in vivo* response. For example, 2D culture systems fail to recreate the three-dimensional microenvironment, and mouse *in vivo* systems don't fully

represent the human species response. And so our attention turned to an all-human microphysiological three dimensional bioreactor system that linked species and three-dimensional culture systems in order to more fully investigate metastatic dormancy and emergence.

7.1 CONCLUSION

We investigated breast cancer metastatic dormancy and emergence in the hepatic niche because this is the most intractable and deadly outcome of nearly 20% of all breast cancer patients. Our research focused on the metastatic microenvironment as providing a favorable niche to host latent breast cancer survival and subsequent lethal emergence from dormancy. We applied experimental techniques across a novel 3D perfused microwell bioreactor, a Markov chain Monte Carlo simulation, and intrasplenic injections of genetically engineered E-cadherin breast cancer cell lines into immune compromised mice. Our investigations revealed that metastatic dormancy is more likely orchestrated by cellular quiescence (versus a balance of proliferation and apoptosis) and that a partial epithelial reversion is conferred in highly invasive, triple negative breast cancer cell lines by the hepatic microenvironment. We also discovered that less invasive, epithelial-like breast cancer cells exhibit a grow-out advantage and mesenchymal shift in the presence of non-parenchymal sinusoidal endothelial cells – strongly suggesting a trigger for emergence from dormancy. These findings are an incremental yet important step in the emerging emphasis of the metastatic niche as a druggable target in order to eradicate or keep at bay the disseminated dormant metastases.

8.0 SPECULATIONS AND NEXT STEPS

Rare opportunities exist where it's acceptable to speculate in scientific writing. One such opportunity is at the end of a thesis, so I shall indulge this opportunity.

My overarching perspective on developing therapies to destroy (or keep dormant) the sub-clinical metastases involves exogenously modulating the body's own physiological mechanisms as opposed to solely targeting the carcinoma cells directly with therapeutic agents. The mutational diversity and multiple drug resistance mechanisms of carcinoma cells present a staggering array of work-around strategies for carcinomas to overcome even targeted therapies such as Trastuzumab. Those drugs certainly have a therapeutic role and are saving patient lives, but even with combination therapies of other agents the metastatic carcinoma cells usually find a way to thwart these interventions.

“It takes a village to raise a child.” This proverb's etiology is unclear but Hillary Clinton resurrected this quotation into the public's lexicon in 1996. Thankfully this thesis is not about politics, but cancer may be. I believe cancer is like the child – notwithstanding parallels to being a voracious consumer of sugar, a fast grower, difficult to control, and behaving one day and derailing the next. Sometimes the more a child acts up, the more a parent wants to directly intervene. Much like the parent-child relationship so has been the drug-cancer relationship. Perhaps too often parents overlook more subtle aspects of the child's environment that may be promoting, sustaining, or inflaming the child's inappropriate behavior. Perhaps those

environmental triggers are subtler and seemingly innocuous to the parent but have grave implications to fueling the child's aversion to authority.

I believe many investigators are still focusing too much effort on what else to take away from the child to change their behavior – so they revoke Xbox® privileges for a week, or ground them from riding their bike. The child responds by surreptitiously playing on their iPod® or riding their friend's bike around the corner. The child will almost always find a way to get what they want. So I think the answer is to still intervene directly with the child with methods that are at least somewhat effective to him/her, but more importantly to leverage the assets in the child's environment (the village) from more unlikely sources in order to reign in their behavior. One method may be to contact the neighborhood parents and request that their children do not share with them any toys, or play with them for a 1-week grounding period. This provides a higher-level, broader enforcement spectrum. Another may be to not remove the Xbox, but instead replace the shoot-em-up games with something like Dora the Explorer® - all but guaranteed to keep a teenager from enjoying the Xbox.

So let's reign in these anecdotes into something more scientifically directed, focusing on the liver as a metastatic niche to breast cancer. The hepatic non-parenchymal cells are a diverse and rich source of secreted cytokines that could attenuate the carcinoma growth. Moreover, that they are dynamic and respond to local microenvironmental cues enables them to adapt to an evolving metastatic microenvironment and change their activation status to stay one step ahead of the cancer. So placing an emphasis on exogenously modulating the non-parenchymal cells in order to educate them to fight cancer I think is a logical, but understudied approach. Next would be the modulating the effects of endocrine signaling from steroid hormones such as hydrocortisone. This hormone is able to elevate blood sugar and has immune suppressive effects

– certainly two characteristics that help promote carcinoma survival and proliferation. Another approach may be to chemically stress the liver parenchyma in order to induce a broad organ stress response pathway that may knock some sense into the cancer cells (to apoptose). This might be akin to sending the child to military school if other less invasive options fail.

One more detailed and certainly speculative mechanistic example of how modulating the microenvironment may indirectly target metastatic breast cancer cells is through the endocrine modulation of hydrocortisone. It's been shown that Vitamin D3 can activate the Vitamin D receptor (VDR) in triple negative breast cancer cells, triggering re-expression of E-cadherin through E-cadherin promoter loss of methylation. However, VDR expression is inhibited by glucocorticoids. Therefore if breast cancer metastatic MER-T is at least in part regulated by VDR activation (through D3 or other ligands), the addition of higher levels of hydrocortisone into the metastatic niche might inhibit E-cadherin reversion and sensitize otherwise dormant carcinomas to succumb to chemotherapeutic agents. So this endocrine stressor may prompt the breast cancer cells back into a more proliferative, mesenchymal phenotype enabling existing therapeutics to be more effective. Because of possible multiple drug resistance mechanisms against hydrocortisone that could be invoked, and within the spirit of, “It takes a village...”, a targeted therapy to Kaiso may be an effective adjuvant. VDR receptors interact with zinc finger and BTB domain proteins of which Kaiso is a member. Perhaps Kaiso can intracellularly activate VDR in certain instances, or perhaps can be secreted extracellularly (such as HMGB1 is from monocytes) – allowing for multiple angles to be addressed simultaneously.

These investigations, however, are high risk and not necessarily conducive to the current trajectory of druggable targets. But with high risk comes high reward and so just like

entrepreneurs who charge ahead when failure is all but certain, I too hope that we breed more scientific investigators willing to take those leaps of faith.

BIBLIOGRAPHY

- Adam AP, George A, Schewe D, Bragado P, Iglesias BV, Ranganathan AC, et al. Computational identification of a p38SAPK-regulated transcription factor network required for tumor cell quiescence. *Cancer Res.* 2009;69(14):5664-72.
- Aguirre Ghiso JA, Kovalski K, Ossowski L. Tumor dormancy induced by downregulation of urokinase receptor in human carcinoma involves integrin and MAPK signaling. *J Cell Biol.* 1999;147(1):89-104.
- Aguirre-Ghiso JA, Ossowski L, Rosenbaum SK. Green fluorescent protein tagging of extracellular signal-regulated kinase and p38 pathways reveals novel dynamics of pathway activation during primary and metastatic growth. *Cancer Res.* 2004;64(20):7336-45.
- Aguirre-Ghiso JA. The problem of cancer dormancy: understanding the basic mechanisms and identifying therapeutic opportunities. *Cell Cycle.* 2006;5(16):1740-3.
- Aguirre-Ghiso JA. Models, mechanisms and clinical evidence for cancer dormancy. *Nat Rev Cancer.* 2007;7(11):834-46.
- Aleamar J, Schuur ER. Progress in using circulating tumor cell information to improve metastatic breast cancer therapy. *Journal of oncology.* 2013;2013:702732. Epub 2013/04/17. doi: 10.1155/2013/702732.
- Almog N, Ma L, Raychowdhury R, Schwager C, Erber R, Short S, et al. Transcriptional switch of dormant tumors to fast-growing angiogenic phenotype. *Cancer Res.* 2009;69(3):836-44.
- Angelucci A, Gravina GL, Rucci N, Millimaggi D, Festuccia C, Muzi P, et al. Suppression of EGF-R signaling reduces the incidence of prostate cancer metastasis in nude mice. *Endocrine-related cancer.* 2006;13(1):197-210.
- Ansieau S, Bastid J, Doreau A, Morel AP, Bouchet BP, Thomas C, et al. Induction of EMT by twist proteins as a collateral effect of tumor-promoting inactivation of premature senescence. *Cancer Cell.* 2008;14(1):79-89.

- Antal T, Krapivsky PL. Outbreak size distributions in epidemics with multiple stages. *J Stat Mech* 2012;2012:p07018
- Auguste P, Fallavollita L, Wang N, Burnier J, Bikfalvi A, Brodt P. The host inflammatory response promotes liver metastasis by increasing tumor cell arrest and extravasation. *Am J Pathol.* 2007;170(5):1781-92.
- Balz LM, Bartkowiak K, Andreas A, Pantel K, Niggemann B, Zanker KS, et al. The interplay of HER2/HER3/PI3K and EGFR/HER2/PLC-gamma1 signaling in breast cancer cell migration and dissemination. *J Pathol.* 2012;227(2):234-44.
- Bednarz-Knoll N, Alix-Panabieres C, Pantel K. Clinical relevance and biology of circulating tumor cells. *Breast Cancer Res.* 2011;13(6):228.
- Benton G, Crooke E, George J. Laminin-1 induces E-cadherin expression in 3-dimensional cultured breast cancer cells by inhibiting DNA methyltransferase 1 and reversing promoter methylation status. *FASEB J.* 2009;23(11):3884-95.
- Berman JJ, Moore GW. The role of cell death in the growth of preneoplastic lesions: a Monte Carlo simulation model. *Cell proliferation.* 1992;25(6):549-57.
- Bombonati A, SgROI DC. The molecular pathology of breast cancer progression. *J Pathol.* 2011;223(2):307-17.
- Brackstone M, Townson JL, Chambers AF. Tumour dormancy in breast cancer: an update. *Breast Cancer Res.* 2007;9(3):208.
- Bresalier RS, Byrd JC, Brodt P, Ogata S, Itzkowitz SH, Yunker CK. Liver metastasis and adhesion to the sinusoidal endothelium by human colon cancer cells is related to mucin carbohydrate chain length. *Int J Cancer.* 1998;76(4):556-62.
- Brodt P, Fallavollita L, Bresalier RS, Meterissian S, Norton CR, Wolitzky BA. Liver endothelial E-selectin mediates carcinoma cell adhesion and promotes liver metastasis. *Int J Cancer.* 1997;71(4):612-9.
- Chambers AF, MacDonald IC, Schmidt EE, Koop S, Morris VL, Khokha R, et al. Steps in tumor metastasis: new concepts from intravital videomicroscopy. *Cancer Metastasis Rev.* 1995;14(4):279-301.
- Chao YL, Shepard CR, Wells A. Breast carcinoma cells re-express E-cadherin during mesenchymal to epithelial reverting transition. *Mol Cancer.* 2010;9:179.
- Chao Y, Wu Q, Shepard C, Wells A. Hepatocyte induced re-expression of E-cadherin in breast and prostate cancer cells increases chemoresistance. *Clin Exp Metastasis.* 2011.

- Chao Y, Wu Q, Acquafondata M, Dhir R, Wells A. Partial mesenchymal to epithelial reverting transition in breast and prostate cancer metastases. *Cancer Microenviron.* 2012;5(1):19-28.
- Chatterjee M, van Golen KL. Farnesyl transferase inhibitor treatment of breast cancer cells leads to altered RhoA and RhoC GTPase activity and induces a dormant phenotype. *Int J Cancer.* 2011;129(1):61-9.
- Chaffer CL, Brennan JP, Slavin JL, Blick T, Thompson EW, Williams ED (2006) Mesenchymal-to-epithelial transition facilitates bladder cancer metastasis: role of fibroblast growth factor receptor-2. *Cancer Res* 66:11271–11278
- Coulthard LR, White DE, Jones DL, McDermott MF, Burchill SA. p38(MAPK): stress responses from molecular mechanisms to therapeutics. *Trends in molecular medicine.* 2009;15(8):369-79.
- Dawson JL, Tan KC. Anatomy of the liver. In: Millward-Sadler GH, Wright R, Arthur MJP, eds. *Wright's liver and biliary disease. Pathophysiology, diagnosis and management*, 3rd ed, vol 1. London: WB Saunders, 1992:3-11.
- Demicheli R. Tumour dormancy: findings and hypotheses from clinical research on breast cancer. *Semin Cancer Biol.* 2001;11(4):297-306.
- Demicheli R, Miceli R, Moliterni A, Zambetti M, Hrushesky WJ, Retsky MW, et al. Breast cancer recurrence dynamics following adjuvant CMF is consistent with tumor dormancy and mastectomy-driven acceleration of the metastatic process. *Ann Oncol.* 2005;16(9):1449-57.
- De Wever O, Nguyen QD, Van Hoorde L, Bracke M, Bruyneel E, Gespach C, et al. Tenascin-C and SF/HGF produced by myofibroblasts in vitro provide convergent pro-invasive signals to human colon cancer cells through RhoA and Rac. *FASEB J.* 2004;18(9):1016-8.
- Divoli A, Mendonca EA, Evans JA, Rzhetsky A. Conflicting biomedical assumptions for mathematical modeling: the case of cancer metastasis. *PLoS computational biology.* 2011;7(10):e1002132.
- Dodds MG, Vicini P. Assessing convergence of Markov chain Monte Carlo simulations in hierarchical Bayesian models for population pharmacokinetics. *Annals of biomedical engineering.* 2004;32(9):1300-13.
- Fausto N, Campbell JS. The role of hepatocytes and oval cells in liver regeneration and repopulation. *Mechanisms of development.* 2003;120(1):117-30.
- Fendrich V, Waldmann J, Feldmann G, Schlosser K, Konig A, Ramaswamy A, et al. Unique expression pattern of the EMT markers Snail, Twist and E-cadherin in benign and

- malignant parathyroid neoplasia. *European journal of endocrinology / European Federation of Endocrine Societies.* 2009;160(4):695-703.
- Fisher B, Anderson S, Bryant J, Margolese RG, Deutsch M, Fisher ER, et al. Twenty-year follow-up of a randomized trial comparing total mastectomy, lumpectomy, and lumpectomy plus irradiation for the treatment of invasive breast cancer. *The New England journal of medicine.* 2002;347(16):1233-41.
- Fridman R, Giaccone G, Kanemoto T, Martin GR, Gazdar AF, Mulshine JL. Reconstituted basement membrane (matrigel) and laminin can enhance the tumorigenicity and the drug resistance of small cell lung cancer cell lines. *Proc Natl Acad Sci U S A.* 1990;87(17):6698-702.
- Gao H, Chakraborty G, Lee-Lim AP, Mo Q, Decker M, Vonica A, et al. The BMP inhibitor Coco reactivates breast cancer cells at lung metastatic sites. *Cell.* 2012;150(4):764-79.
- Graff JR, Herman JG, Lapidus RG, Chopra H, Xu R, Jarrard DF, Isaacs WB, Pitha PM, Davidson NE, Baylin SB (1995) E-cadherin expression is silenced by DNA hypermethylation in human breast and prostate carcinomas. *Cancer Res* 55: 5195– 5199
- Griffith LG, Swartz MA. Capturing complex 3D tissue physiology in vitro. *Nat Rev Mol Cell Biol.* 2006;7(3):211-24.
- Gunasinghe NP, Wells A, Thompson EW, Hugo HJ. Mesenchymal-epithelial transition (MET) as a mechanism for metastatic colonisation in breast cancer. *Cancer Metastasis Rev.* 2012.
- Haeno H, Michor F. The evolution of tumor metastases during clonal expansion. *J Theor Biol.* 2010;263(1):30-44.
- Hanahan D, Folkman J. Patterns and emerging mechanisms of the angiogenic switch during tumorigenesis. *Cell.* 1996;86(3):353-64.
- Harris T. The theory of branching processes. United States: Air Force Project RAND;1964:1-248
- Haustein V, Schumacher U. A dynamic model for tumour growth and metastasis formation. *Journal of clinical bioinformatics.* 2012;2(1):11.
- Hurst DR, Edmonds MD, Scott GK, Benz CC, Vaidya KS, Welch DR. Breast cancer metastasis suppressor 1 up-regulates miR-146, which suppresses breast cancer metastasis. *Cancer Res.* 2009;69(4):1279-83.
- Imai T, Horiuchi A, Shiozawa T, Osada R, Kikuchi N, Ohira S, et al. Elevated expression of E-cadherin and alpha-, beta-, and gamma-catenins in metastatic lesions compared with primary epithelial ovarian carcinomas. *Human pathology.* 2004;35(12):1469-76.

- Inman S. Integration of Real Time Oxygen Measurements with a 3D Perfused Tissue Culture System: Massachusetts Institute of Technology; 2011.
- Jiao Y, Torquato S. Emergent behaviors from a cellular automaton model for invasive tumor growth in heterogeneous microenvironments. *PLoS computational biology*. 2011;7(12):e1002314.
- Jungermann K, Kietzmann T. Oxygen: modulator of metabolic zonation and disease of the liver. *Hepatology*. 2000;31(2):255-60.
- Kamiya N, Suzuki H, Endo T, Yano M, Naoi M, Nishimi D, et al. Clinical usefulness of bone markers in prostate cancer with bone metastasis. *International journal of urology : official journal of the Japanese Urological Association*. 2012.
- Kienast Y, von Baumgarten L, Fuhrmann M, Klinkert WE, Goldbrunner R, Herms J, et al. Real-time imaging reveals the single steps of brain metastasis formation. *Nat Med*. 2010;16(1):116-22.
- Kim RS, Avivar-Valderas A, Estrada Y, Bragado P, Sosa MS, Aguirre-Ghiso JA, et al. Dormancy signatures and metastasis in estrogen receptor positive and negative breast cancer. *PLoS One*. 2012;7(4):e35569.
- Klein CA, Holzel D. Systemic cancer progression and tumor dormancy: mathematical models meet single cell genomics. *Cell Cycle*. 2006;5(16):1788-98.
- Klein CA. Framework models of tumor dormancy from patient-derived observations. *Curr Opin Genet Dev*. 2010.
- Kmiec Z. Cooperation of liver cells in health and disease. *Advances in anatomy, embryology, and cell biology*. 2001;161:III-XIII, 1-151.
- Kobayashi A, Okuda H, Xing F, Pandey PR, Watabe M, Hirota S, et al. Bone morphogenetic protein 7 in dormancy and metastasis of prostate cancer stem-like cells in bone. *J Exp Med*. 2011;208(13):2641-55.
- Kowalski PJ, Rubin MA, Kleer CG. E-cadherin expression in primary carcinomas of the breast and its distant metastases. *Breast Cancer Res*. 2003;5(6):R217-22.
- LaPorta CAM, Zapperi S, Sethna JP. Senescent cells in growing tumors: population dynamics and cancer stem cells. *PLoS Comput Biol* 2012;8:e100216
- Lin Q, Balasubramanian K, Fan D, Kim SJ, Guo L, Wang H, et al. Reactive astrocytes protect melanoma cells from chemotherapy by sequestering intracellular calcium through gap junction communication channels. *Neoplasia*. 2010;12(9):748-54.

- Luzzi KJ, MacDonald IC, Schmidt EE, Kerkvliet N, Morris VL, Chambers AF, et al. Multistep nature of metastatic inefficiency: dormancy of solitary cells after successful extravasation and limited survival of early micrometastases. *Am J Pathol.* 1998;153(3):865-73.
- Mani SA, Guo W, Liao MJ, Eaton EN, Ayyanan A, Zhou AY, et al. The epithelial-mesenchymal transition generates cells with properties of stem cells. *Cell.* 2008;133(4):704-15.
- Marshall JC, Collins JW, Nakayama J, Horak CE, Liewehr DJ, Steinberg SM, et al. Effect of inhibition of the lysophosphatidic acid receptor 1 on metastasis and metastatic dormancy in breast cancer. *Journal of the National Cancer Institute.* 2012;104(17):1306-19.
- Matsumura T, Takesue M, Westerman KA, Okitsu T, Sakaguchi M, Fukazawa T, et al. Establishment of an immortalized human-liver endothelial cell line with SV40T and hTERT. *Transplantation.* 2004;77(9):1357-65.
- Michalopoulos G, Cianciulli HD, Novotny AR, Kligerman AD, Strom SC, Jirtle RL. Liver regeneration studies with rat hepatocytes in primary culture. *Cancer Res.* 1982;42(11):4673-82.
- Michalopoulos GK, DeFrances MC. Liver regeneration. *Science.* 1997;276(5309):60-6.
- Michalopoulos GK. Liver regeneration. *J Cell Physiol.* 2007;213(2):286-300.
- Michor F, Nowak MA, Iwasa Y. Stochastic dynamics of metastasis formation. *J Theor Biol.* 2006;240(4):521-30.
- Mocellin S, Hoon D, Ambrosi A, Nitti D, Rossi CR. The prognostic value of circulating tumor cells in patients with melanoma: a systematic review and meta-analysis. *Clin Cancer Res.* 2006;12(15):4605-13.
- Nash KT, Phadke PA, Navenot JM, Hurst DR, Accavitti-Loper MA, Sztul E, et al. Requirement of KISS1 secretion for multiple organ metastasis suppression and maintenance of tumor dormancy. *Journal of the National Cancer Institute.* 2007;99(4):309-21..
- Naumov GN, MacDonald IC, Weinmeister PM, Kerkvliet N, Nadkarni KV, Wilson SM, et al. Persistence of solitary mammary carcinoma cells in a secondary site: a possible contributor to dormancy. *Cancer Res.* 2002;62(7):2162-8.
- Naumov GN, Akslen LA, Folkman J. Role of angiogenesis in human tumor dormancy: animal models of the angiogenic switch. *Cell Cycle.* 2006;5(16):1779-87.
- Naumov GN, Folkman J, Straume O, Akslen LA. Tumor-vascular interactions and tumor dormancy. *APMIS : acta pathologica, microbiologica, et immunologica Scandinavica.* 2008;116(7-8):569-85.

- Onder TT, Gupta PB, Mani SA, Yang J, Lander ES, Weinberg RA. Loss of E-cadherin promotes metastasis via multiple downstream transcriptional pathways. *Cancer Res.* 2008;68(10):3645-54.
- Pantel K, Schlimok G, Braun S, Kutter D, Lindemann F, Schaller G, et al. Differential expression of proliferation-associated molecules in individual micrometastatic carcinoma cells. *Journal of the National Cancer Institute.* 1993;85(17):1419-24.
- Phadke PA, Vaidya KS, Nash KT, Hurst DR, Welch DR. BRMS1 suppresses breast cancer experimental metastasis to multiple organs by inhibiting several steps of the metastatic process. *Am J Pathol.* 2008;172(3):809-17.
- Radisky DC. Epithelial-mesenchymal transition. *J Cell Sci.* 2005;118(Pt 19):4325-6.
- Rakha EA, Putti TC, Abd El-Rehim DM, Paish C, Green AR, Powe DG, et al. Morphological and immunophenotypic analysis of breast carcinomas with basal and myoepithelial differentiation. *J Pathol.* 2006;208(4):495-506.
- Ranganathan AC, Zhang L, Adam AP, Aguirre-Ghiso JA. Functional coupling of p38-induced up-regulation of BiP and activation of RNA-dependent protein kinase-like endoplasmic reticulum kinase to drug resistance of dormant carcinoma cells. *Cancer Res.* 2006;66(3):1702-11.
- Reddy JK, Rao MS. Hepatic ultrastructure and adaptation. *Monographs in pathology.* 1987(28):11-42.
- Riethmuller G, Klein CA. Early cancer cell dissemination and late metastatic relapse: clinical reflections and biological approaches to the dormancy problem in patients. *Semin Cancer Biol.* 2001;11(4):307-11.
- Sahai E. Mechanisms of cancer cell invasion. *Curr Opin Genet Dev.* 2005;15(1):87-96.
- Seer.cancer.gov [Internet]. Bethesda, MD: National Cancer Institute. Available from: <http://seer.cancer.gov>. Accessed August 22, 2013.
- Shi Y, Massague J. Mechanisms of TGF-beta signaling from cell membrane to the nucleus. *Cell.* 2003;113(6):685-700.
- Simpson PT, Reis-Filho JS, Lambros MB, Jones C, Steele D, Mackay A, et al. Molecular profiling pleomorphic lobular carcinomas of the breast: evidence for a common molecular genetic pathway with classic lobular carcinomas. *J Pathol.* 2008;215(3):231-44.
- Sosa MS, Avivar-Valderas A, Bragado P, Wen HC, Aguirre-Ghiso JA. ERK1/2 and p38{alpha}/{beta} signaling in tumor cell quiescence: opportunities to control dormant residual disease. *Clin Cancer Res.* 2011.

- Tanaka H, Kono E, Tran CP, Miyazaki H, Yamashiro J, Shimomura T, et al. Monoclonal antibody targeting of N-cadherin inhibits prostate cancer growth, metastasis and castration resistance. *Nat Med.* 2010;16(12):1414-20.
- Taub R. Liver regeneration: from myth to mechanism. *Nat Rev Mol Cell Biol.* 2004;5(10):836-47.
- Taylor DP, Wells JZ, Savol A, Chennubhotla C, Wells A. Modeling boundary conditions for balanced proliferation in metastatic latency. *Clin Cancer Res.* 2013;19(5):1063-70. Epub 2013/01/19. doi: 10.1158/1078-0432.CCR-12-3180.
- Thiery JP. Epithelial-mesenchymal transitions in tumour progression. *Nat Rev Cancer.* 2002;2(6):442-54.
- Thiery JP. Epithelial-mesenchymal transitions in development and pathologies. *Curr Opin Cell Biol.* 2003;15(6):740-6.
- Townson JL, Chambers AF. Dormancy of solitary metastatic cells. *Cell Cycle.* 2006;5(16):1744-50.
- Uhr JW, Pantel K. Controversies in clinical cancer dormancy. *Proc Natl Acad Sci U S A.* 2011.
- Van den Eynden GG, Majeed AW, Illemann M, Vermeulen PB, Bird NC, Hoyer-Hansen G, et al. The multifaceted role of the microenvironment in liver metastasis: biology and clinical implications. *Cancer Res.* 2013;73(7):2031-43.
- Venet D, Dumont JE, Detours V. Most random gene expression signatures are significantly associated with breast cancer outcome. *PLoS computational biology.* 2011;7(10):e1002240.
- Vlodavsky I, Fuks Z, Bar-Ner M, Ariav Y, Schirmacher V. Lymphoma cell-mediated degradation of sulfated proteoglycans in the subendothelial extracellular matrix: relationship to tumor cell metastasis. *Cancer Res.* 1983;43(6):2704-11.
- Wagenaar GT, Chamuleau RA, Pool CW, de Haan JG, Maas MA, Korfage HA, et al. Distribution and activity of glutamine synthase and carbamoylphosphate synthase upon enlargement of the liver lobule by repeated partial hepatectomies. *J Hepatol.* 1993;17(3):397-407.
- Wang W, Wyckoff JB, Frohlich VC, Olyeynikov Y, Huttelmaier S, Zavadil J, et al. Single cell behavior in metastatic primary mammary tumors correlated with gene expression patterns revealed by molecular profiling. *Cancer Res.* 2002;62(21):6278-88.
- Watson HW, Galton F. On the probability of the extinction of families. *J Anthropol Inst Great Brit Ireland* 1875;4:138-44.

- Weibel ER, Staubli W, Gnagi HR, Hess FA. Correlated morphometric and biochemical studies on the liver cell. I. Morphometric model, stereologic methods, and normal morphometric data for rat liver. *J Cell Biol.* 1969;42(1):68-91.
- Wells A, Yates C, Shepard CR. E-cadherin as an indicator of mesenchymal to epithelial reverting transitions during the metastatic seeding of disseminated carcinomas. *Clin Exp Metastasis.* 2008;25(6):621-8.
- Willis L, Alarcon T, Elia G, Jones JL, Wright NA, Tomlinson IP, et al. Breast cancer dormancy can be maintained by small numbers of micrometastases. *Cancer Res.* 2010;70(11):4310-7.
- Wyckoff JB, Jones JG, Condeelis JS, Segall JE. A critical step in metastasis: in vivo analysis of intravasation at the primary tumor. *Cancer Res.* 2000;60(9):2504-11.
- Ycart B. Fluctuation analysis with cell deaths. arXiv preprint arXiv 2012: e1207.4375
- Yates C, Shepard CR, Papworth G, Dash A, Beer Stolz D, Tannenbaum S, et al. Novel three-dimensional organotypic liver bioreactor to directly visualize early events in metastatic progression. *Adv Cancer Res.* 2007;97:225-46.
- Yates CC, Shepard CR, Stolz DB, Wells A. Co-culturing human prostate carcinoma cells with hepatocytes leads to increased expression of E-cadherin. *Br J Cancer.* 2007;96(8):1246-52.
- Yu W, Kim J, Ossowski L. Reduction in surface urokinase receptor forces malignant cells into a protracted state of dormancy. *J Cell Biol.* 1997;137(3):767-77.
- Zou L, Hazan R, Roy P. Profilin-1 overexpression restores adherens junctions in MDA-MB-231 breast cancer cells in R-cadherin-dependent manner. *Cell motility and the cytoskeleton.* 2009;66(12):1048-56. Epub 2009/07/14. doi: 10.1002/cm.20407.